Stony Brook University

Low Intensity Vibrations Mitigate Cancer-Induced Bone Loss with Indications of Reduced Tumor Progression

A Dissertation Presented

by

Gabriel M. Pagnotti

to

The Graduate School

in Partial Fulfillment of the

Requirements

for the Degree of

Doctor of Philosophy

in

Biomedical Engineering

Stony Brook University

August 2014

* Chapter 2 (as presented) has already been published and is used with permission by Elsevier: Pagnotti et al., *Bone*. 2012 Sep; 51(3):570-7.

Stony Brook University

The Graduate School

Gabriel M. Pagnotti

We, the dissertation committee for the above candidate for the

Doctor of Philosophy degree, hereby recommend

acceptance of this dissertation.

Clinton T. Rubin, Ph.D. – Dissertation Advisor
Distinguished Chair of Biomedical Engineering, Stony Brook University
Director of Center for Biotechnology, Stony Brook University

Richard A. Clark, M.D.
Professor of Biomedical Engineering and Dermatology, Stony Brook University
Director of Center for Tissue Engineering, Stony Brook University

Sanford Simon, Ph.D.
Adjunct Professor of Biomedical Engineering and Professor of Biochemistry, Cell Biology, and Pathology, Stony Brook University

Kenneth R. Shroyer, M.D., Ph.D.
Professor and Chair of Department of Pathology, Stony Brook University School of Medicine

This dissertation is accepted by the Graduate School

Charles Taber
Dean of the Graduate School

Abstract of the Dissertation

Low Intensity Vibrations Mitigate Cancer-Induced Bone Loss with Indications of Reduced Tumor Progression

by

Gabriel M. Pagnotti

Doctor of Philosophy

in

Biomedical Engineering

Stony Brook University

2014

Osteopenia is a comorbidity frequently observed in patients being treated for and recovering from cancer treatment, elevating their risk of fracture. These skeletal losses are compounded by chemotherapy and irradiation, damaging both bone and contents of the marrow, thereby undermining recovery efforts. Exercise is commonly prescribed as a non-pharmacological means of maintaining bone mass. However, in those with compromised bone strength, the loads imposed by rigorous exercises may facilitate a fracture it was intended to prevent. Low intensity vibrations (LIV), a mechanical signal demonstrated as anabolic to bone by biasing mesenchymal stem cells (MSCs) towards an osteogenic endpoint, may represent a novel strategy to circumvent the bone losses induced by cancer if it is able to do so without negatively affecting survivability. Two murine models of cancer were employed to assess the effects of LIV in mitigating cancer-induced bone loss. Following 1y of LIV administration, a murine model of spontaneous granulosa cell ovarian cancer demonstrated significant preservation of bone quantity and quality as evidenced by micro-CT analysis of tibial and vertebral trabecular bone without negatively influencing animal survivability. In quantifying tumor burden, fewer tumor foci pervaded the system in LIV mice. MSC populations were significantly lower in the marrow of LIV as compared to controls, indicating a modulation of stem cell progenitor differentiation towards skeletal endpoints while reducing their capacity to contribute towards neoplastic tissue expansion. Additionally, an immunocompromised mouse strain was xenografted with human multiple

myeloma cells, inducing diffuse infiltration of aberrant plasma cells in the host bone marrow. Significant cortical osteolysis and trabecular destruction was observed after 8w. However, micro-CT analysis of the injected mice exposed to 8w of LIV revealed retention of trabecular bone in the distal femur and reduced instance of cortical perforations, all without influencing the survivability of the mice. Histological assessment of the femoral marrow cavity further demonstrated the infiltration of myeloma cells throughout the length of the medullary cavity, both across the diaphysis and extending past the epiphyseal growth plate resulting in anemic and neutropenic outcomes in both groups. Osteolysis was clearly evident in the diseased groups, particularly at the distal femur, as woven bone and cortical resorption pits were a consequence of disease progression. The bone marrow phenotype, as assessed by FACS analysis and histological evaluation, was also highly disrupted, reflected by the elevated hematopoietic stem cell and lineage-specific populations. A trend towards reduced pathology, including necrotic tumor and fewer tumor cells, were quantified in diseased animals exposed to LIV. These skeletal and marrow outcomes, however, were mildly reduced in those mice initially treated with LIV. Together, the data taken from these studies reinforce the known destructive capacity of cancer on the skeletal system and the constituents of bone marrow but in two different murine models of the disease. In addition, the two cancer models studied which demonstrate different mechanisms of cancer-induced bone loss, also reveal the positive effects low intensity vibrations impart on the skeletal system during tumorigenesis without negatively affecting survival outcome. Further, the outcomes of administering low intensity vibrations to ameliorate consequences of disease support its potential clinical use in mitigating cancer-induced bone losses and, perhaps, in slowing progression of the disease itself.

Dedication Page

These works are dedicated, in no small part, to two different bodies of inspiration. First, and foremost, as one of millions of biomedical researchers, I humbly extend this dedication to those across all disciplinary spectrums of engineering and medicine who have expended far more precious time than I and devoted their lives dedicated to the understanding, treatment of those with, and elimination of cancer. Secondly, and most importantly, I would like to thank my parents for instilling in me at a young age the notion that if you want to achieve something badly enough, you can, but one has to earn it. Without your support and guidance, the ways of the world would have been an impossibility.

"Always dream and shoot higher than you know you can do. Do not bother just to be better than your contemporaries or predecessors. Try to be better than yourself." - William Faulkner

"Nothing's ever easy…" - Michael F. Pagnotti Jr.

Table of Contents

List of Figures – Tables -- Illustrations

Figures

X. Histological sections of nuclear-stained (H&E) femurs (6.3x) at the distal metaphysis.

XI. Gross histological quantification of total percentage of the plasmacytoma infiltration throughout the marrow cavity.

XII. Micro-CT analysis of segmented bone parameters in the femur and tibia were used to measure differences in bone quantity and quality.

XIII. Dot plot FACS analysis of $CD138^{+}$-tagged cells from *in vitro* and bone marrow and peripheral blood cultures at 8w-post-injection.

XIV. FACS analysis of hematopoietic lymphocyte populations in the femoral bone marrow: $CD138^{+}$, LSK^{+}, $CD11c^{+}$/$F4\text{-}80^{+}$ and $NK1.1^{+}$. These populations are increased in MM as compared to AC and decrease in LIV as compared to MM.

XV. 3D μCT reconstructions of segmented distal femur sections proximal to the epiphyseal growth plate detailing extensive trabecular bone loss and cortical thinning in MM as compared to AC. Trabecular bone was preserved in LIV as compared to MM.

XVI. Transverse μCT 3D reconstructions of the proximal tibia.

XVII. Focal necrosis of the tumor within the bone marrow.

Tables

Illustrations

List of Abbreviations

Ab:	Antibody; A type of protein, in varying isoforms, secreted by plasma cells used to identify and tag foreign bodies for elimination
AC:	Age-matched Control
ALP:	Serum Alkaline Phosphatase (Marker for Bone Formation)
BC:	Baseline Control
BM:	Bone Marrow
BV:	Bone Volume; A µCT parameter
BV/TV:	Bone Volume Fraction; A µCT parameter measuring the volume of thresholded bone contained in a pre-prescribed volume within a scan
CD:	Cluster of Differentiation; nomenclature for cell surface receptor designation
CD138:	Syndecan-1; A plasma cell surface marker for normal and malignant neoplasms
CD105:	Endoglin; A cell surface marker widely expressed on hematopoietic and mesenchymal stem cell surfaces
CD44:	Homing Cell Adhesion Molecule; A stem cell surface marker implicated in cell-cell adhesion and the homing and migration of stem cells to the bone marrow
CD90.2:	Thy-1b; A cell surface marker expressed on a wide-array of circulating cells, including mesenchymal and hematopoietic stem cells
CIBL:	Cancer-Induced Bone Loss
C-Kit:	CD117; Mast stem cell growth factor
Ct.:	Cortical bone
Ct.Th.:	Cortical Thickness; A µCT parameter

CTX:	Serum CTX; Carboxy-terminal collagen crosslinks (Marker for bone turnover)
DKK-1:	Dickkopf-1; Mediator of osteoblast suppression
DMEM:	Dulbecco's Modified Eagle's Medium; Cell culture growth media
DPBS:	Dulbecco's Phosphate-Buffered Saline
EndoV:	Endosteal Volume; A μCT parameter quantifying the volume bounded by the endosteal surface of the cortical shell
EMT:	Epithelial-to-Mesenchymal Transition
FACS:	Fluorescence-Activated Cell Sorting (i.e. Flow cytometry)
FBS:	Fetal Bovine Serum
g:	Earth's gravitational acceleration ($9.8 m/s^2$)
GCT:	a). Granulosa cell tumors of the ovary or b). A strain of mice prone to developing this disease (F1-SWRxSWXJ-9, *The Jackson Laboratory*)
gct1:	Locus on chromosome 4 pertaining to site of granulosa cell tumor susceptibility
Gy:	Grey; SI unit of measurement for ionizing radiation
HSC:	Hematopoietic Stem Cells
Hz:	Hertz (frequency units as cycles/second)
IHC:	Immunohistochemistry
Ig:	Immunoglobulin; Alternative designation for "antibody"
IL (#):	Interleukin; Indicating a class of signaling, soluble cytokines synthesized intracellularly and secreted into the cytoplasm and/or extracellularly.
L5:	Referring to the 5^{th} lumbar vertebrae
LSK:	Lin^-, $Sca1^+$, C-kit^-; Designation for short-term hematopoietic precursor cells exhibiting this receptor phenotype

Lin^-:	Lineage negative; Early lymphoid progenitors that have not undergone maturation within the thymus
LIV:	Low Intensity Vibrations; Experimental treatment of mechanical signals
MGUS:	Monoclonal Gammopathy of Undetermined Significance; A clinically irresolute diagnosis following plasma cell clonal proliferation, but which precedes diagnosis of multiple myeloma
mL:	Milliliter
MM:	a.) Multiple myeloma or b.) Experimental group of mice engrafted with human multiple myeoma cells which did not receive LIV treatment
mRNA:	Messenger Ribonucleic Acid
MSC:	Mesenchymal Stem Cells
NBF:	Neutral Buffered Formalin; Tissue fixative
NF-κβ:	Necrosis Factor-kappa beta; Protein that is responsible for cell survival and cytokine production
NOD:	Non-Obese Diabetic; Referring to the inbred mouse strain exhibiting defects in T-cell immunity
NOG:	The NOD/SCID/gamma immunocompromised mice strain (NOD/SCID/γ_c^{null}, *Taconic)*
Nsd:	Not-significantly different; With regards to statistical measures
NSG:	The NOD/SCID/gamma immunocompromised mice strain (NOD.Cg-*Prkdc*^{scid} *Il2rg*^{tm1Wjl}/SzJ, *The Jackson Laboratory*)
NTX:	Serum NTX; N-terminal collagen crosslinks (Marker for bone turnover)
OB:	Osteoblast
OC:	Osteoclast

OPG:	Osteoprotegerin, also known as osteoclastogenesis inhibitory factor; Protein that inhibits NF-κβ, acts as a decoy receptor for RANKL and is a member of the TNF-supergroup
PB:	Peripheral Blood; The blood circulating throughout the vasculature
P/S:	Penicillin and Streptomycin; Standard broad spectrum antibiotics
RANKL:	Receptor-Activated Necrosis factor-Kappa beta Ligand
RBC:	Red Blood Cells; Erythrocytes
ROI:	Region-Of-Interest; As it pertains to µCT evaluations
ROS:	Reactive Oxygen Species
RT-PCR:	Real Time-Reverse Transcription-Polymerase Chain Reaction
RunX2:	Runt-related transcription factor-2 gene
Sca-1:	Stem cell antigen-1; One of the canonical HSC markers
SCID:	Severe Combined Immune Deficient; Pertaining to the mutation used in mouse models lacking mature lymphocyte functionality
SMI:	Structure model index; A µCT parameter; An indicator of bone quality
SPKLS:	"Side Population" of hematopoietic stem cells gated from LSK^+ cells; The long-term, primitive HSC population
Tb.:	Trabecular bone; A µCT parameter
Tb.N.:	Trabecular Number; A µCT parameter
Tb.Sp.:	Trabecular Spacing; A µCT parameter
TGF-β:	Transforming Growth Factor-Beta
TNF-α:	Tumor Necrosis Factor-Alpha; An inflammatory cytokine
TV:	Total Volume; A µCT parameter

U266β1:	Immortalized human multiple myeloma cell line (TIB-196, *ATCC*)
µCT:	Micro-Computed Tomography
µm:	Micron(s)
VCAM-1:	Vascular Cell Adhesion Molecule; Protein that promotes the adhesion of cells to vascular endothelium
Wnt/β-catenin:	A canonical signaling pathway (as opposed to the non-canonical pathway); Regulator of a variety of axial developments, stem cell differentiation pathways, and bone remodeling
WT:	Wild-type

Acknowledgments

Nothing worthwhile is ever accomplished in a single breath, and no one is ever without influence from another. In this vein, I would like to acknowledge the many people that were a part of this venture from its inception to completion: an idea that began on a hunch has stretched so far now. To all of those who have contributed to this body of work throughout my tenure at Stony Brook, your roles in completing these studies were crucial. Equally so, I'd like to thank those who were in my life in the years prior to my departure from FL, who supported (and endured) my pipe dreams about moving to NY, changing career paths, and undergoing this feat of mental stamina.

Family/Friends: My parents, Michael and Diane Pagnotti, who have always been a source of inspiration and a benchmark for success; my accomplished younger sister, Jenna, who makes us all proud; my supportive girlfriend, Abigail Laurence; my extended family and incredible group of friends I've made and maintained along the way…your continued love and support has gotten me to where I am today. I'm grateful to have you in my life.

Mentor: Professor Clinton Rubin, advisor extraordinaire, whose voracious appetite for data has afforded me this incredible opportunity, to contribute to an untouched area of biomedical research that bridged my two academic interests: tissue engineering and cancer research. Your guidance, mentorship, and friendship over the past five years has made me a better scientist and helped me reach one of the proudest achievements of my life.

Thesis Committee: Professors Richard Clark, Sandy Simon, and Kenneth Shroyer, three gentlemen at Stony Brook who have been secondary advisors during my time at Stony Brook and have always been a voice of wisdom and advice. Your valuable time and expert guidance throughout the remainder of these studies have contributed so much to what I hope will one day have a positive clinical impact on those facing disease.

Stony Brook University Colleagues: Roughly 12 hours a day with the same group of people, especially in a laboratory environment, tends to build relationships that border on family. From 2009-14, the Rubin, Judex, and Qin group were like that. Dr's Steven Tommasini, Gunes Uzer, Sarah Manske, Nilsson Holguin, Sardar Zia Uddin, Liangjun Lin, Frederick Serra Hsu, Jesse Muir, Meilin Ete Chan, Andrea Kwaczala, Benjamin Adler, Danielle Green; soon-to-be-Dr's Elizabeth Fivelsohn, Ada Tsoi, Vihita Patel, Jeyantt Sankaran, Tee Pamon, Danielle Frechette, Divya

Krishna, Alyssa Tuthill and Aparna Kadam; and the remainder of the lab, some of whom have moved on, Kofi Appiah-Nkansah, Nirukta Patri, James Lennon, Denis Nguyen, and SWC3 were all considerably key in performing the many experiments it has taken to complete this degree. Whether it was in the mountains of upstate, the beaten of NYC, the serenity of Long Island's East End, or surfing on a South Shore beach, Katarzyna Sawicka, Tabitha Shen, Chris Mahrer, Michael Budassi, Oliver Brutus, Harrison Seidner, William Hauser, Jordan Rustad, and Dan Dedora were the SBU friends that reminded me that life existed outside of the lab.

Shroyer Pathology Lab Core (Stony Brook): Stephanie Burke, Mallory Korman, Dr. Daniel Mockler, Dr. Yupo Ma, and Dr. Kenneth R. Shroyer schooled me in the "arts" of histopathology, gave me a second home in their lab, and facilitated the diagnoses needed to validate this work.

Division of Laboratory Animal Research (Stony Brook DLAR): It takes a caring and trained group of people to handle as many animal research studies as those which pass through this facility. Jean Rooney, Laurie Levine, Nicole Motta, Nick Ortiz, Tom Zimmerman, Tami Darvin, Alan Supovitz, and Mike Gliganic took special care of my animals when I could not. Maintaining animal care as smoothly as it had gone certainly would not have succeeded without these people.

Flow Cytometry Core (Stony Brook): Todd Rueb, Rebecca Connor, and Nancy Boehm, a seemingly endless pool of expertise in flow cytometry, managed to keep their sense of humor despite the overwhelming sample-sets submitted to their doorstep at every study sacrifice.

Stony Brook University BME Faculty: Michael Hadjiargyrou for being an ear; Stefan Judex for trusting me with μCT oversight; Paul Vaska, and Helene Benveniste for facilitating ovarian cancer pilot studies; and Nubia Andrade, Anne-Marie Dusatko, and Jessica Kuhn for keeping me on track throughout my time here.

University of Central Florida Colleague and Mentor**:** Dr. Lawrence Ayong and Professor Debopam Chakrabarti for providing me with my first step towards graduate school, the opportunity to spend evenings and weekends "ghost-volunteering" in their parasitology lab, developing basic lab skills whilst untangling the complexities of malaria. This was an indispensable opportunity and I could never thank them enough.

Former Colleagues: Timothy Malone, my first employer as a professional engineer, for taking in a then-recent electrical engineering graduate with minimal experience, and giving me a chance to

build my skillset from the ground up, and to allow, at times, the chance to step away from multi-million dollar contracts long enough to fulfill my biomedical pursuits: for this I will always be grateful. Dan Gherrity, Randy Crosby, Mike Edwards, and Pete Vega for all teachings ITS related. Penny Kamish and Jason Summerfield for your lasting friendships through the tough times on the road. We'll always have Jacksonville!

Music: Perhaps the most inseparable facet of my life, one which I do not go a day without and one to which I must give some sense of acknowledgement to, is my ever-present, overabundant, and eclectic catalog of music. It does not only facilitate the completion of my work but drives and inspires me in all that I do.

Thank you, all. Achieving these ends would not have been possible otherwise.

Chapter 1: Interactions of Bone, Marrow and Cancer

Overview

Osteopenia is a comorbidity frequently observed in patients being treated for and recovering from cancer treatment. Maintaining bone mass and marrow health over the course of cancer progression and remission is essential to achieving positive outcomes, from both the perspective of fracture risk prevention and from an immunological standpoint. Pharmacological interventions lack true target-specificity, corrupting marrow and damaging healthy tissue, subsequently disrupting immune health, which makes recovery efforts increasingly difficult. Radiotherapies, though effective in ablating cells especially sensitive to irradiation, are undoubtedly disruptive to healthy regulation of blood and bone. Pharmaceutical interventions designed to curb the subsequent skeletal losses are typically accompanied by unfavorable consequences or show marginal affectivity. Alternatively, from a non-pharmacological position, exercise is commonly prescribed as a means to maintain bone strength and sustain immunity. However, in the case of those with significant reductions in bone strength, the loads imposed by rigorous exercises may actually facilitate a fracture it was initially aimed at preventing. In general, mechanical signaling, a component of physical activity and exercise that promotes anabolic tissue growth, is vital to maintaining bone and muscle strength, whereas the absence of such loading results in accelerated muscle and bone catabolism, as evidenced by those subjected to chronic bed-rest. Filtering out the intense magnitudes experienced during exercise and administering the remaining spectral content of muscle contractibility has proven to be an effective strategy in curbing age and osteoporotic-related bone losses in animal and human research efforts and in the clinic. Specifically, low intensity vibrations (LIV), a class of high-frequency, low-magnitude signals, have been suspected of biasing stem cell growth towards osteogenic endpoints. With demonstrated efficacy in promoting osteogenic growth in models of osteoporosis, diet-induced obesity, and reambulation, LIV may represent a novel strategy by which to circumvent the critical bone losses that are observed in the wake of cancer's onset. As with any translational research, degree of safety must be established before treatment efficacy can be assessed in human. Quantifiable differences in bone mass following use of this strategy in *in vivo* models of disease, without negatively affecting mortality rate, may demonstrate preliminary clinical efficacy.

1. Bone: Dynamic Tissue

The musculoskeletal system is a dynamic construct, adapting to and accommodating alterations in loading stresses by modulating its mass and morphology. Skeletal remodeling is a natural phenomenon, resorbing weak or dead bone and replacing it with newer, healthier bone (Illustration 1). First postulated by Wolff [1, 2], bones and muscle are now known as being uniquely adept at responding to discrepancies in metabolic and loading challenges by remodeling their architecture to reflect these changes. When the body is aging or facing illness, it has a reduced capacity to sustain excessive loading and, thus, becomes increasingly susceptible to fracture, reinforcing the prescribed notion to maintain skeletal health by remaining physically active. Vital organs are protected by the hard material properties of bone and gait and posture rely on the integrity of skeletal system to function properly. Bones ravaged by metabolic imbalance are especially susceptible to fracture which can compromise these critical tissues. The composition of bone helps illustrate its vulnerability to these changes.

From a material standpoint, bone is a composite of organic and inorganic substituents organized into an array of cell types and minerals that allow it to undergo unique alterations. Together, this bone matrix, comprised of dense, inorganic minerals of hydroxyapatite, phosphate, and calcium in combination with collagen fibers, endows skeletal tissue with viscoelastic mechanical properties. The orientation of the components enable bone to withstand extreme loads as well as tolerate a moderate degree of deformation. Metabolically, it is also utilized as a depot for calcium to maintain adequate calcium levels in the blood. An architecture consisting of both compact cortical and cancellous trabecular bones allow the skeleton to resist mechanical loads. Trabecular bone, strut-like formations at the extreme ends of long bones and through the vertebral body of spinal vertebrae, resist compressive forces as well as tensile loads and bending moments. Cortical bone, the osseous, more highly dense, and rigid exterior surface of the bone, offers protection to the bone marrow housed within the medullary cavities of bones within the cortices, while also interfacing with the skeletal muscles. A high ultimate stress permits axial, torsional and bending loads [3-5]. Skeletal muscle that attaches at distinct locations on bone also contributes to skeletal loading through transmission of mechanical forces during muscle contractions. Cyclical bouts of these stresses, at physiologically tolerable magnitudes, can positively influence skeletal health [6, 7].

A human skeleton remodels at a rate of approximately 10% per year, as it has an inherent ability to regulate its own growth. This is a natural process that permits replacement of old, damaged or dead bone with healthy tissue over time; however, a requisite for this phenomenon is that bone cells embedded within bone, perceive a mechanical load, either through gravitational means, shear forces across cell surface membranes, or transmissible signaling via internal stresses [8]. The cell syncytium senses these skeletal loads, and these mechanical signals prompt bone to remodel itself to adapt to these new functional challenges through tightly orchestrated osteoclast-mediated resorption and osteoblast-mediated formation, in a coordinated effort to restore loading capacity and healthy bone [9] (Illustration 1). Just as bones are mechanosensitive, responding to various loading challenges, so, too, are they sensitive to the absence of these mechanical loads. Microgravity (long-term space flights) or chronic bedrest (the infirm) result in reduced bone formation, thus, causing musculoskeletal atrophy.

At the molecular scale, levels of signaling proteins are indicate imbalances in the bone remodeling pathway. Variations in bone resorption are indicated by concentrations of certain proteins detected in the serum, such as collagen type-1 cross-linked C- or N-telopeptide (CTX and NTX, respectively) and tartrate-resistant acid phosphatase 5b (TRAP5b). Serum indicators of bone formation are detected via assays specific for alkaline phosphatase (ALP), osteocalcin (OCN), and serum type-1 pro-collagen (C-terminal/N-terminal: C1NP or P1NP). Receptor-activated nuclear-factor kappa ligand (RANKL) is a secreted protein that binds to membrane-bound RANK, promoting bone resorption [10, 11]. Osteoprotegerin (OPG) is another secreted molecule that binds to RANKL, acting as a decoy which prevents excessive bone resorption. The ratio of RANKL to OPG as detected in the serum is an important diagnostic measurement of bone mass and quality, as imbalances in favor of increased RANKL concentrations may be a prognostic indication of multiple myeloma.

In addition to physical influences on bone mass and morphology, disruptions caused by diet (calcium insufficiency), age (age-induced osteoporosis), and disease (cancer-induced bone loss) can disrupt mechanically-mediated adaption and put the skeleton at risk. Dietary alterations, myelodysplastic syndromes that utilize bone marrow space, and fallacies in the endocrine system are examples of systemic conditions that disrupt the delicate balance in the pathway. A surface β-receptor for estrogen and the focal adhesion kinase, for instance, regulate the osteoblastic activity

needed to drive bone formation [12, 13]. Agonistic and inhibitory signaling play reciprocating roles to keep bone at optimal loading capacity.

2. Bone Marrow: Epicenter of Systemic Homeostasis

Bone marrow, the viscous tissue within the cortical shell of almost all bones, functions as a discrete "micro-environment" housing cells of most subtypes and secreted factors that work in concert to regulate solid tissue regeneration, such as bone, and maintain systemic immunity through hematopoiesis. Discrete "niches" within these spaces are the regulatory sites of tissue homeostasis, housing pluripotent stem cells capable of self-renewal and differentiation into one of the two primary subsets of cell lineages in the body. These include those of blood cell origin, deemed hematopoietic stem cells (HSC), which include all cells of the myeloid and lymphoid lineages (Illustration 3), and those cells which ultimately constitute the connective, epithelial, and nervous tissue found throughout the body, are of the mesenchymal lineage (MSC), some of which include bone, cartilage, muscle, fat and are often referred to as the cells responsible for repair and regeneration of tissues [14-21] (Illustration 2), especially those of the musculoskeletal system. Though comparatively few, stem cells are the body's most important resource, imparting the ability to self-renew, regenerate lost and damaged tissue, and to respond to external pressures through proliferation or tissue specific-differentiation. Recruitment of both MSC and HSCs to sites of tissue damage exemplifies the role of the marrow space, not just as a stem cell reservoir, but also as a primary regulator of repair and regeneration.

The bone marrow "microenvironment" is the site for hematopoiesis, the process by which stem cells (HSC's) of the blood obtain cues both locally and remotely to undergo proliferation and lineage-specific differentiation [22-24]. Here, cells of both the lymphoid and myeloid lineages begin their journey towards maturation and specificity. The immune system as a whole functions systemically to sequester and eliminate foreign insults. Immunological components (erythrocytes, platelets, granulocytes, and lymphocytes) and specialized progenitor and stem cells, regulate inflammation [22, 24]. Initiation of inflammatory cascades is most commonly the result of trauma or lesion, but chronic inflammation in bone can be a consequence of excessive resorption. In an effort to repair itself, the body releases soluble factors that increase circulation and signal that reparative resources, such as MSCs, HSCs, and other injury-receptive cell types, migrate to the

"injured" site, repair the damaged site. A primary means of communication to perform such actions comes in the form of circulating white blood cells who perform distinct roles in surveying the body for "non-self" or foreign entities, be they viral, fungal, or bacterial in nature. However, not all insults are foreign in nature, as tumor cells, those that have undergone some mutation, have the ability to evade detection, capture, or apoptotic self-elimination. Cytotoxic activity (natural killer and cytotoxic CD8-T-cells) mediate apoptosis of tumorigenic cells via surface recognition. Dysregulation of their cell cycle DNA replication program permits unregulated cell division and, thus, the persistence of a particular clonal population is ensured [25]. This self-renewal and high-proliferative capacity is reminiscent of hematopoietic stem cell characteristics [26]. Undermining immune surveillance, dysplastic tissue develops at a faster rate than that of normal tissue, with both normal and cancerous cells vying for resources to sustain themselves [27].

As mentioned, the bone marrow encases the largest pool of pluripotent stem cells. Organization of these distinct niches is dictated by available resources and proximity to concentrated populations of specific cells types, especially in the long bones. The mesenchymal stem cell has the ability to differentiate into osteoblastic cells that are responsible for bone formation. [15, 17, 19, 20, 28]. This is an attractive concept that recent research has been geared toward, particularly to promote osteogenesis by culturing on mechanically rigid substrates [29-35] and to aid in wound healing [36]. MSC differentiation towards higher-ordered tissue formation, such as bone and muscle, proceeds in response to mechanical signaling [33, 37] (Illustration 1). Because of this mechanosensitivity, the MSC plays a critical role in the homeostatic regulation of bone mass. Therefore, maintaining the composition of the marrow is essential to the preserving skeletal integrity.

Cancer cells, however, heavily disrupt the balance within the bone marrow microenvironment [27, 38-40] and its stem cell reservoirs. This space may be involved by certain primary and hematopoietic cancers, converting what was once a tightly regulated control center, to a microenvironment conducive to tumor growth. Both healthy and malignant cells within the bone marrow compete for the mass of sustainable blood supply and space, disrupting the bone remodeling process. The more highly proliferative cell type dominates this space. Tumor cells constitutively produce and secrete inflammatory cytokines and angiogenic factors, thereby,

engaging and facilitating the immune system to sustain their growth. Conversely, an immune response can also lead to tumor cell destruction.

3. Osteoporosis

Osteoporosis, the disease characterized by high incidence of porotic bone, loss of bone mineral density (BMD) and strength, can be observed in the elderly, post-menopausal, inactive patient population, or those under a large metabolic burden [41, 42]. The Center for Disease Control and Prevention cites osteoporosis as one of the most globally prevalent diseases. Influencing 1:3 women and 1:5 men over the age of 50. Osteoporosis accounts for 8.9M fractures annually, leading to increased susceptibility to secondary fractures of the forearm, hip, vertebrae, and femoral neck. Of these populations, post-menopausal women experience the greatest decrease in BMD. Densitometry measurements using dual-energy X-ray absorptiometry (DXA) and CT evaluations reveal dramatic decreases in bone mineral density and extreme reductions in bone quality, as evidenced by cortical thinning and loss of trabecular bone. On the microscale, mounting porosities are visible across the cortical shell. To demonstrate the severity of these losses, just a 10% reduction at the vertebrae can more than double the chance that a fracture will occur. Disuse as a consequence of physical inactivity, especially in the aging population, contributes immensely to the acceleration of bone loss. Additionally, post-menopausal women experience large reductions in ovarian production of estrogen, in turn lowering bone formation. Over time and in combination with reduced activity due to aging, osteoporotic bone develops as resorption outpaces formation, resulting in a net loss of bone, disposing these populations to increase fracture risks. Here, the coupled activity of resorption to formation becomes less efficient.

Estrogen is a hormone that plays an essential role in initiating bone formation [43, 44], mediated specifically at the cellular level through binding interactions with estrogen receptors α and β [45, 46]. These associations are gradually lost in the elderly, particularly in women. Deficits in systemic estrogen, which naturally occur in women whose ovaries (specifically, the theca interna cells) have exhausted their means of producing the hormone. Its absence is the catalyst driving osteoporosis in post-menopausal women and aging men. Ovariectomy studies on rats have demonstrated this very phenomenon that, in as little as one month post-ovarian resection, extensive adipose accumulation in the bone marrow and significant losses in bone density measures were made across the tibiae, vertebrae, and femora [47, 48].

Inflammation plays a strong role in the onset of osteoporosis. The factors contributing to these bone losses are largely a consequence of hematopoietic stem and progenitor cells involvement. As mentioned, inert growth factors and cytokines are embedded in the cortices of bone. Upon release, whether from trauma or excessive bone resorption, the cytokines embedded in the bone matrix become activated and can impart additional local or systemic inflammation, accelerating resorptive activity. Soluble inflammatory cytokines, such as TNF-α, IFN-γ, and IL-2, promote osteoclast activity, release of local reactive oxygen species, and creation of hypoxic environments which have a high concentration of bone dissolving molecules. Chronic inflammation, such as autoimmune conditions, increase rates of resorption thereby causing increased tissue damage.

4. Cancer-Induced Bone Loss

The high incidence of comorbidities that result as a byproduct of cancer and its accumulating array of treatment modalities, or simply in concert with age-related factors, demonstrates how systemically taxing cancers become **[49]**. Osteoporosis and cachexic wasting are also consequences of cancer, where metabolism is highly affected, disrupt bone turnover rates [49-51]. These consequences are further compounded and accelerated in those undergoing cancer-related treatment.

Widespread data on cancers demonstrate their catabolic effects on bone. Granulosa cell tumors of the ovary, a non-epithelial, stromal-derived cancer, involves excessive and then muted concentrations of estrogen. Specifically, granulosa cell neoplasia can occur in two disparate forms, either juvenile or adult, becoming extensively large and incapacitating [52]. In either case, both susceptible populations are inherently at risk of osteopenic outcomes [53]. Radiation treatments are typically administered to ensure the elimination of the tumorigenic cells [54]. This combined with reductions in serum-bound estrogen secondary to ovariectomy contributes to reductions in bone mass.

Neoplasias that are directly associated with the bone, some of which develop from osteoblasts (bone-forming cells) or chondrocytes (cartilage cells) and, still others, which are derived from cells residing within the marrow, are highly disruptive to bone and marrow. Of the

former, osteosarcomas and chondrosarcomas, tumors resulting from bone and cartilage, respectively [25], are dysplasias which develop in or near the epiphyseal growth plate, arising from tissues that are of mesenchymal origin. Leukemias, conversely, derive from mutations in blood cells that comprise the hematopoietic lineage and are detectable in the bone marrow. Despite recovery efforts, adolescents that have gone into remission from leukemia and glioblastoma, are often met with a lifetime of compromised skeletal integrity [55-59]. Women who have undergone treatment for breast cancer most often present with post-surgical bone deficits [60, 61].

Multiple myeloma (MM), a clonal expansion of malignant plasma cells, manipulates the local bone marrow microenvironment, promoting extensive bone resorption that outcompetes bone formation. An aggressive bone marrow cancer, MM is known to incite severe osteolysis, resulting in highly porotic bone and systemic toxicity [62, 63]. Cortical osteolysis and trabecular destruction compromise skeletal integrity, decreasing the skeletal system's ability to withstand loads. This reduction in bone density elevates risk of fracture to the long bones or vertebral compression, of which paralysis is a possible outcome.

Occult breast metastases have a high affinity to bone. Though not technically bone cancers, these lesions result from cancer cells that have invaded and metastasized from the primary tumor to bone where they adapt and thrive on the local environment. These metastasic lesions are so detrimental that they cause fracture rates and higher mortality rates in individuals versus death from the primary disease.

Each dysplasia detailed above account for a particular form of cancer-induced bone loss, developing a negative relationship with the surrounding bone and the marrow microenvironment. Addressing and mitigating the critical bone losses leading to osteoporosis, particularly through strategies already identified as safe and osteogenic, may help to reduce skeletal loss in patients with cancer.

5. Cancer Treatment Modalities: Contributors Compounding Osteopenia

Clinical treatment for leukemias and other forms of aggressive cancers consist of total body irradiation in order to reduce the tumor burden. This may be followed immediately by a bone

marrow transplantation. Total body irradiation causes destruction of whole blood, in turn lowering immunity, increasing delayed toxicity, and lowering the bone quality of the irradiated region by compromising its mineral content [64]. Irradiation also devastates the bone marrow microniche and its resident stem cell populations [65, 66], making recovery efforts more difficult to attain. Fractionated low-dose radiation treatments (a total of 20-30Gy delivered in 10 equal fractions) are used in most cases of MM, lytic lesions, or as necessitated for bone palliation [67]. High-dose radiation (>30Gy) is used in severe cases, such as when patients experience a spinal cord compression event, as the tumor burden and osteoclast activity within vertebral marrow has caused significant cortical destruction, resulting in collapsed load-bearing bone and potential nerve damage [68]. Following these treatment modalities percutaneous cement is used to prevent fractures in MM on load bearing bone [69]. These strategies are highly invasive and detrimental to skeletal integrity and marrow quality.

Suppressing the rapidly dividing tumor burden, while mitigating the mounting bone losses, is best achieved by adjuvant therapy. Combinational therapies are more effective forms of treatment than administration of any single drug or therapy. Total body irradiation and autologous stem cell transplantation (or simply bone marrow transplantation) are two such modalities that are used to control and reduce a growing tumor burden. Side effects come at the risk of ablating whole bone marrow and destroying bone progenitor and circulating blood cells, but the cumulative skeletal damage is a hidden consequence that patients do not easily, if at all, overcome.

Chemotherapy is most often prescribed for those with advance-staged cancers or those that are difficult to resect, but this results in extensive side effects due to low target-specificity and extensive toxicity [68]. Common side effects observed following chemotherapy include nausea, vomiting, extreme fatigue, and hair loss. There are, however, more extreme side effects of chemotherapy, as it is essentially altogether toxic to the body. For the non-epithelial stromal cell tumor of the granulosa cells, gross resection of the tumor is necessitated before chemotherapy is used. Once the bulk of the tumor is removed or the cancer is in a more advanced stage, platinum-based BEP (bleomycin, etoposide, and cisplatin) treatments are employed in 3-5 cycles to combat the residual tumor burden [70]. In the case of the bone marrow-based cancer MM, several other, more aggressive chemotherapy options are employed, in particular, the MPT option (Melphalan,

prednisone, and thalidomide) [71]. Melphalan, for example, is an alkylating drug used to treat chemo-resistant cancers [72, 73] (e.g. late-stage ovarian and plasmacytomas), yet in humans it is mutagenic, resulting in bone marrow damage and increased susceptibility to leukomogenesis [67, 74-76] and teratogenesis [77]. Thalidomide is an agent is prescribed for MM patients because of its potency, yet because of its lack of target-specificity, reports of nerve damage are prevalent. Two to four-drug combinations are used to varying degrees depending on the geographical region, such as lenalidomide, bortezomib, bendamustine, and vinicristine, amongst others [71]. Autologous stem cell transplantation, post-chemotherapy, is typically performed on fit individuals.

Pharmacological treatment strategies for CIBL are as extensive as they are mechanistically different. Bisphosphonates, are a class of oral and/or intravenous drugs that are prescribed to prevent osteoporotic-related bone losses, and in some cases, reduce metastatic lesions in bone-associated cancers. Specifically, pamidronate (*Aredia*) and zoledronic acid (*Reclast*), are indicated in those with extensive bone losses as means to prevent further bone loss, but they have been oft-cited with serious side effects, such as osteonecrosis of the jaw [68, 78, 79]. Anabolic treatments [80], such as parathyroid hormone (PTH; commercial name *FORTEO*), are designed to elevate osteoblast-mediated formation, though it has been strongly linked to increased risk of osteosarcomas in rats and several human cases over long-term use. Given the overwhelming risks assumed when undergoing cancer treatments, alternative strategies to encourage anabolic enhancement of bone and muscle through non-pharmacological means are heavily desired.

Remaining physically active is critical to maintaining bone strength and has been shown to promote an array of health benefits in the individual [81]. Exercise, a regimented form of physical activity, has long been prescribed as a means to maintain bone strength by imposing subtle loads across the skeleton and sustaining systemic health [82-84]. NIH guidelines state that regimented exercise of moderate impact at least five days a week can improve indices over a range of many disease types, from osteoporosis and Type II diabetes, to systemic inflammation and obesity [85]. It is commonly prescribed as a strategy to prevent bone loss and as a cancer preventative [84, 86-90]. Cancer-associated bone losses are critical clinical problems that are difficult for patients to endure and overcome, considering that the stresses imposed during regimented exercise may expose their fragility [86, 91].

Mechanical signaling has been demonstrated to significantly alter the morphology of bone [92, 93]. These forces are inherently present, at varying frequencies and magnitudes, during physical activity and aerobic exercise regimens. The high frequencies derived from the fast twitch, type-II skeletal muscles, are of specific importance. The summation of these muscle contractions on bone over time is sufficient to modulate bone remodeling activity. Tennis players, for instance, are known to have higher BMD in their dominant playing arm, resulting from the many small magnitude forces transmitted through the forearm.

As a non-pharmacological intervention, mechanical signaling may be an attractive route to retain bone formation without coupling to increases in the disease. As described, mechanical loading is essential in maintaining homeostatic regulation of bone health. Bone is naturally removed and rebuilt time and again in order to reestablish optimal loading capacity and to remove weak and diseased bone. Mechanical signaling may serve to regulate homeostatic bone remodeling activity, which includes periodic resorption and formation. Effects of this dynamic loading promotes osteoblast activity at certain magnitudes and frequencies and has been reflected in increased MSC activity [92, 94, 95] and bone formation markers amounting to significantly greater bone density and improvements in overall bone quality. This is accomplished through regulation of the *Wnt* signaling pathways, either directly or indirectly. *Wnt*/β-Catenin transduction is responsible for axial development, cell proliferation and migration, ovary development, sex cell development, and hematopoiesis, where β-Catenin translocated to the nuclear acts as a strong transcriptional regulator. Mechanical strain on bone is directly facilitated through the non-canonical arm of the *Wnt*/β-catenin signaling pathway (Illustration 1); however, these activities may indirectly modulate *Wnt* through the canonical pathway. Controversially, *Wnt* and other pathways are shared amongst the exercise and mechanical loading transduction pathways as well as with the signaling that is implicated in many cancer developments and metastases through mutations in *β*-catenin [96, 97]. With these commonalities in mind, broad guidance on the issue has been met with caution.

Recent work has shown that low magnitude (<5 microstrain) mechanical signals can be administered using low intensity vibrations (LIV) to act as a surrogate for exercise regimens [93].

Low intensity vibrations are a specific form of mechanical signal that recapitulates the high frequency content of muscle contraction with a force magnitude considerably lower (1000x) of that which is imposed on the body during moderate to vigorous exercise regimens [98]. Instead, uniaxial loading of a sub-gravitational (<1g) magnitude and high-frequency (30-90Hz) is administered using a stationary loading vibration platform. Slight oscillations along the z-axis (longitudinal) of the body at subtle magnitudes can safely reach the cervical vertebrae [92, 99]. This is accomplished without aerobic activity, yet it is osteogenic enough to observe bone retention in osteoporotic, post-menopausal women [100], disabled children [101], and in studies demonstrating its effect on strict bedrest [102, 103], and then upon reambulation [104]. In addition to bone, LIV has demonstrated efficacy in increasing muscle fiber density [105], improving balance measures in patients. While these anabolic effects have been shown [106], LIV has also been demonstrated to deter adipose accumulation [107], suggesting its utility in promoting not just any tissue, but primarily healthier tissue. *In vitro* studies provide supportive evidence that indeed MSCs are driven towards osteoblastogenesis and away from adipogenesis [108-110] after exposure to regimented treatments of low magnitude mechanical signals [111]. Indications of this at the cellular level show that mechanical control of cells occurs along the non-canonical β-Catenin signaling axis in a pro-osteogenic manner [8, 95, 112, 113]. Indeed, MSC exposure to LIV has been demonstrated to upregulate cytoskeletal regulators [114] and calcium deposition, perhaps akin to strain where mechanical forces increase actin fiber development and number of focal adhesions [115].

In considering LIV's anabolic tendencies toward MSC proliferation and differentiation, its use as a mediator of bone growth along β-Catenin in those with cancer is concerning. This apprehension is compounded when considering the data demonstrating MSC's controversial role in tumor progression as both a supportive [116, 117] and a deterrent [118, 119] element. Would administration of a mechanical signal preferentially increase osteoblastogenesis, without signaling for rapid expansion of the tumor? Further, does the mechanical signal reaching the MSC promote stromal expansion of the tumor? Additionally, are the MSCs that respond to the mechanical signal universally sensitive to particular frequencies and magnitudes that would drive one response over another? Since bone marrow-derived MSC's are responsive to LIV, do other cell types in the

marrow microenvironment respond to it as well, which may also have secondary effects on cancer outcomes?

In order to determine the ability of low intensity vibrations as a means to mitigate bone loss in models of cancer, two different models of cancer will be employed. Though the mechanism of bone loss secondary to disease progression is not expected to be equivalent across both diseases, LIV's effects on bone retention may provide an indication of its ability to non-exclusively mitigate these losses, independent of the means of the skeletal deficit.

The first model explored in these studies employs a crossbred strain of *SWR* mice that develop granulosa cell tumors (GCT) of the ovary. This strain of mouse spontaneously develops enlarged ovarian tumors, as they are genetically predisposed to the mutation in *gct1*. GCT's are classified as ovarian stromal tumors and are considered rare in humans, occurring in one out of every 200,000 people per year, comprising just 2% of all malignancies arising from the ovary [52, 53]. Despite the rarity in occurrence, if the ability to induce bone loss subsequent to disease progression is a systemic one, this may demonstrate the scope of LIV to combat these losses at multiple anatomical sites along the skeleton. More so, if the effects of GCT on bone loss are largely hormonal in nature and secondarily invoke resorption of bone (or inhibition of bone formation) across several pathways then the ability to drive osteogenesis using LIV while these catabolic or inhibitory factors are influencing bone, could indicate that the anabolic mechanisms of mechanical signaling act independently. Are low intensity vibrations capable of modulating hormonal activity as well as differential selection of MSC fate? Additionally, the spontaneity of the disease in this model allows us to understand whether LIV, as a known anabolic signal, precipitates the disease from those who are predisposed to its development. To these ends, if bone preservation can be observed utilizing LIV without contributing to provocation of tumorigenesis, then, perhaps the same outcomes are obtainable in a lytic cancer which directly interfaces with bone.

Countering systemic bone losses secondary to cancer progression in the first model is contrasted by the second model which was designed to address whether bone loss as a direct interaction of cancer cells with the bone interface can possibly be mitigated using mechanical signaling. Multiple myeloma and the plasmacytomas that engulf the bone marrow are highly lytic

lesions, as discussed previously, but the degree to which they influence these tissues in murine models has not been tested against low intensity vibration treatment. If indeed the aggressive bone losses that are anticipated in this model are mitigated solely by the administration of LIV, then the strong interactions that perpetuate localized bone resorption in multiple myeloma may be uncoupled or counteracted using this strategy. Further, the influence of regimented mechanical loading, perhaps by progressive stiffening of the cytoskeletal matrix, may suffice as an osteogenic signal to counter the bone resorption brought on by tumor cell interaction with the bone marrow microenvironment. The strong associations of stem and stromal cells with malignant cells drive the pathogenesis of MM. Understanding the how and where low intensity vibrations on the bone and elements of the bone marrow relative to viable tumor and healthy marrow may demonstrate their formative (or resorptive) effects on cortical and trabecular tissue. The colocalization of these outcomes with stem cells could further indicate the ability of LIV to bias stem cell fate towards osteoblastogenesis in parallel with cancer-induced bone resorption. Combined outcomes from these two models will provide extensive evidence as to whether LIV is limited to countering deficits in bone quantity and quality resulting from inactivity or obesity, or if, despite the nature of malignancy in promoting bone loss, encouragement of an osteogenic endpoint is obtainable.

Global Research Objectives

Mechanical signaling, in the form of low intensity vibrations, preserves bone mass in murine models of cancer by altering the bone marrow microenvironment without compromising host survival.

Specific Aim 1: *Determine the extent to which low intensity vibrations (LIV) influence survivability while preserving bone mass in a spontaneous murine model of cancer.*

Sub-hypothesis 1a: Systemic bone loss will be observed following 1y of disease progression.

Sub-hypothesis 1b: Administration of LIV over 1y to a mouse model genetically predisposed to ovarian cancer will not adversely affect survivability.

Sub-hypothesis 1c: Bone will be preserved in LIV-treated animals, in contrast to the losses observed in AC, following the 1y administration of LIV.

Specific Aim 2: *Determine the effects of low intensity vibrations (LIV) on survivability while preserving bone mass in a multiple myeloma induced-murine model of symptomatic plasmacytoma.*

Sub-hypothesis 2a*:* Osteolytic lesions, systemic bone losses, and disruption of the bone marrow phenotype will be observed in diseased animals at 8w post-injection of human multiple myeloma cells.

Sub-hypothesis 2b: Animal survivability will not be negatively impacted by the 8w administration of LIV to mice engrafted with human multiple myeloma cells.

Sub-hypothesis 2c: Cancer-induced bone losses observed in disease animals will be mitigated following 8w of LIV-treatment.

Chapter 2: Mechanical Signaling Mitigates Bone Loss without Affecting Survivability

Introduction

Cancer progression is often complicated by rapid declines in bone density. This osteopenia is exacerbated by the catabolic pressures of irradiation, immunosuppressive therapy following bone marrow transplantation, or chemotherapeutic interventions, placing the individual at an elevated risk of fracture [58, 61, 66, 120-123]. Just as exercise is considered an effective means of reducing the risk of cancer [82, 86-88, 124, 125], sedentary individuals are at an increased risk of developing tumors at a wide range of anatomic sites [88, 126, 127]. Both cancer and its treatment regimens disrupt adult stem cell reservoirs residing in the bone marrow, populations essential to maintaining and regenerating injured tissues and organs, further suppressing the ability to repair damaged connective tissue [66, 128-130]. Taking advantage of the skeletal system's inherent sensitivity to mechanical stimuli [1], recent evidence indicates that low-magnitude, high-frequency mechanical signals induced via low intensity vibration (LIV) are anabolic to bone, perhaps serving as an exercise surrogate by introducing the spectral content of muscle contractibility into the skeletal system [92, 94, 95, 131-133]. This spectral content consists of a specific magnitude and frequency of mechanical force that skeletal muscle exerts on bone during load-bearing activity. To some degree, the osteogenic nature of these mechanical signals is realized by biasing bone marrow-derived MSCs towards osteoblastogenesis, while suppressing the formation of adipose tissue in fat pads and within the marrow [107, 111, 114, 134]. Conversely, sedentary individuals, the infirm, or those subject to disuse due to injury, shift the fate of the bone marrow progenitor pool towards adipogenesis [94, 131, 134], undermining the pool of cells that contribute to skeletal mass and regeneration [135-137]. These preclinical and clinical data indicate that the absence of mechanical signals potentiates a “default” pathway of fat formation, while physical stimuli, such as exercise, can encourage lineage commitment to higher order connective tissues, including bone, muscle, ligament, and tendon.

The capacity of exercise in general, and LIV in particular, to be anabolic to bone suggests that mechanical signals may be a suitable means of protecting bone from the catabolic consequences of cancer and its therapies. However, considering the capacity of LIV to influence

stem cell activity in the bone marrow [111, 134, 138], it is also reasonable to raise concern that these mechanical signals may enable the formation of a stromal framework of solid tumors [139-142], thus, facilitating progression of the disease. This concern is magnified at the molecular level, where β-catenin, through its cytoplasmic association with the intracellular domain of E-cadherin, serves to partially mediate *Wnt*/β-Catenin osteoblastogenic signaling in response to mechanical signals [8, 95, 113, 143-146], yet, as an oncogene, it is implicated in a wide array of human cancers [96, 117, 147-149], mediating roles in the cell cycle and in epithelial-to-mesenchymal transition (EMT) [142, 150]. Further, the MSC itself is suggested to be a key component of the 'tumor microenvironment", with evidence for a role in both suppressing [118, 119, 151, 152], and promoting [116, 117, 153, 154] tumor growth. Recent work from Mclean et al. (2012), which considered MSC harvested from human epithelial ovarian microenvironments showed, in comparison to non-pathological MSCs, that cancer-MSC were able to enhance ovarian tumorigenesis [155]. This suggests that mechanical regulation of MSC commitment could have far-reaching effects on cancer growth, both by driving MSC towards the formation of bone, and/or influencing the progression of the tumor itself.

Materials and Methods

The experiments reported herein use a mouse model genetically prone to tumorigenesis to determine if the introduction of LIV compromises longevity, protects bone density, promotes tumor formation, and/or biases the fate of bone marrow-derived progenitor populations. The uniqueness of this mouse strain resides in the development of spontaneous granulosa cell tumors (GCT) of the ovary within ~30% of the population [156, 157]. Tumorigenic onset occurs at approximately 3 months of age, which then proceed to metastasize to the lungs and liver [156-158].

In order to assess the safety and efficacy of low intensity vibrations as a strategy in preserving bone in cancer models, 70 12w-old female mice (F1- *SWRxSWXJ-9*, The Jackson Laboratory) of a strain prone to spontaneously developing granulosa cell tumors of the ovary, were randomized into baseline control (BC: n=10), age-matched control (AC: n=30), and LIV (n=30). The latter of these groups received LIV via a vertically oscillating platform (0.3*g* +/- 0.025 @ 90Hz) for 15m/d, 5d/w over the course of 1y, while AC received mock treatment (i.e. vibration platform left unpowered). Longevity data for AC and LIV was tracked until the study sacrifice in order to address treatment influence on animal survivability. *Ex vivo* μCT analysis was performed to determine the extent of bone loss or retention across key anatomical sites. Flow cytometric analyses (FACS) was used to quantify progenitor and lymphocyte cell populations of interest throughout the circulation and marrow that may be "mechanosensitive". The number of primary and focal lesions were quantified to assess tumor burden and disease pervasiveness.

Animal Model

All experiments and procedures were reviewed and approved by the Stony Brook University Institutional Animal Care and Use Committee (IACUC). An F1 strain of 70 female, *SWRxSWXJ-9* mice (The Jackson Laboratory; Bar Harbor, ME), crossbred to create a *gct1* mutation, was chosen for its genetic propensity to develop spontaneous granulosa cell tumors at around 3 months of age. Tumorigenesis occurs naturally and spontaneously in these animals, meaning that no external pressures, such as those administered through chemical induction or cell line injection, were used at the beginning time point in the study. Importantly, acquiring the disease

is not a certainty in these mice. This mouse strain was selected for that very "attribute", to establish if the mechanical signals influenced the appearance of the disease and/or provoked an early death.

Environmental conditions remained at 12h light/dark cycles in a 20°C facility. Animals were housed individually, fed ad libitum, and weighed weekly. Distribution of animals into Baseline Control (BC), Age-Matched Control (AC), and Low Intensity Vibration (LIV) groups were determined using a *Matlab* program that specifically randomizes large sample sizes by weight matching.

Daily Mechanical Loading Protocol

The daily loading regimen consisted of placing animals into individual 12cm × 12cm containers on a fixed, vertically-oscillating platform (modified from *Marodyne Medical*; Lakeland, FL) to administer the LIV signal; 90Hz for 15 min/day for 5 days/week at 0.3g ± 0.025 (where 1g = Earth's gravitational field, or 9.8m/s^2). The displacements necessary to cause such accelerations at this frequency are less than 100μm, and are barely perceptible to human touch. AC underwent identical handling and loading protocols as LIV, but without the platform being activated. Animal age at the beginning of the experimental protocol was 3 months, with the goal of extending the experiment for 1 year (15 months of age). Other than determining survivability curves, no data from AC or LIV mice that died naturally during that one year experimental period were used in the analyses listed below.

Tissue Harvesting and Pathological Analyses

Mice surviving the 1 year experimental protocol were first anesthetized using isoflurane inhalation, at which point whole blood was collected via cardiac puncture, heparinized and aliquoted (100μl), followed by erythrocyte lysis (1× Pharmalyse; *BD Biosciences*, San Jose, CA) for FACS analysis. Euthanasia was completed by cervical dislocation. Right tibiae and femora were removed from each mouse and stored in 70% ethanol (EtOH). Marrow from left tibiae and femora were preserved in Dulbecco's modified eagle's medium (DMEM) containing 2% FBS, 10mM HEPES Buffer, and 1% penicillin–streptomycin (DMEM$^+$) for FACS analysis. Tissues for histological staining, including excised tumors, were fixed in 10% neutral buffered formalin (NBF), replaced at 48h with 70% EtOH. Tissue samples of interest were sectioned and processed

in 10% NBF. 5μm, paraffin-embedded tissue sections were stained with hematoxylin and eosin (H&E). After deparaffinization, antigen retrieval was performed in citrate buffer (20 mmol/L (ph 6.0)) at 120˚C for 10min in a Decloaking Chamber. Sections were incubated using mouse monoclonal anti-calretinin (Cat. Number 610908; *BD Biosciences*; San Diego, CA), diluted 1:100, and mouse monoclonal CD45 staining (Cat. Number 550539; *BD Pharminogen*; San Diego, CA), diluted 1:20, followed by detection of an avidin-biotin based system (Vectastain ABC) and development with 3, 3′-diaminobenzidine. After dilute hematoxylin counterstaining, sections were dehydrated and coverslipped for bright-field microscopy. Negative controls were performed by substituting the primary antibody solution with TBST buffer. Diagnosis of granulosa cell tumors by histologic examination was confirmed by immunohistochemical staining using calretinin (*Abcam*; Cambridge, MA), a molecular marker that is known to be widely expressed in GCT's. To confirm sites of leukocyte recruitment, CD45 staining (Cat. Number 550539; *BD Pharminogen*; San Diego, CA) was also performed. All analyses were performed blind to the experimental group each animal was in by a trained histopathologist (Kenneth R. Shroyer, M.D., *Stony Brook Medicine*).

Flow Cytometry

Flow cytometric analyses employed the use of a FACSAria cytometer (*BD Pharminogen*; San Diego, CA). Fluorescent antibody tagging utilized specific markers (*BD Pharminogen*; San Diego, CA) for hematopoietic precursors, MSCs, and immunogenic tissues. Flow cytometry data reported for AC and LIV groups represented the average of all cell populations quantified separately for each animal, processed individually for a single marker. For each sample, cells were homogenized and dissociated from their respective tissues in 3mL of $DMEM^{+}$ in order to maximize cell viability before tissue processing. Subsequent washing steps consisted of the addition of DPBS and centrifugation (4°C, 2000rpm, 10min). $2x10^{6}$ cells from each tissue (with the exception of blood) were quantified individually from each animal using an automated cell counter (Scepter, Millipore; Billerica, MA), fixed with 1% neutral buffered formalin (NBF) in Hank's buffered salt solution (HBSS), and stained for specific hematopoietic markers. Specific leukocytes ($CD3^{+}$, $CD4^{+}$: helper T-cells; $CD3^{+}$, $CD8^{+}$: cytotoxic T-cells; $CD3^{-}$, $CD19^{+}$: B cells; $CD11c^{+}$: dendritic cells; $CD335^{+}$: natural killer cells) were quantified based on staining for distinct surface markers. Sca-1^{+}, c-kit^{+}, $CD90.2^{+}$, $CD105^{+}$ and $CD44^{+}$ were designated as unique MSC cell surface

identifiers and populations positive for all five markers were sub-gated accordingly [111, 159, 160]. Hematopoietic stem cells (HSC's) were quantified using known "LSK" markers (Lineage^{-}, Sca-1^{+}, and c-kit^{+}) in conjunction with side population (SP^{LSK}) staining (Vybrant Dyecycle Violet, *Invitrogen*; Rockville, MD) [23, 161].

Micro-computed Tomography

A range of bone morphology parameters of the proximal tibial metaphysis and L5 vertebrae was quantified *ex vivo* using high-resolution X-ray micro-computed tomography (μCT, *Scanco Medical*; Wayne, PA). These included bone volume (BV), bone volume fraction (BV/TV), trabecular number (Tb.N.), thickness (Tb.Th.) and spacing (Tb.Sp.), and structure model index (SMI) [162].

Proximal Tibia

Beginning 300μm distal to the growth plate, 1200μm of the metaphysis was evaluated at 12μm resolution and 55keV intensity settings. A threshold for each slice was set exclusively for cortical and trabecular bone using an automated script [163]. The reconstructed solid 3D images were then used to quantify bone microarchitecture.

L5 vertebrae

A 400μm cylindrical sample of trabecular bone from the center of the vertebral body (diameter = 0.8mm; height = 0.4mm; composed of 40 slices at 10μm intervals) at 10μm resolution and 70keV intensity settings. The reconstructed slices generated a 3D rendering used to quantify microarchitecture as a representative region of the spine. The axial skeleton was not harvested from BC, so baseline comparisons for L5 could not be made.

Statistical Analysis

Significance ($p \leq 0.05$) between LIV and AC groups, and between healthy and those animals with visible evidence of tumor pathology upon gross dissection, was determined using Student's *t*-test. One-way ANOVA was used for μCT analysis for baseline control and Tukey's post hoc with a significance of $p \leq 0.05$. The Mann–Whitney test was used to determine the statistical significance of nonparametric data. A Kaplan Meier Survival Analysis was performed

to determine if there was a difference in longevity between LIV and AC. Chi-square tests were performed to determine if the LIV signal influenced the number of animals with tumors relative to AC, and if LIV influenced the number of organs with pathology relative to those in AC.

Results

Longevity

Over the course of the study, 8 animals were lost within the LIV group (27%), while 10 were lost in AC (33%), indicating similar survivability over the 1 year course of the study (Fig. 1; p=0.62). Unless otherwise noted, data from animals that died over the course of the study were not included in the analysis.

Bone Morphology

Micro-CT analyses of the proximal tibia indicated that trabecular bone volume (Tb.BV) and bone volume fraction (Tb.BV/TV) in the 64w old AC had decreased by −47% ($p<0.01$) and −45% ($p<0.01$), respectively, from 12w BC (Fig. 2). In contrast, Tb.BV in 64w LIV mice was +25% greater ($p<0.03$) and Tb.BV/TV +24% higher ($p<0.02$) than AC. In the axial skeleton, Tb.BV was +15% ($p<0.03$) and TV.BV/TV was +16% higher ($p<0.02$) in the L5 vertebrae of LIV mice as compared to AC (Fig. 3). Within the same region of the L5 vertebrae, the structure model index (SMI) was 40% ($p<0.01$) more plate-like in LIV than AC. No significant differences between AC and LIV were observed for trabecular number (Tb.N.), trabecular thickness (Tb.Th.), or trabecular spacing (Tb.Sp.). No differences were measured in cortical bone indices.

Histology and Pathology

Animals bearing mature granulosa cell tumors (GCT) were readily identifiable due to distension of the abdomen. Upon dissection, the most prominent of all lesions were the primary solid ovarian tumors. Solid and cystic ovarian tumors measuring up to $8mm^3$ were noted. Histological examination of the tumors revealed sheets of cells with central necrosis, nuclear grooves, Call-Exner bodies, and numerous mitotic figures. Immunohistochemical staining confirmed that these lesions were calretinin$^+$ and CD45$^-$, consistent with the diagnosis of granulosa cell tumors (Fig. 4) [53, 157]. Mature ovarian tumor growth extended from the pelvic cavity into the abdominal cavity. Gross examination of the excised, mature GCT typically revealed adhesion to the kidneys and occasional extension to the thoracic spine.

Upon further inspection of the abdominal cavity, those animals with visually evident tumors were also noted to have enlarged lymph nodes along the subcutaneous lymphatic vasculature adjacent to the hind-limb musculature, the mediastinum, and in the inguinal regions. Enlarged LN's were found in the para-aortic regions as well but not to the extent as those of the peripheral LN's. Histological examination of the lymph nodes revealed metastatic granulosa cell tumors with focal necrosis.

Combining the overall incidence of primary tumors and metastatic lesions in the ovaries, peripheral and aortic lymph nodes, liver and lung, this pathology pervaded 54% of AC mice, while evident in 38% of LIV that survived to 15 months of age ($p=0.27$). Though non-significant, trends were identified in those mice with pathology evident in multiple organ systems (i.e., liver, ovary, and lung), which was approximately 45% lower in mice subject to the LIV signal ($p=0.09$). There was no discernible, qualitative site-specific difference in sites of tumor metastasis or tissue pathology between the groups.

Flow Cytometry

At the end of the protocol, the 1 year total cell counts quantified from the marrow of AC and LIV were 12.5×10^6 and 11.5×10^6 cells, respectively, while healthy mice vs. mice with pathology contained 12.3×10^6 and 11.5×10^6 cells, respectively (nsd). Based on the five positive cell surface markers, marrow populations enriched for MSCs were −52% lower ($p=0.01$) in LIV mice as compared to AC (Fig. 5a, Table 1). Regardless of treatment group, comparing MSCs in mice with no visible pathology versus those containing gross pathologic tissues showed a trend of being −31% lower (Fig. 5b; $p=0.08$). The lower number (−8%) of HSC-enriched populations in the bone marrow of LIV as compared to AC mice was not significantly different ($p=0.25$; Table 1). Flow cytometry data was not processed at baseline and, therefore, could not be used for comparison (simultaneous processing was not possible).

Mice with Pathology: LIV vs. AC

In an effort to evaluate the influence of mechanical signals on those animals with evidence of the disease, both bone and MSC parameters were compared between AC and LIV mice with visual evidence of tumor pathology. Tb.BV/TV of the tibiae and of the L5 vertebrae of LIV mice

bearing pathology showed evidence of a trend towards being higher than AC mice with pathology (+17%, $p=0.12$; and +13%, $p=0.29$, respectively; Fig. 6). The population of MSC's quantified from the hindlimb BM of LIV remained significantly lower than AC by −60% ($p<0.04$).

Discussion

Osteoporosis, a common co-morbidity of cancer [55, 61, 164-166], is often exacerbated by aggressive chemo- and irradiation-therapies [41, 55, 58, 66, 167]. Cancer-associated declines in bone strength ultimately increase the risk of fracture, while disease or treatment-based disruption of the bone marrow stem cell pool can compromise tissue repair processes [168]. While antiresorptive agents (e.g., bisphosphonates) have helped cancer patients to mitigate these losses [169-171], concerns arise regarding long-term complications, including cases of osteonecrosis of the jaw [78, 79, 172, 173] and atypical fractures of the femur [174]. Further, the skeletal benefits of using anabolic agents may not balance concerns surrounding their role as a potential promoter of neoplastic cell expansion, and thus, their use is restricted [80]. In some contrast to pharmacologic strategies, physical activity is universally promoted as a means to help preserve bone density [175]. Unfortunately, the very nature of cancer and/or its treatments is such that participating in even a mild exercise regimen can be difficult [91] and, during extreme bone loss, such as those resulting from osteolytic lesions, might precipitate the very fracture it is intended to prevent.

Mechanical signals both large (resulting in > 2,000 microstrain at the bone surface) and small (< 10 microstrain) [92], several orders of magnitude below those generated by strenuous activity [176], can positively influence bone mass, even under the added duress of disuse [104]. These mechanically-mediated enhancements in bone density are achieved, at least in part, by biasing the MSC population towards formation of skeletal tissue and away from adipose accumulation, most notably by driving MSC differentiation through the *Wnt/β*-catenin pathway [16, 110, 112, 114, 134, 138, 177].

To consider the use of mechanical signals as osteoprotective agents while combating cancer, whether or not in concert with cancer treatments, care must be taken to ensure that tumor growth is not accelerated. To this point, β-catenin – a key mediator of mechanically induced bone remodeling – is known to have a role in tumor growth and metastasis [96, 117, 147, 178]. The data presented here indicate that brief, daily exposure to extremely low magnitude mechanical signals helped to preserve bone density but did not compromise survivability or promote disease progression in mice with a high propensity for the spontaneous development of GCT.

Supporting previous studies which reported the ability of LIV to protect bone morphology [179, 180], both the trabecular bone volume and bone volume fraction indices of the tibiae and vertebrae in LIV mice were significantly higher than that measured in their AC counterparts. The structure model index (SMI), an index of bone quality [162], indicated that the LIV signal protected trabecular architecture as more plate-like, than rod-like structures, a morphology considered to be stronger and more resilient to fracture [84].

These studies also indicate that the fate of certain bone marrow-derived mesenchymal lineages can be influenced by mechanical loading, with a lower fraction of MSC being measured in bone marrow of the LIV mice as compared to the AC. In parallel, a trend was observed in that MSC-enriched populations were higher in the bone marrow of those mice bearing visible pathology – whether AC or LIV – as compared to those mice lacking tumors evident upon dissection.

The emphasis of the data presented here has been on the comparison of LIV vs. AC mice and determining if the osteoregulatory potential of mechanical signals also promoted extent of the disease. Nevertheless, as anticipated, mice from each group succumbed to the disease through the 12-month protocol, and (AC: n=9, LIV: n=7), showed evidence of pathology when examined at 15 months of age. When considering only those mice with pathology, there was a trend, though not statistically significant, towards higher bone density in the tibia and spine of the LIV group as compared to AC, paralleled by a significantly lower level of MSC in the bone marrow. Whether the lower MSC is simply correlated to a lower tumor burden in the diseased mice, or is actually responsible for the suppression of pathology, cannot be concluded from this study. Nevertheless, when considered with the longevity data, these results suggest that mechanical signals – which perhaps serve as a surrogate to exercise – represent a non-pharmacological means of protecting bone structure in those susceptible to cancer – and those which carry the disease – without enabling the disease itself.

The contributing role of MSC to the "tumor microenvironment" is controversial, with evidence for both promotion and suppression of tumor progression [151, 153]. In the case of epithelial ovarian carcinoma, not only are MSC "universally present" in human ovarian cancer, but these cancer-associated MSCs promoted the growth and abnormal characteristics of co-

cultured ovarian cell lines *in vitro* [155]. Our data suggests that, not only do mechanical signals have the capacity to suppress MSC number in the bone marrow, but that a corollary is also true — that an increasing tumor burden is associated with an elevated MSC progenitor pool. Importantly, the reduction of the MSC pool by the mechanical signals in the LIV group at 1 year was achieved without affecting HSC levels, indicating that this was cell specific, and not a systemic response per se. As such, the capacity of exercise in general, or mechanical signals distilled from the exertion, may reduce tumor progression by potentially limiting ongoing interactions between MSC and cancer stem cells, while biasing MSC fate towards higher order connective tissues such as bone.

As an indication of the spread of the disease, separate metastatic foci were quantified revealing that enlarged aortic lymph nodes were actually metastatic foci, contributing further to tumor pervasion in addition to the primary ovarian tumors. A role for the suppression of tumor growth by mechanical signals was further supported by a trend of reduced tumor number in the LIV mice, as compared to AC, and the lower number of LIV mice with disease that involved more than one organ system. These data taken in combination with decreased levels of MSC-enriched populations observed in LIV mice are interpreted as a possible reflection of the benefits of exercise in reducing disease pathogenesis, perhaps by driving MSC differentiation towards higher-ordered connective tissue, such as bone or muscle, thus hindering their contribution to the stromal framework of neoplastic tissue. This perspective is supported by clinical evidence that sedentary and/or obese individuals are more susceptible to cancer [127, 181, 182], indicating that the absence of mechanical signals is permissive to the formation of adipose and neoplastic tissues. Perhaps, in the absence of the regulatory signals commanded by mechanical stimuli, the ability of progenitor populations to proliferate and spread in an undirected manner remains unheeded and unchallenged.

There are a number of limitations in this study, including that the model itself does not approach 100% onset of tumorigenesis for all animals within 15 months of age (i.e., 66% of AC suffered from pathology). As the goal of the study was to determine if the mechanical signals promoted appearance of the disease, this uncertainty was considered an attribute of the model, allowing us to compare not only effects on longevity, but on incidence. It should also be pointed out that the lineage selection (FACS) data were only compared at the endpoint, with no comparison to baseline measures. While this would have provided a strong index of change, confidence in

FACS measures is typically derived from measures made at the same sacrifice date, using the same reagents; something that was not possible given the difficulty of breeding these mice. Importantly, this study reports only the bone loss which occurs with 15 months of aging, rather than the bone loss which may be compounded by chemical or irradiation treatment for cancer, interventions which are certain to accelerate this loss [65]. Nor was the bone lost with age compared to that which might have occurred in a WT control. Nevertheless, the LIV signal did help protect bone quantity and quality in the skeleton, relative to the untreated age-matched controls.

Given the bone morphology measures that were made, we are not able to conclude if this mechanical protection of the skeleton was realized by an increase in bone formation, a suppression of bone resorption, or a change in levels of bone turnover. As this is an ovarian cancer, however, fluctuating hormone levels, such as that of estrogen derived from dysplasia, might contribute to variances in normal trabecular bone remodeling, a point of consideration for future work in elucidating the underlying mechanism-of-action. Severe osteolysis that is observed in occult breast skeletal metastases and primary lesions of multiple myeloma, do not appear in this model.

Conclusion

In summary, using a mouse model of spontaneous granulosa cell ovarian cancer, low magnitude mechanical signals, induced non-invasively using low intensity vibration, mitigated the long-term loss of bone relative to age-matched controls. This skeletal endpoint was achieved without compromising survival. Further, the decreased tumor burden, considered in concert with significantly lower mesenchymal stem cell populations measured in the bone marrow of LIV mice, suggest that both the skeletal and disease benefits of mechanical-based interventions, including exercise, may involve biasing these progenitors towards higher-order connective tissues such as bone. Considering the brief exposure and low magnitude of these mechanical signals, these preliminary data support the potential of low intensity vibration as an intervention to mitigate bone loss in cancer patients, particularly those that are infirm or are inactive. Further, these objectives were safely met and achieved without the aid of pharmaceutical intervention. Demonstration of these aims against other cancer models, especially those that interact directly with bone remodeling mechanisms, may advocate the drive towards preclinical efficacy.

Chapter 3: Mechanical Signaling Influence on Bone Marrow Cancer

Introduction

In the United States, the risk of acquiring the primary bone cancer multiple myeloma (MM) over the course of one's lifetime is 1 in 149 (0.67%) [183]. Although globally very rare, MM is statistically regarded as the 2nd most prevalent hematologic malignancy [25, 184], representing approximately 10-15% of all hematologic cancers [71]. The American Cancer Society estimates that during 2014 approximately 24,000 new cases will be diagnosed in the U.S., over half of which will be male [183]. While therapeutic interventions are presently prolonging lifetimes (a 35% 5-year survival rate), the mortality rate is still 11,000 per year; therefore, few, if any, patients outlive the disease. The defining comorbidity associated with multiple myeloma is the extent of osteolysis observed in patients, thereby reducing overall skeletal quality, increasing fracture susceptibility, and degrading quality-of-life. Disease onset also has a profound effect on the immune system as resident hematopoietic populations falter in the wake of cancer's onset.

MM is characterized by a marked increase in plasma cell proliferation which devastates skeletal tissue, ultimately usurping the bone marrow and, in the process, causes unrestricted bone resorption that results in osteolysis [62, 63, 184] (Illustration 5). Dissemination of these cancerous cells leads to diffuse infiltration throughout other marrow spaces, forming osteolytic lesions and destruction of healthy marrow. Neoplastic cells develop a unique interaction with their environment, as MM is primarily marrow-centric and is surrounded by resources that are vital to sustaining the cancer [38, 39]. Specifically, this bone marrow microenvironment transforms into a tumor supportive niche, and progressively fewer attributes of its original functionality, such as a site for bone remodeling and of hematopoiesis, remain over the course of tumor persistence. Self-sustaining autocrine and paracrine feedback mechanisms in concert with MSCs, HSCs, and osteoclast mediators of bone resorption facilitate this transformation [38, 63, 184]. Here, osteoblast activation (i.e. bone formation) is suppressed [184] through the secretion of dickkopf-1 (DKK-1), preventing the secretion of osteoprotegerin (OPG) which typically acts as a decoy protein for RANKL (in homeostatic regulation of bone remodeling). Instead, the secretion of RANKL from MM cells binds to osteoclast-bound RANK at high concentration, upregulating bone resorption. Extensive osteolysis occurs via osteoclast-mediated resorption, progressively thinning the cortical

shell and dissolving trabecular bone and predisposing the patient to increased fracture incidence. Once the supportive capacity of the marrow to promote plasma cell proliferation has been exceeded, MM plasma cells enter the circulation and migrate to other suitable tissue sites. Metastatic attachment to distant tissue and organs increase sites of tumorigenesis, compounding the systemic tumor burden and elevating osteolytic outcomes.

Both plasmacytomas and "monoclonal gammopathies of undetermined significance" (MGUS) are clinically premalignant, asymptomatic B cell dysplasias, which do not necessarily become, but do precede all, myeloma cases. Multiple myeloma diagnoses are confirmed on the basis of four primary symptoms; "C.R.A.B." being the clinical acronym used to identify each of the major symptoms (C = Hyper**C**alcemia; R = **R**enal dysfunction; A = **A**nemia; B = Lytic **B**one lesions). Hypercalcemia refers to the detection of higher-than-normal levels of calcium in the blood and urine. Saturation of calcium in the blood and kidneys is the result of the severe osteolysis instituted by osteoclast resorption of cortical bone. Renal dysfunction, another by-product of multiple myeloma, occurs as a result of both light-chain cast nephropathy and higher-than-normal creatinine levels, a condition onset by flooding of the blood and urine with monoclonal free light chains and calcium and the kidneys' inability to clear them. As a result of plasma cell infiltration into the marrow, the native hematopoietic cells of healthy marrow (erythrocytes, lymphocytes, and granulocytes) are outcompeted for space and resources, conferring anemia, leukopenia, and neutropenia on an ailing immune system. In addition to the extreme skeletal losses contributing to fracture the patient is, therefore, also at an increased susceptibility to infection and decreased capacity to reduce the tumor burden occupying the marrow space. Treatment strategies range from high-dose chemotherapy to fractionated radiotherapies [67, 68].

Reduction in tumor burden is critical in mitigating skeletal events. Irradiation is an effective approach to combat plasma cell expansion [68] due to the radiosensitive nature of the cells. Subsequent to these radiotherapies, autologous or allogeneic bone marrow transplantation is required, which brings the likelihood for secondary side effects, such as graft-versus-host disease, acute myelodysplastic leukemia, or myelodysplastic syndrome [75, 185, 186]. Immunosuppressives, such as corticosteroids, are administered to mitigate autoimmune reactivity and permit greater tolerance of a graft.

Chemotherapies are used clinically to address the tumor burden; however, renal toxicity is a byproduct and can lead to impairment of erythropoiesis, further contributing to the anemia occurring as a result of the tumor burden in the marrow [67]. Both anti-resorptives (bisphosphonates) and pro-anabolics (PTH) are used to mitigate bone loss or promote bone growth, respectively. Targeting of bone loss using bisphosphonates secondary to disease progression is limited by inconsistent results and undesired side effects. Osteosarcomas have been contraindicated following use of pro-anabolic drugs (FORTEO) designed to treat osteoporotic bone, thereby limiting its utility in treating cancer-induced bone loss.

Mechanical loading plays a large role in regulating tissue anabolism. Since exercise is a largely recognized as a deterrent of cancer and as a means to maintain musculoskeletal strength, prescribing it as an effective strategy seems the obvious choice. However, in the case of patients with multiple myeloma, even a moderate exercise regimen can facilitate a skeletal event. In an effort to incorporate non-pharmacological strategies for those with reduced skeletal loading capacity, low-intensity vibrations (LIV), a mechanical signal recently demonstrated to preserve bone in a murine model of ovarian cancer without accelerating the disease [187], was hypothesized to mitigate bone losses resulting from multiple myeloma. LIV has been demonstrated to encourage healthy, higher-ordered tissue synthesis, such as bone and muscle, meanwhile reducing the instance of lower-ordered tissue development.

Rodent knockout strains offer the ability to model diseases utilizing mutational defects in their immune surveillance [188-191]. Specifically, immunodeficient mouse models now offer wider ranges of compromised hematopoiesis, making human cell line xenografts with the intent to mimic diseases, increasingly consistent. Severe combined immune deficient (SCID) murine models, specifically in mice, are genetically engineered to exhibit defects in T and B cell lymphocyte development and function [189, 190, 192-195]. Immortalized human cancer cell lines have also provided the opportunity for *in vitro* diagnostics, particularly for drug-cell interactions as simulations and preliminary efficacy. Mimicking the clinical manifestations of multiple myeloma in a rodent model promoted drug-based testing against progression of the disease. We hypothesized that with this reduced immune surveillance, successful engraftment of a human cell line could occur in a murine marrow cavity, proliferate, and institute the disease consequences that occur following plasmacytoma development in human.

Materials and Methods

Animal Model

In order to investigate the role of low intensity vibrations in mitigating bone loss during the early onset of a primary bone cancer of the marrow, U266β1 (TIB-196, *ATCC*) human multiple myeloma cells were engrafted via intravenous injection into immunodeficient mice (NSG, *The Jackson Laboratory).* Distribution of animals into Baseline Control (BC), Age-Matched Control (AC), Myeloma-Injected (MM), and Myeloma-Injected plus Low Intensity Vibration treatment (LIV) groups were determined using a *Matlab* program that specifically randomizes large sample sizes by weight matching. While tracking animal survivability throughout the 9w-study period, disease induction efficacy was validated using FACS analysis and histological comparison of saline-injected controls against U266β1-injected animals. An injected ("diseased") group incorporated a low intensity vibration-regimen. These signals were administered to LIV mice for 15m/d, 5d/w (0.3*g* ± 0.025 @ 90Hz), while AC and MM mice received mock LIV treatment (i.e. vibration platform left unpowered). AC mice also underwent mock-injection using saline. Animal survivability was tracked throughout the study period and analyzed at its conclusion, as to whether there is any significant deviation between MM and LIV. At sacrifice, comparisons were made to determine the extent of plasmacytoma infiltration and the impact of disease and mechanical signaling on marrow populations housed in the hind-limb using FACS analysis. Evaluation of disease institution and sites of abnormal bone resorption were assessed using μCT and histological analyses.

Cell Culturing

A cryogenically preserved human-myeloma cell line "U266β1" (*ATCC;* Manassas, VA) was subsequently thawed at 37˚C for approximately 2min and immediately transferred to 9mL of growth media (RPMI-1640, *GIBCO*, supplemented with 10% FBS and 1% penicillin/streptomycin) using aseptic techniques. Centrifugation of the sample (4˚C, 125g, 6min) was performed in order to retrieve a cell pellet and remove dimethyl sulfoxide (DMSO) from the media. Pellet was resuspended in a 25cm^2 tissue culture flask with 10mL of growth media and incubated horizontally at 37˚C in a 5% CO_2 atmosphere in order to establish a healthy cell suspension. Cell viability was tested every 3 days using an automated cytometer (Countess;

Invitrogen) until cultures were confluent (~97% viability), at which time the suspension was centrifuged (24˚C, 2200rpm, 5min), resuspended, and split 1:3 into 75cm^2 tissue culture flasks. Subculturing of the U266β1 cells was maintained at a density of 3.5x10^5 and 1x10^6 cells/mL until injection.

Disease Induction

A study was designed to demonstrate efficacy in utilizing 7w-old immunocompromised mice (n=40; NSG, *The Jackson Laboratory*) to test whether a xenograft model of human myeloma could be successfully observed in a mouse via tail-vein injection following an 8w induction period. Briefly, 26 NSG mice were injected with a 0.3cc solution composed of 2x10^6 U266β1 cells suspended in sterile saline via tail-vein injection (1cc syringe, 27AWG needle), while baseline controls (BC; n=6) and age-matched controls (AC; n=8) were each saline-injected with 0.3cc of sterile saline. BC animals were sacrificed at study baseline (day of injection). Of the 26 myeloma cell-injected animals, 13 were subjected to 8w of low intensity vibration (LIV), while the remaining 13 received placebo-treatment (MM). All of the animals were restrained but injected into the dorsal tail vein without use of anesthesia by a trained veterinary-specialist (Jean Rooney, SBU Division of Laboratory Animal Resources).

Daily Mechanical Loading Protocol

The daily loading regimen consisted of placing animals into individual 12cm × 12cm containers on a fixed, vertically-oscillating platform (modified from *Marodyne Medical*; Lakeland, FL) to administer the LIV signal; 90Hz for 15 min/day for 5 days/week at 0.3 ± 0.025g (where 1g = Earth's gravitational field, or 9.8m/s^2). The displacements required to cause such accelerations at this frequency are less than 100μm, and are barely perceptible to human touch. AC and MM underwent identical handling and loading protocols as LIV but without the platform being activated.

Tissue Harvest and Preservation

For euthanasia mice were first anesthetized using isoflurane inhalation, at which point whole blood was collected via cardiac puncture, heparinized and aliquoted (100μl), followed by

erythrocyte lysis (1X Pharmalyse; *BD Biosciences*, San Jose, CA) for FACS analysis. Euthanasia was confirmed by cervical dislocation. Marrow from left tibiae and femora were briefly preserved on ice in Dulbecco's modified eagle's medium (DMEM) containing 2% FBS, 10mM HEPES Buffer, and 1% penicillin–streptomycin ($DMEM^{+}$) for FACS analysis. Tissues for histological staining, including kidneys, right tibiae, right femora, pelvis, right humeri, and whole spine were fixed in 10% neutral buffered formalin (NBF), replaced at 48h with 70% EtOH, and subsequently sectioned and processed in 10% NBF. Bone sections were initially treated with a decalcification solution (DECAL; *Decal*, Suffern, NY). 5μm paraffin-embedded sagittal cross-sections were then stained with hematoxylin and eosin (H&E). Diagnosis of multiple myeloma was made using pathological verification via histologic examination. All analyses were performed blind to the experimental group of each animal by a trained histopathologist (Kenneth R. Shroyer, M.D., *Stony Brook Medicine*).

Flow Cytometry

Flow cytometric analyses employed the use of a FACSAria cytometer (*BD Pharminogen*; San Diego, CA). Fluorescent antibody tagging utilized specific markers (*BD Pharminogen*; San Diego, CA) for hematopoietic precursors, MSCs, and immunogenic tissues. Flow cytometry data reported for AC, MM, and LIV groups represented the average of all cell populations quantified separately for each animal, processed individually for a single marker. For each sample, cells were homogenized and dissociated from their respective tissues in 3mL of $DMEM^{+}$ in order to maximize cell viability before tissue processing. Subsequent washing steps consisted of the addition of DPBS and centrifugation (4°C, 2000rpm, 10min). $2x10^{6}$ cells from each tissue (with the exception of blood) were quantified individually from each animal using an automated cell counter (Scepter, *Millipore*; Billerica, MA), fixed with 1% neutral buffered formalin (NBF) in Hank's buffered salt solution (HBSS), and stained for specific hematopoietic markers. $CD138^{+}/CD3^{-}$: Myeloma plasma cells; $CD11c^{+}/F4\text{-}80^{+}$: mature macrophages; and $NK1.1^{+}$: natural killer cells were quantified based on staining for distinct surface markers. $Sca\text{-}1^{+}$, $c\text{-}kit^{+}$, $CD90.2^{+}$, $CD105^{+}$ and $CD44^{+}$ were designated as unique MSC cell surface identifiers and populations positive for all five markers were sub-gated accordingly [111, 159, 160]. Hematopoietic stem cells were quantified from two populations using known "LSK" markers (Lin^{-}, $Sca\text{-}1^{+}$, and $c\text{-}kit^{+}$) (Illustration 4) in conjunction

with side population (SP^{KLS}) staining (Vybrant Dyecycle Violet, *Invitrogen*; Rockville, MD) [23, 161].

Bone Morphology

A range of bone morphology parameters and extent of bone loss of the proximal tibial metaphysis and distal femoral metaphysis were quantified *ex vivo* using high-resolution (10μm) X-ray micro-computed tomography (μCT40, *Scanco Medical*; Wayne, PA). These measurements included trabecular and cortical bone volume fraction (BV/TV); trabecular tissue mineral density (Tb.Mean1); trabecular number (Tb.N.), thickness (Tb.Th.) and spacing (Tb.Sp.); cortical thickness, porosity, and endosteal volume; and structure model index (SMI) [162].

Proximal Tibia and Distal Femur

Starting 700μm distal to the epiphyseal growth plate in the tibia and 700μm proximal to the epiphyseal growth plate in the femur, 1000μm of the metaphyseal regions were evaluated at 10μm resolution and 55keV intensity settings. A threshold for each slice was set exclusively to separate cortical and trabecular bone using an automated script [163]. The reconstructed solid 3D images were then used to quantify bone microarchitecture.

Statistical Analysis

Significance ($p \leq 0.05$) between MM and LIV groups alone as a function of pathological outcomes, was determined using Student's *t*-test. The Shapiro-Wilk test was used to assess the normality of the FACS and μCT sample distribution. One-way ANOVA was used for μCT analysis of AC versus MM and LIV if data was normally distributed. Kruskal-Wallis test was used to run a one-way ANOVA on non-parametric data. Tukey's post hoc test was used with a significance of $p \leq 0.05$.

Results

Survival and Behavior Analyses

Utilization of NSG mice engrafted with human myeloma cells were divided into 4 groups at 7w of age: baseline control (BC; n=6), age-matched control (AC; n=8), diseased (MM; n=12), and diseased mice treated with LIV (LIV; n=13). No visible signs of duress were visible over the 8w study protocol; however, myeloma-injected animals (MM and LIV) showed a mild reduction in activity. There were no deaths throughout the study duration. Animal weights were tracked throughout the study (Fig. 7). Though these were non-significant, a -1% decrease in MM weights as compared AC was observed, while a +1% increase in LIV was shown as compared to MM ($p=0.73$). No differences in chow consumption were observed between groups (Fig. 7).

Pathological Analysis of Xenograft

This animal strain is genetically bred without the capability of developing mature lymphocytes, including terminally-differentiated B cells (i.e. plasma cells). Therefore, presence of plasma cells in any section would indicate U266β1 infiltration. Histological assessment of the disease pathology in the femoral, tibial, humeral, and pelvic marrow cavities revealed extensive plasma cell infiltration throughout the medullary cavity in both MM and LIV as compared to AC, resulting in displacement of healthy BM constituents, phenotypically consistent with gross anemia, leukopenia, and neutropenia (Fig. 8, 9). Confluent plasmacytomas were clearly distinguishable in contrast to the healthy marrow and, frequently, an interface between the distinct marrow qualities was visible (Fig. 9). Extending further into the healthy marrow, plasma cells were diffusely visible amongst the reticulocyte, granulocyte, and erythrocyte populations. Resorption pits adjacent to myeloma cell infiltration of the medullary cavity were evident along the endosteal surface in MM and LIV (Fig. 10). Woven bone, an outcome of poorly remodeled, diseased bone, was visible within the cortical bone of MM and LIV (Fig. 10). Semi-quantitative pathological estimates of the tumor burden in the viable cellularity across the femoral marrow space indicate a 75% infiltration of the disease in MM, with a 61% ($p=0.07$) invasion in LIV (Fig. 11). The same analysis was performed with the tibial marrow space resulting in 69% occupation of MM marrow, contrasted by 57% ($p=0.18$) in the marrow of LIV (Fig. 11). These analysis were not statistically significant; however, a trend toward a decreased tumor encroachment within the marrow space of LIV mice

was observed. Sites of tumor necrosis within the viable cellularity of the bone marrow were evident in tibial sections of MM but were absent from the bone marrow of those of LIV animals. Necrotic tumor was bordered by viable tumor but not healthy marrow, indicating a more advanced stage of tumor progression in the non-LIV-treated animals (Fig. 17).

Red marrow obtains its hue from erythrocytes and their precursor cells which are confluent in healthy marrow. Upon visual inspection, even without the use of microscopy, regions along the length of the long bones, sternum, and pelvic bones devoid of red marrow were evident in MM and LIV as compared to AC, which maintained the confluent red marrow phenotype. Healthy marrow in NSG mice (Fig 8) consists of modest amounts of adipocytes, granulocytes, immature leukocytes, and an abundance of erythrocyte precursors. Gross histological examination of these regions would later confirm that these paler sites were indeed plasmacytomas, the lack of color indicative of an anemic response. In fact, these plasma cells were so devastating to the marrow that the predominance of regions occupied by viable tumor lacked any of the components of healthy marrow. In essence, where there was tumor, there was nothing else. This is consistent with more advanced stages of symptomatic myeloma, where anemia, neutropenia, and leukopenia are observed. In some cases, as expansion of the plasmacytoma reached critical levels, it exhausted the supportive capacity of the marrow, starving out the surrounding hematopoietic populations and, in the end, depleting the resources it needed to thrive. In some cases (n=6), necrotic tumor was visible in the tibial bone marrow adjacent to viable tumor. Viable tumor in both femur and tibia was observed adjacent to other viable marrow in two histological fashions. First, a defined boundary between plasmacytomas and healthy marrow provided easily distinguish tumor and normal marrow. The alternative pattern consisted of a gradient of tumor cells which proceeded into a heterogeneous mix of healthy and malignant cells, which concluded in healthy marrow. Sites of extensive cortical bone resorption were visible, including deep pits that sometimes breached the periosteal surface in MM. Tumor was always present adjacent to the sites of resorption in both MM and LIV. Interestingly, gross analysis of marrow pathology demonstrated modest decreases in viable tumor in both femora and tibiae.

Visual inspection of femoral bone from 3D reconstructions revealed how thin the bone in MM and LIV had become. Micro-CT analyses showed profuse skeletal degradation in the distal metaphysis of MM and LIV as compared to the undisturbed shell of the AC counterparts. Extensive

evidence of cortical thinning (-16%, $p<0.03$) was observed in distal femurs of the MM group. This was accompanied by the devastation of trabecular bone in distal femora and proximal tibiae. Segmented bone in the femur and tibia further revealed extensive bone loss in MM as compared to AC. The dramatic (-73%, $p<0.04$) loss of femoral trabecular bone volume in MM as compared to AC only further indicates the severity of the disease. Quality of the bone was also compromised as evidenced by the -39% reduction in tissue mineral density. In contrast to these losses, the mechanically-stimulated LIV group had a +36% ($p<0.05$) greater trabecular BV/TV as compared to the disease-only MM group. Cortical BV/TV in LIV, though not statistically different and still lower than AC, revealed a trend that was 6% greater than MM. Quality of bone was also improved as a result of the LIV administration as a +13% (nsd) increase was measured as compared to MM. These data reinforce the utility of LIV in mitigating cancer-induced skeletal degradation as demonstrated by the modest improvements in bone quantity and quality as a result of exposure to LIV.

Micro-CT Analyses

Micro-CT analyses (Fig. 12) of the distal femora and proximal tibiae demonstrated a -73% ($p<0.04$) and -79% ($p<0.0004$) decrease in trabecular bone volume fraction (Tb.BV/TV), respectively, in MM versus AC, while increasing by +36% ($p<0.05$) and +29% (nsd) in LIV versus that of MM. Across the distal femur, cortical bone volume fraction (Ct.BV/TV) was decreased by -16% ($p<0.03$) in MM from AC while increasing by +6% (nsd) in LIV. Micro-CT of the distal femora demonstrated a -73% ($p<0.04$) lower Tb.BV/TV, in MM as compared to AC. In contrast, the mechanically stimulated LIV group had a +36% greater BV/TV ($p<0.05$) as compared to MM. Ct.BV/TV of the femoral diaphysis was -16% ($p<0.03$) lower in MM as compared to AC, while LIV was +6% greater than MM (nsd). Tissue mineral density in the tibiae (Tb. Mean 1) was -39% ($p<0.001$) lower in MM as compared to AC, while a +13% (nsd) increase was measured in LIV as compared to MM

Qualitative 3D-reconstructions of the distal femur (Fig. 15) revealed an intact cortical shell in AC. Extensive porosities are visible along the periosteal surface proximal to the growth plate in MM. Dissecting the 3D image along the sagittal and transverse axes revealed these porosities were not superficial but extended through to the endosteal surface. These perforations through the

cortical shell were not visible in LIV femora. Transverse sections detail the extensive trabecular bone loss and cortical thinning in MM as compared to AC. Though some degree of bone was lost in LIV, these measures were moderately lower as compared to MM. Proximal tibiae also reveal cortical thinning and extensive trabecular destruction in MM as compared to AC. These losses were visibly reduced in LIV as compared to MM.

Flow Cytometric Analyses

Engraftment efficacy of U266β1 was partially determined by FACS analysis (Fig. 13). *In vitro* characterization was performed on the plasma-cell surface marker CD138 (syndecan-1), a cell-membrane protein responsible for cell-matrix interactions, for the U266β1 cell line. At sacrifice, peripheral blood was harvested and tested for presence of $CD138^+$ cells, which were undetected in all animals. Homing of the injected cells exclusively to the bone marrow cavity was confirmed in 25 of the U266β1-injected animals, reflecting the phenotype observed from *in vitro* cultures.

At sacrifice and as compared to AC, flow cytometric analysis of BM from the left femur of LIV revealed a negligible population of $CD138^+$ cells in AC. A -37% ($p=0.08$) decrease in $CD138^+$ cells was quantified as compared to MM. Natural killer cells ($NK1.1^+$) in MM were +1330% ($p=0.0029$) greater than in AC, while there were -20% ($p=0.94$) fewer in LIV as compared to MM. Total mature macrophages ($CD11c^+$, $F4\text{-}80^+$) were +61% greater in MM as compared to AC, while there were -10% ($p=0.75$) fewer in LIV as compared to MM. Long-term-hematopoietic stem cells (LSK^+) were +187.5% ($p=0.08$) greater in MM as compared to AC, while there were -20% fewer in LIV versus MM.

Discussion

Cancer progression and the subsequent array of treatment strategies physicians employ to combat the disease, often complicate clinical outcomes causing drastic reductions in bone quantity and quality [49, 51, 56, 58, 167, 169, 196]. These are not only correlated with an increased risk-of-fracture [123, 164, 166] but their use imparts negative impacts on the bone marrow (BM) niche [38, 62, 66], disrupting stem cell populations that are critical for tissue repair and immune regulation [40, 129, 130]. Despite this, cancer alone is enough to offset the bone remodeling pathway, either through humoral means or by directly interfering with the bone remodeling pathway. Multiple myeloma promotes accelerated cortical resorption and destruction of healthy marrow [38, 197]. Exercise is recognized by the NIH as a non-pharmacologic strategy for preserving bone strength in cancer patients [124, 125, 198-200], and also serves to suppress inflammation [81, 87]. In an effort to investigate non-pharmacological strategies to aid in cancer treatment in those with a reduced skeletal loading capacity we found that mechanical signals, a component of exercise, were significantly effective in mitigating bone loss in a murine model of spontaneous ovarian cancer without compromising longevity [187]. The treatment appeared to have influenced MSC-fate in the BM towards osteogenesis, as evidenced by increased trabecular bone volume and reduced numbers of MSC in LIV-treated animals; however, this mechanism must be studied further to understand how LIV imparts its osteogenic effects. While successfully demonstrating LIV's safety and efficacy, additional investigation on LIV's ability to deter cancer-induced bone loss must also be tested against a cancer whose mechanism-of-action and sustainability are tightly regulated by marrow constituents. For these reasons, an unmet clinical need exists to develop anabolic agents to repair damaged bone.

To address this, our studies were designed to evaluate if low intensity vibrations could mitigate the symptomatic bone loss consistent with human multiple myeloma. A highly aggressive and invasive cancer, MM causes diffuse osteolytic lesions across the cortical shell, providing the ideal model to study LIV's effects on bone skeletal losses stemming from a primary bone cancer-related deficit. $2x10^6$ U266β1 human myeloma cells from an immortalized cell line were injected intravenously into the dorsal tail veins of an immunocompromised mouse strain (NSG). A subset of this group of injected mice was exposed to daily bouts of LIV, at high-frequency, sub-gravitational magnitudes, in parallel with the "disease-only" mice, over the course of the study.

Intravenous tail vein injection was a safe and efficient route of administration, as compared to the invasiveness and inconsistencies that are encountered during intracortical, intracardiac, or subcutaneous injections, yielding a 100% success rate of the full 0.3cc injection.

The injected MM plasma cells homed exclusively to the bone marrow, likely through adherent proteins that are intrinsic to the endosteal surface of the bone marrow, as there was no evidence of soft tissue lesions at other susceptible tissues (lungs, kidney, and liver) at sacrifice. One way this is likely to have occurred is by the binding of CD138 (syndecan-1), a surface marker on multiple myeloma cells, and VCAM-1 to stromal and mesenchymal stem cells that naturally inhabit the bone marrow microniche [201]. This association is important in the progression of the disease and is reminiscent of the mechanism by which hematologic metastatic cells home in and attach to the marrow as a consequence of identified chemokines and binding proteins. Following the 8w investigation period, bones across the appendicular and axial skeleton were harvested.

Marrow occupation by the malignant plasma cells tilts the bone remodeling pathway heavily in favor of resorption, whereas, upon institution of regimented mechanical loading, here LIV, factors are driving a modest preservation of trabecular bone. Whether these are realized as a result of increased formation or from decreased resorption has yet to be determined. MM is dependent on elements of the *Wnt/β*-Catenin pathway [96] and that LIV has been demonstrated to modulate activity along a shared pathway indicates mechanical signals as a modulatory agent. One possible mechanism that this may be achieved is by reducing the encroachment of the cancer into the bone marrow microenvironment. Critical stem cell populations involved in the tumor development are also tightly associated with bone formation and resorption; however, resulting from the disease (Illustration 5) myeloma cells secrete DKK-1, an antagonist of the *Wnt*/β-Catenin pathway, thereby inhibiting bone formation. The strength of the RANK:RANKL osteoclast-activating signal derived from stem cell and myeloma expression, may have overwhelmed the fidelity of LIV at these magnitudes and at 8w. If so, this could partially explain the limited preservation of cortical bone mass. Additionally, bone remodeling is cyclically completed at 3 months; therefore, the duration of LIV-treatment may require a longer period to significantly preserve bone, though the trends presented here are convincing.

At the same rate, HSCs can differentiate into OC-precursors, whose activation may become critical in accelerating bone resorption. The nearly three-fold increase in LSK (HSCs) and +61% in mature macrophages increase in MM demonstrates the ability of HSC to undergo proliferation in the face of disease, migrate to cite of dysplasia (here the marrow), possibly contributing to resorption via inflammatory means [22, 24]. Perhaps their presence contributes to some degree to the macrophage-like, osteoclast behavior that promotes bone resorption. The clinical range of this phenomenon extends from breast cancer metastases [202] to acute myeloid leukemia [203] and multiple myeloma [204]. Further, the highly proliferative, stem-like SP^{KLS} population is almost universally detected in most cancers, especially those with high metastatic propensity [205]. While not a heterogeneous tumor in the traditional sense, for example an ovarian cancer may have a stem like germinal center, stromal exterior, and is highly vascularized, myeloma is mostly a homogenous lesion. Again, its expansion into the marrow depends on its almost parasitic associations with the microenvironment and its constituents [206]. The proliferative response of these marrow populations in the face of disease reflects their contribution to the disease state. Reductions in the populations that were quantified following introduction of LIV suggests that the marrow may have strengthened the bone against atypical resorption.

The long-term, catabolic repercussions of chemotherapy, irradiation, and immunosuppressive therapies on bone endpoints contribute heavily to post-treatment osteopenia and faltering immune health, especially for the very young, frail elderly, and immunodepressed. For reasons discussed previously, maintaining skeletal integrity is vitally important to achieving positive clinical outcomes, even when patients are successfully in remission. With the cortical shell compromised, the marrow is subject to damage, making recovery efforts increasingly difficult to overcome. To this end, utilizing low intensity vibrations to combat skeletal losses as a comorbidity of cancer in this animal model without disrupting host survivability elevates LIV towards a preclinical strategy. Additionally, the histopathological data suggest that, perhaps, modulation of the marrow microenvironment via LIV, secondary to bone retention, has had a modest effect on the tumor component in the marrow. Through signaling pathways not yet understood, it is possible that mechanical signaling plays duals roles in engaging the stem cell populations towards osteoblastogenesis or away from osteoclastogenesis, while minimizing the signaling pathways that are conducive to disease.

This study has several limitations, chiefly those surrounding the administration of disease. Though human myeloma does reach the vasculature when its leaves marrow space, it is not universally disseminated to all marrow spaces at once. That every bone of the injected animals presented with a lesion suggests that the concentration of injected cells may have overwhelmed the body's innate ability to defend itself, reflected by the significant increase in natural killer cell, macrophage, and LSK cells in MM and LIV. Naturally, the innate immune system, even in this immunocompromised mouse strain, effectively mounted an immune response in the femoral bone marrow. Inducing the disease in this fashion, though exhibiting many of the facets of myeloma, undermines the chronic time line and the manner in which myeloma presents. The aggressive nature of tumor infiltration, osteolytic lesions along the cortex, and subsequent neutropenia within the occupied marrow reflects clinical presentation of the disease [25, 62]. The intentions of this study were not from a preventative standpoint but, rather, to determine if bone loss could be curbed earlier on in the disease stage, corresponding roughly to symptomatic Stage I-II myeloma. A study aimed at preventing the disease would test a group of animals that had undergone LIV treatment over a period of priming, perhaps 8w, and then were subjected to instatement of the disease at more subtle concentrations. It is also important to highlight that, as a limitation of the animal model, while innate immunity (granulocytes, NK cells, monocytes) is conserved, the adaptive, mature lymphocyte populations are not available to combat the early, smoldering onset of plasma cell proliferation. Thus, proliferation of the neoplasm is not under the suppression of an intact immune system as would generally be observed in the clinical sense.

Disease progression was subjectively lower in both the femur and tibia of LIV animals than the diseased animals alone. Of these regions, necrotic tumor in the bone marrow accounted for over 1/3 (n=6) of the observations in tibiae of the MM group only. Follow-up studies should address the range of time at which necrotic tissue is bound to happen and if these animals who undergo LIV treatment, fall in this range. Perhaps, this is due to the reduced volume of the tibia versus that of the femur. If the disease were to have progressed to 16w, necrosis of the femur may have been observed as well. In addition, it is interesting to note that NK cell activity in LIV is the same as that in MM, suggesting that the immune response is still strong enough to handle tumor expansion.

Taken together, these data demonstrate the destructive capability of inducing U266 human multiple myeloma cells into the circulation, and thereby significantly and negatively impacting bone remodeling through elevated bone resorption in the marrow. Infiltration and disruption of the bone marrow alters hematopoietic outcomes, elevating key cells involved in the tumorigenesis of multiple myeloma as well as inciting an immune response. Introduction of regimented treatment using low intensity vibrations afforded significant mechanical protection to trabecular bone, reducing the risk-of-fracture, which in turn protects the bone marrow. Perhaps this is achieved through the uncoupling of the critical crosstalk that occurs between the myeloma cells and the surrounding microenvironment (Illustration 5) that maintains disease, in turn, driving healthier tissue growth. We also appear to be slowing progression of the disease effects on bone, perhaps by modulating osteoclast activity. In modulating osteoclast activity, we may reduce the amount of bone being resorbed. One possible mechanism in which this may be achieved is through the influence of low intensity vibrations as an agonist for osteoblast activity, independent of the cancer cells, whereby increased levels of secreted OPG may serve to bind to RANKL, thereby, preventing the binding of RANKL to RANK on osteoclast precursors. The response of the bone marrow in response to LIV may bridge the ameliorating capacity of mechanical signaling in preventing trabecular bone loss to the modulation of the bone marrow phenotype in multiple myeloma. Future studies will focus on the duration of LIV administration beyond the 8 weeks allotted for this study, to determine the nature of bone retention, the role of LIV in mediating inflammatory outcomes, and if disease progression was truly reduced in LIV. While preliminary, of course, it appears that the introduction of mechanical signals – perhaps as a surrogate to exercise – helps slow disease-related damage to bone.

Conclusion

In summary, the skeletal data reported herein have demonstrated that, at the system level, administration of low intensity vibration in an induced, aggressive murine model of multiple myeloma can safely intervene and mitigate long-term osteopenic and osteolytic insults to metabolically active areas of bone. These skeletal gains were achieved without accelerating tumor progression or influencing survival outcomes. Further, we have presented evidence indicating a reduced tumor burden via histological evaluation and flow cytometric analyses, perhaps through the modulation of the bone marrow microenvironment. Constituents of the bone marrow markedly influenced by the presence and persistence of the disease, had somewhat normalized over the course of LIV administration. These data demonstrate the singular potential of mechanical signaling in reducing a primary symptom of plasmacytomas as well as influencing phenotypic aspects of the bone marrow microenvironment. Modulating activity of cells known to harbor inflammatory mediators coupled with reduced area of viable tumor suggests that LIV may influence more than just osteogenic and adipogenic outcomes. As combinational therapies have historically benefited those undergoing treatment, a novel clinical strategy may complement LIV with other treatment modalities, such as chemotherapy or irradiation, to mitigate myeloma-associated osteolysis while also reducing the tumor burden. Adverse effects that are observed following current interventions in comparison to the nearly non-invasive effects of LIV reinforces its translational potential as a possible treatment modality to safely stem the skeletally destructive capacity broadly observed in osteolytic cancers. While advocating physical activity as a means to maintain overall health and bone strength, it appears that LIV, a surrogate for exercise, may have deeper implications in slowing the progression of cancer. In the future, LIV may aid in combinational therapeutic strategies to target and mitigate these skeletal deficits while reducing the extent of tumor progression.

Chapter 4: Future Directions

We have shown that in the wake of cancer, significant bone destruction is likely to occur. These deficits are highly detrimental to bone integrity and disrupt bone marrow along with its stem cell reservoirs. Presenting a novel, non-pharmacological direction by which to attenuate the insults associated with cancer-induced bone loss is an attractive clinical approach, as drug-based interventions are typically accompanied by secondary consequences. Our studies have demonstrated preliminary *in vivo* efficacy using a novel means of preserving bone mass and protecting the marrow without compromising the survival of the host. These studies widen the reach of mechanical signaling as a device to combat cancer-driven bone deficits, strengthening support in favor of exercise, in the broadest sense, and low magnitude skeletal loading, specifically, as a strategy to maintain bone quality and, potentially, to improve overall health.

Within these aims we have demonstrated the ability of two different cancers to cause bone loss through different mechanisms of disease, both systemically (granulosa cell tumors) and through local interaction at the bone marrow interface (plasmacytomas). Mice that develop granulosa cell tumors demonstrated a systemic response secondary to tumor progression for bone loss. It is suspected that this occurs, rather than through pathways directly involved in the bone remodeling pathway, either hormonal or cytokine factors involved in the pathogenesis of the disease. A humanized mouse model for multiple myeloma was developed that demonstrated extensive localized bone resorption as a consequence of plasmacytoma manipulation of the bone remodeling components. Of course, both types of cancer thrive off distinct stromal interactions: GCT through an external tissue, and MM, by engaging the bone marrow. Granulosa cell tumors present with a high degree of metastases, whereas, the plasmacytomas appeared confined to the bone marrow, likely through adhesion factors which keep malignant plasma cells attached to the stroma of the bone marrow. Additionally, the bone marrow phenotype of both animals was altered subsequent to disease onset, but in different capacities. However, the GCT mice appear to have an unperturbed immune reactivity within the marrow, suggesting the potential that hormonal shifts or inflammatory mediators secreted by diseased tissue, act as the causal agents of bone loss. Further, MSC quantification was significantly reduced in both the non-diseased and LIV-treated animal cohorts. This suggests that mechanical signals may bias MSC differentiation towards a

higher-ordered tissue state, such as that of bone or muscle, whereas in their absence, an unstimulated pool of MSC's may be susceptible to fueling progression of neoplastic tissue. Conversely, in the bone marrow of mice bearing plasmacytomas, the pathogenesis of disease mounted a hematopoietic response, markedly upregulating cell activity along this lineage. LSK^+, macrophage, and $NK1.1^+$ cells demonstrated dramatic proliferative expansion after 8w of disease onset. The MSC data from these animals is being evaluated to determine if population differences can be identified. To what degree does the MSC contribute to stromal expansion of the tumor and can LIV modulate their migration to sites of tumorigenesis?

Both studies contained a cohort of animals subjected to low intensity vibration treatment. While GCT mice were tracked for 1y, mice bearing plasmacytomas were only tracked for 8w. Further, the survivability of the GCT exposed to LIV, though not 100%, did not significantly deviate from its AC counterpart. Additionally, mice injected with myeloma cells (n=25) lasted the study duration without a fatality, despite exposure to LIV. Clearly, this demonstrates that systemic and local models of bone disease are not directly antagonized by mechanical signals. As importantly, trabecular bone volume was significantly preserved in both models and at two anatomical sites. The observations taken from these studies indicate that, independent of disease, mechanical signals have the capacity to influence bone outcomes. To what degree this occurs appears exclusive to each type of cancer.

Elucidating the means by which LIV mitigates bone loss in two different cancer models, without stirring the potential for disease, may be indicated through histological means. Depending on the calcein double-marker staining, dynamic histomorphometry of the bones of GCT mice may reveal the degree of bone formation at 1y. In combination with these labels, immunohistochemical (IHC) staining of MSCs and osteoblasts would demonstrate which of these cell type propagates to sites of bone formation. Conversely, regions devoid of double labels may be stained with TRAP to confirm that osteoclast activity is responsible for the lack of mineralization of new bone. In the MM animals, IHC could be used to determine the degree of TRAP (bone resorption) or alkaline phosphatase (bone formation) staining on the endosteal surface of the cortex co-localized with surface markers for MSCs. Or, since the trabecular bone appears to have responded more strongly to LIV-treatment, are the markers for MSC and bone formation, instead, observed across the trabeculae? If observed, in what proximity to the tumor mass are these bone remodeling markers

located? Do the MSC's adjacent to sites of resorption show any distinct, morphological characteristics that may demonstrate a response to mechanical strain? In either scenario, the increased expression of OPG may indicate increased osteoblast activity. Conversely, if either IL-6 or DKK-1 expression was reduced across the tumor mass in LIV bone marrow, this may hint at reduced effects of the tumor on osteoclast activity. Are the same effects observed in the diseased mice not subjected to LIV? As there was a degree of healthy marrow in each cohort of diseased animal (MM and LIV), quantifying viable MSC, osteoclast, and osteoblast numbers versus those in the diseased portion of the bone may reveal how and where LIV acts as an osteogenic agent.

While LIV has been efficacious in small animal models of cancer to the extent studied here, further investigation is needed to determine safety in more complex models of disease. For instance, how do those with a greater degree of bone loss, at more advanced stages of cancer, or those more susceptible to the disease, react to LIV administration? Our first study on granulosa cell ovarian cancer returned no adverse indications of survivability. Perhaps, the same 1y duration of treatment can be tested on a model of multiple myeloma that exceeds the 8w treatment period tested in SA3. Additionally, is age a factor? While the granulosa cell tumor-bearing mice lived past a year (comparatively long for a mouse) and the myeloma-bearing mice just short of 4 months, both animals acquired the disease at a younger age. Is an aged population, one who may be systemically taxed by obesity, physical inactivity, or of faltering health afforded the same protective skeletal benefits of LIV as those of a younger, more vital population?

Since the role of *Wnt*/β-catenin is known to regulate anabolic growth, as well as induce tumorigenesis, we must understand which regulatory pathway is most responsive to LIV. The mechanisms by which the MSC and HSC perceive and respond to mechanical loads, and how these discrete pathways may intercept and combat those which institute programs leading to bone loss (osteopenia and osteoporosis), are ongoing. While preservation of bone quantity and quality has been studied in other models of metabolic disease (osteoporosis, diabetes, and high-fat diets), the capacity to target cells responsible for making bone without influencing a highly proliferative, neoplastic condition can have profound effects on the way clinicians now approach treatment. *In vivo* tracking of stem cell and cancer lines using endogenous fluorescent markers could confirm how the disease progresses over time and how these stem cell populations contribute to mitigation of the bone losses associated with the disease.

In vitro assays used to isolate the responses of different cancer cells following administration of mechanical signals will provide data on transcription factor activity of mechanotransduction, proliferative capacity, cell cycle senescence, and migratory ability. These are important elements in the scope of cancer progression. Previous studies have utilized *in vitro* assays to determine importance of cell-cell adhesions of MM cells to those of its stroma. In this vein, co-culture assays may be designed to understand how cancer cells interact with stem cells during mechanical signaling. If an immunomodulatory role is suspected, then inflammatory cytokine secretion, such as IL6 or TNF-α, or genes regulating their synthesis may be down-regulated. If so, these results may provide further explanation into the phenomenon seen in our second aim, that hematopoietic mediators of inflammation and osteoclastogenesis may have reduced reactivity to LIV. In addition to understanding the role of LIV on inflammation, RT-PCR of bone marrow-derived MSCs isolated from the hindlimbs can determine if there is an upregulation in RunX2 (osteoblastic gene) or down-regulation of the RANKL gene.

Serum was harvested from animals in these studies. Immunoglobulin-E, a clonal immunoglobulin of plasma cells, and IL6, an interleukin responsible for osteoclastogenesis, are secretory molecules that U266β1 constitutively synthesizes. In an effort to determine the extent of osteolysis, *in vitro* assays designed to quantify these markers should be performed as well. In the same vein, calcium is leached from bones during excessive resorption, disrupting kidney function over time. Molecular indications of bone formation (serum-alkaline phosphatase; ALP) and bone resorption (tartrate-resistance-acid phosphatase; TRAP-5b) should be quantified to determine whether, in LIV, if bone formation was increased or resorption decreased. Factors that inhibit bone formation, such as DKK-1, and those that upregulate resorption (RANKL, IL6, TNF-α), can indicate where along the pathway LIV plays its critical role and if the uncoupled bone remodeling process was bridged to any degree. Longitudinal assessment of all of these factors in the serum may help track disease progression. Do low intensity vibrations reduce the amount of resorption, and if so by what means? If HSC populations senesce or if osteoclast-precursors, a type of macrophage, are no longer heavily activated through RANKL:RANK interaction, this may explain how bone was preserved. Still, based on what was observed from the GCT mice, MSCs may be signaled to become bone, thereby increasing rates of formation to counterbalance the bone resorption. The mechanism of systemic bone loss may be mediated by inflammatory factors, as

chronic inflammation from rheumatoid arthritis is primary to systemic bone degradation. In this regard, the demonstrated effects of LIV on reducing inflammation may be another possible mechanism by which trabecular bone retention is achieved.

It can be reasoned that the systemic effects of cancer on bone loss can be mitigated by LIV either through modulating inflammatory mediators that may exacerbate osteoclast activity, and therefore reduce bone resorption, in combination or alone with biasing MSC fate selection towards osteoblastogenesis, accomplished by causing rearrangement and stiffening of their cytoskeleton. In contrast, plasmacytoma disruption of the marrow – bone interface literally uncouples the bone remodeling pathway. If the MSC's engaged in the tumorigenic, vicious cycle of the disease are susceptible to erroneous signaling in the absence of mechanical signaling, then perhaps LIV serves to deter these MSC's from contributing to the cycle of tumor progression. In that case, MSC differentiation is a deterrent from its contribution towards osteoclast activation. Maybe this two-pronged approach, committing SCs to a specific fate and secondarily reducing the amount of osteoclast-activating cytokines or inflammatory mediators driving their secretion, is how LIV remains effective in cancer models that directly engage the bone. One final point of consideration is the possibility of LIV's direct effects on cancer cells. If indeed stem cells and other lineage-committed cells are susceptible to mechanical loading, alteration of their cytoskeletal framework, or transcription of specific genes as a sole consequence of LIV exposure, then it is reasonable to infer that neoplastic tissue may also be susceptible to modulation of these outcomes. In doing so, the disrupted cell cycle of the tumor cells may be forced to senesce and, ultimately, apoptose.

Follow-up studies will examine the extent of mechanical signals in suppressing bone loss and cancer progression in other induced models of the disease, such as occult breast metastases to the bone or osteosarcomas, with a continued focus on the lineage selection of the mesenchymal and hematopoietic progenitors and their involvement with and migration to sites of tumorigenesis. Similarly, the mechanism(s) by which mechanical signals influence bone indices but fail to drive neoplastic tissue expansion must be understood if this therapy is to be used in the clinic. As importantly, *in vivo* animal studies must be combined with *in vitro* protocols used to determine if, and how, hyperplasia in cancer cells can be suppressed by mechanical signals, perhaps through pathways already identified as mechano-responsive in MSC [109]. Additionally, these models of

cancer utilize LIV as a preventative and ongoing therapeutic to mitigate bone loss before or at the onset of tumorigenesis. Research into LIV's effects on bone once the cancer has reached more critical stages of care, reflecting a larger percentage of clinical cases, must also be addressed. Discerning the extent of LIV's immunomodulatory effects, suppression of inflammation, and preservation of bone quantity and quality respective to cancer models treated by fractionated irradiation and low- and high-dose chemotherapy would provide even further justification for preclinical efficacy. If indeed LIV has a salutary effect, perhaps "priming" the bone marrow before irradiation or chemotherapy may resist the catabolic aftermath on skeletal outcomes.

Taking into consideration that treatment modalities do elicit positive outcomes, if only for a short duration, it would be important to determine the peak efficacy of each approach. With these ranges discerned, combinational therapies can be used to target different aspects of the disease. For instance, and as detailed above, irradiation is the gold-standard when it comes to eliminating the radio-sensitive plasmacytomas in symptomatic myeloma. Use of low intensity vibrations, as a means to curb skeletal insults while irradiation focuses on eradicating the tumor burden, may be one such bi-modal approach, but these efforts must only be addressed following clinical efficacy with LIV alone.

What are the true mechanosensitive targets in the bone marrow? The degree of variation in MSC populations in LIV-treated animals as compared to AC in the GCT study suggests they are a major mechanosensitive population, at least when a systemic bone loss is incurred indirectly by a cancer. Conversely, in the myeloma study, our immature lymphocyte populations have demonstrated sensitivity to LIV as did the long term hematopoietic group. While HSC populations were relatively static in marrow of GCT mice, they reacted very differently when challenged by myeloma, a disease that utilizes a hematopoietic response to initiate osteoclast-precursor activity, yet also interacts with MSC's to perpetuate tumor cell growth. Two exclusively different models of cancer were addressed. Observing parallel outcomes in marrow activity between GCT and MM murine models of cancer would have been unlikely, further advocating the need to test against other models of the disease.

Our data has demonstrated that low intensity vibrations are effective in reducing the dramatic bone losses associated with the disease at both 1y and at 8w. Future studies should investigate the full extent of this mechanical signal, whether its efficacy is limited to mitigation of osteopenia, a symptom of the disease, or if the underlying mechanism of LIV is truly reducing disease progression through modulation of the marrow phenotype.

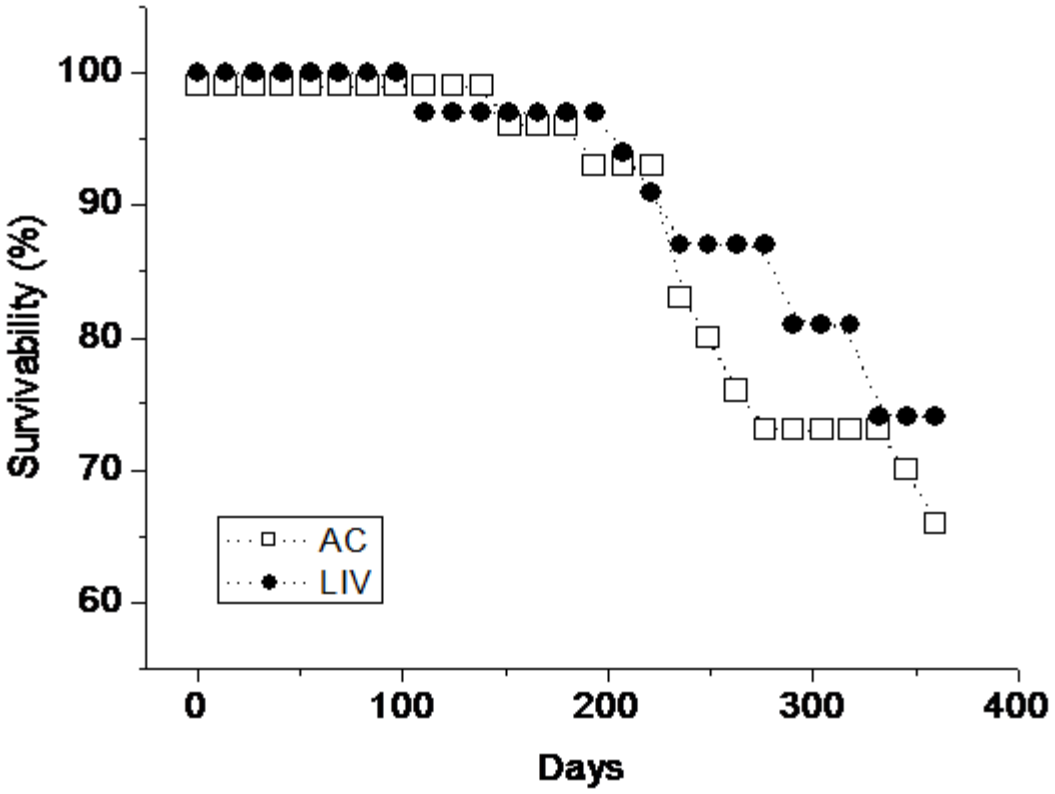

Figure 1. Survivability curve for LIV (n=30) and AC (n=30) mice, with the experimental protocol beginning at 3 months of age. Both AC and LIV groups followed similar declines over the course of the 1y period (p=0.62), indicating that exposure to the mechanical signal did not compromise life expectancy.

* Images reprinted with permission from Pagnotti et al., *Bone*. 2012 Sep; 51(3):570-7.

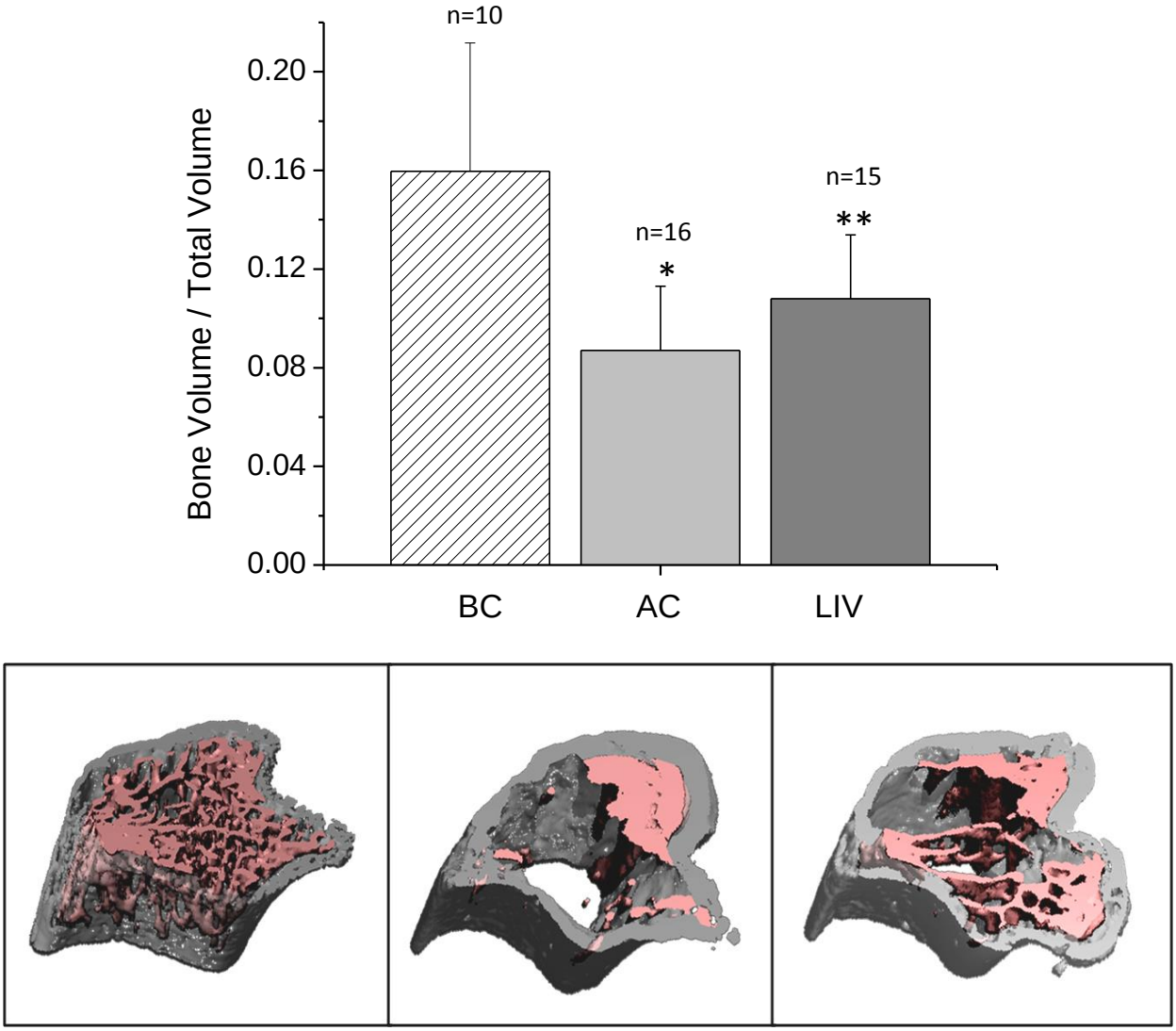

Figure 2. Reconstructions of cortical and trabecular bone in the tibial metaphysis, assayed by μCT, are shown for baseline control (BC) (left: 3 months of age), age-matched control (AC) (center: 15 months), and low intensity vibration mice (LIV) (right: 15 months). While bone quantity (BV/TV) dropped relative to BC in both AC and the mechanically stimulated (LIV) mice, the loss was mitigated in LIV by daily exposure to the mechanical signals (AC and LIV are both different from BC at $p<0.01$, shown by *; AC different from LIV at $p<0.02$,shown by **).

* Images reprinted with permission from Pagnotti et al., *Bone*. 2012 Sep; 51(3):570-7.

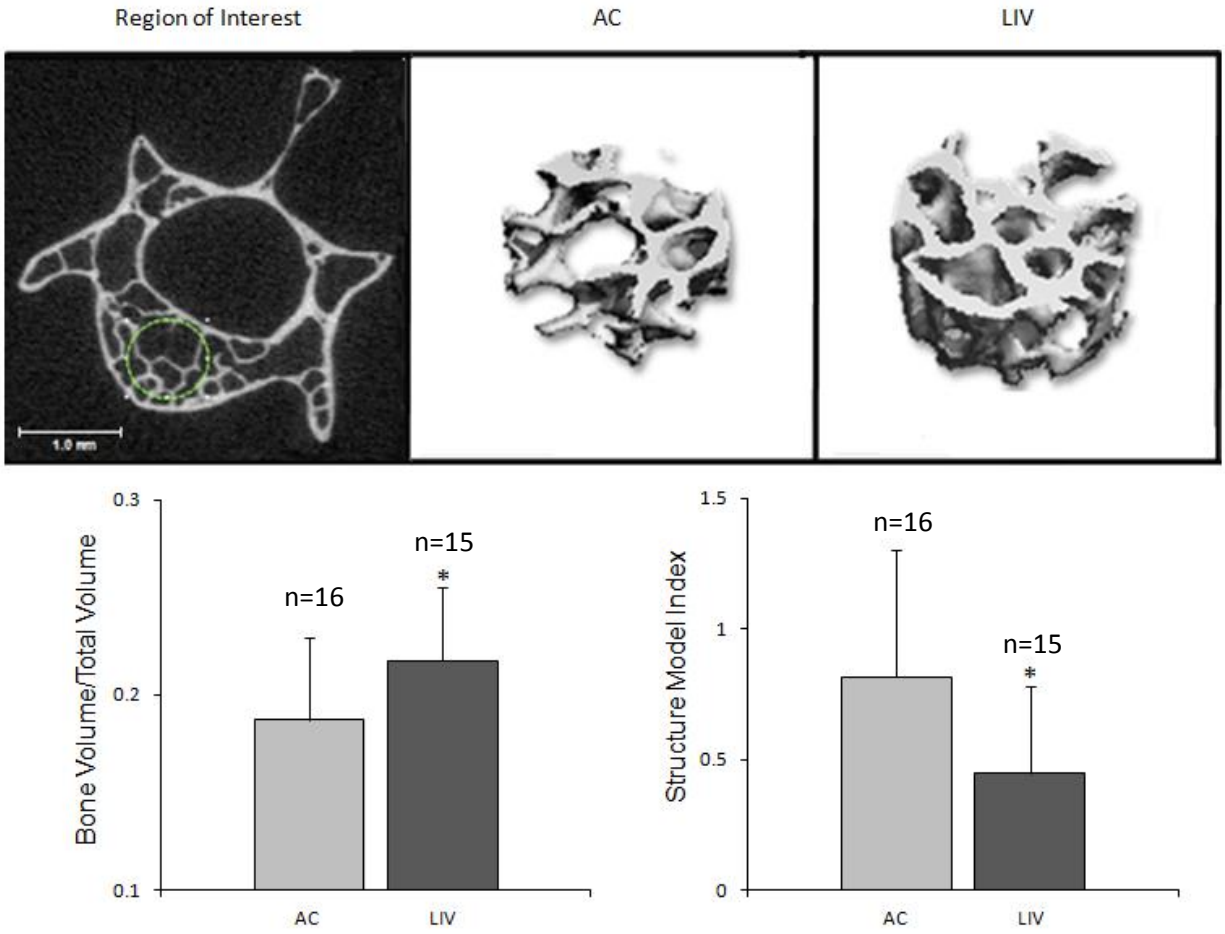

Figure 3. Reconstructions of trabecular bone volume, Tb.BV, as derived from μCT scans of L5. A cylinder (0.8mm in diameter and 0.4mm in length) was fit into the center of the vertebral body (top left; Region of Interest represented by dashed line), such that a defined volume was taken for each specimen. The 3D reconstruction of the LIV mice (top right), revealed a bone volume fraction, Tb.BV/TV, to be +16% higher than that of the age matched controls (bottom left; $p<0.02$). The SMI, 40% different between groups (bottom right; $p<0.01$), indicated the trabecular morphology of the mechanically stimulated mice to be more plate-like in structure, rather than the rod-like struts measured in the age-matched controls. Scale is 1mm; * = $p<0.02$.

* Images reprinted with permission from Pagnotti et al., *Bone*. 2012 Sep; 51(3):570-7.

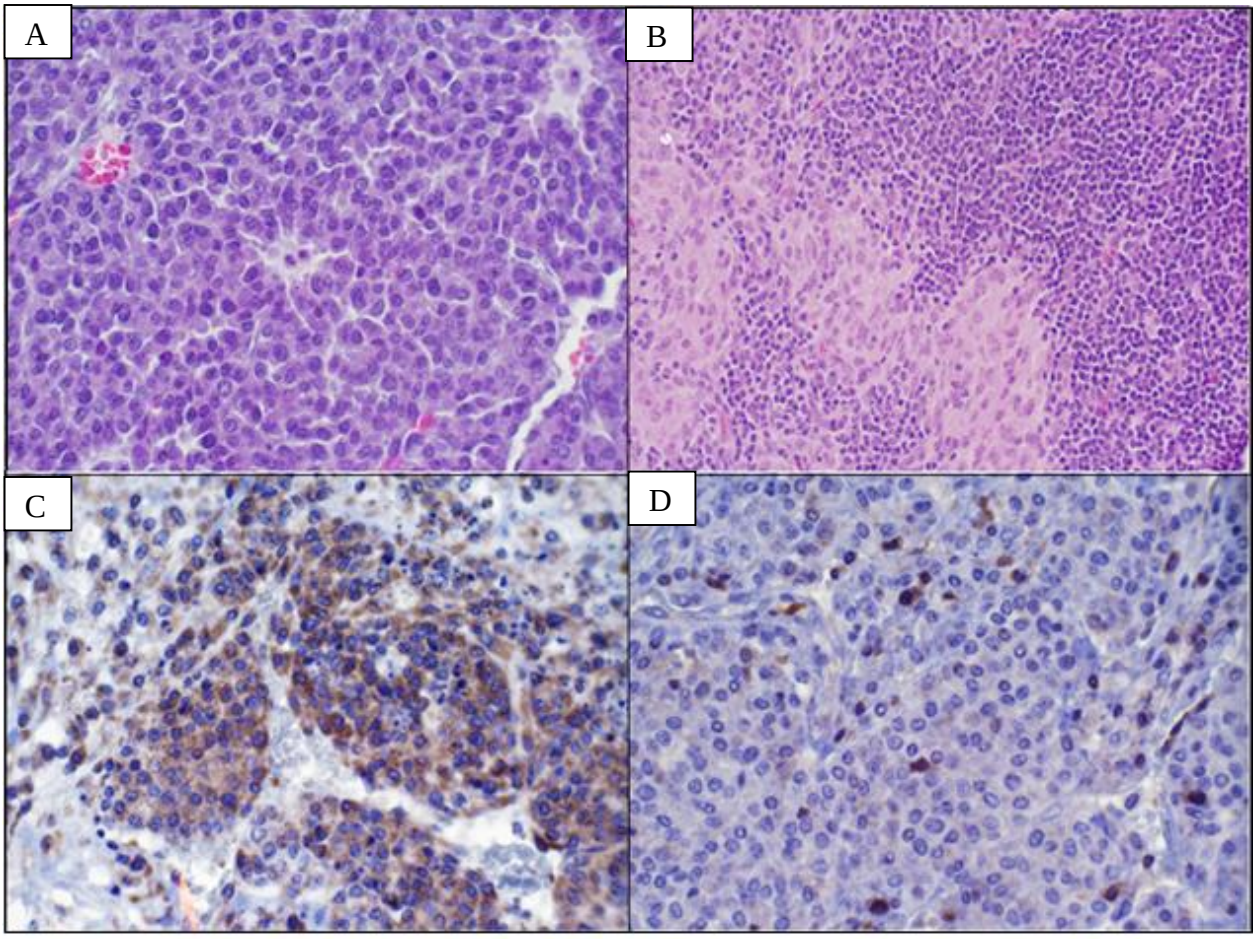

Figure 4. Histological and immunohistochemical tissue sections. A: Sheets of tumor cells forming Call-Exner bodies (40×). B: Sinus histiocytosis observed in enlarged lymph nodes both along the abdominal aorta as well as in the peripheral subcutaneous tissue (40×). C: The histologic diagnosis of granulosa cell tumor was confirmed with calretinin staining (1:100; 60×). D: Immunoreactivity of tumor infiltrating lymphocytes but not tumor cells for CD45 (1:20; 40×).

* Images reprinted with permission from Pagnotti et al., *Bone*. 2012 Sep; 51(3):570-7.

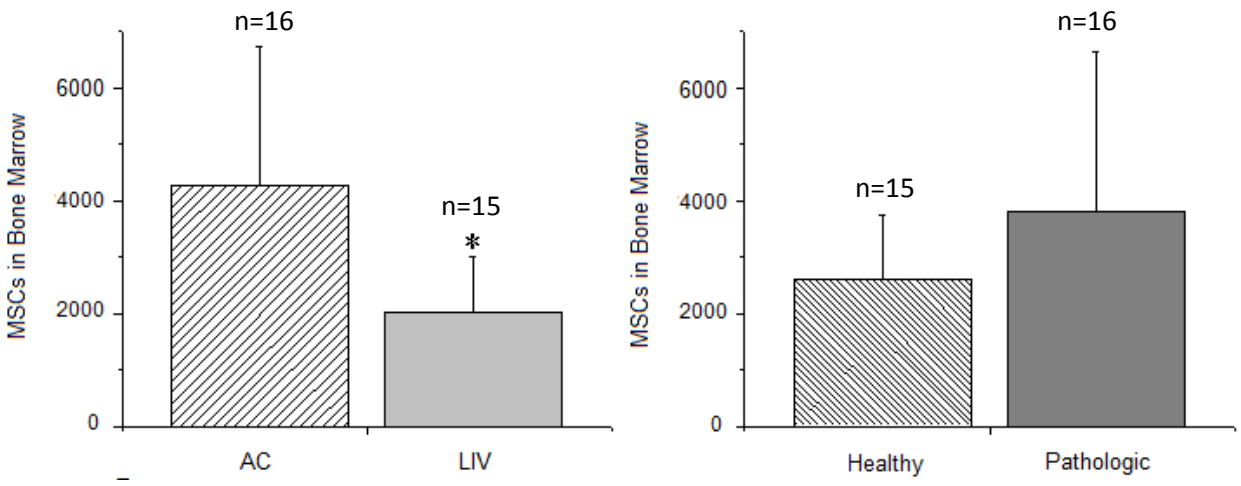

Figure 5. MSC-enriched populations estimated from pooled hind limb bone marrow as taken from FACS analysis. MSC numbers were 52% lower in LIV mice as compared to age matched control (left; $p<0.01$), suggesting these signals either suppress MSC proliferation or promote lineage commitment towards higher-order musculoskeletal tissues. This perspective was supported when the MSC populations from diseased mice were +31% greater than those with no evidence of pathology (right; $p=0.08$).

* Images reprinted with permission from Pagnotti et al., *Bone*. 2012 Sep; 51(3):570-7.

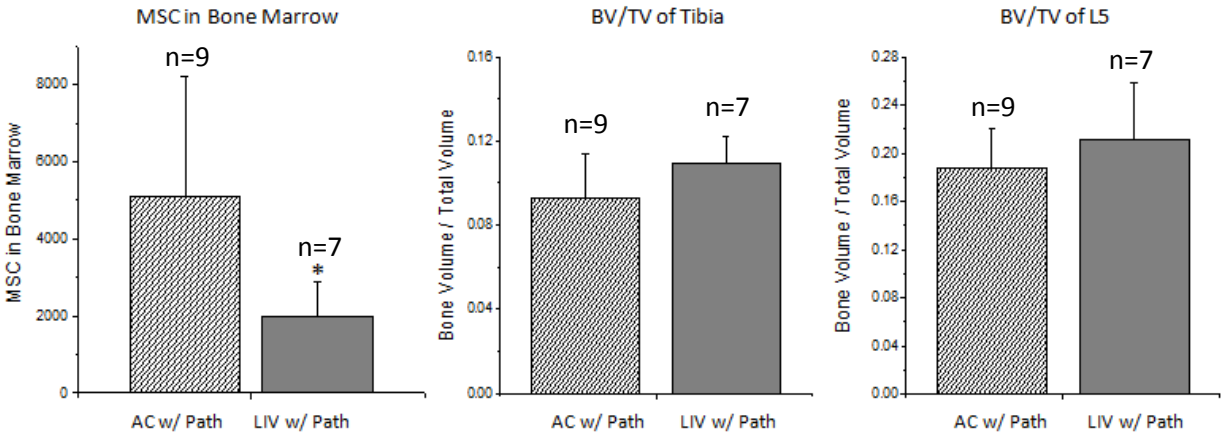

Figure 6. When considering only those animals that had visible evidence of pathology, there were −61% fewer MSC in the bone marrow of the LIV as compared to the AC mice (left; $p<0.04$). The BV/TV of the tibia (middle) and L5 vertebrae (right) of LIV mice with pathology showed a trend towards being higher than age-matched controls (17%, $p=0.12$ and 13%, $p=0.29$, respectively). These data indicate that the mechanical signals served to suppress MSC proliferation within the bone marrow even in mice with a tumor burden, and suggest some benefit in preserving bone quality despite carrying the disease.

* Images reprinted with permission from Pagnotti et al., *Bone*. 2012 Sep; 51(3):570-7.

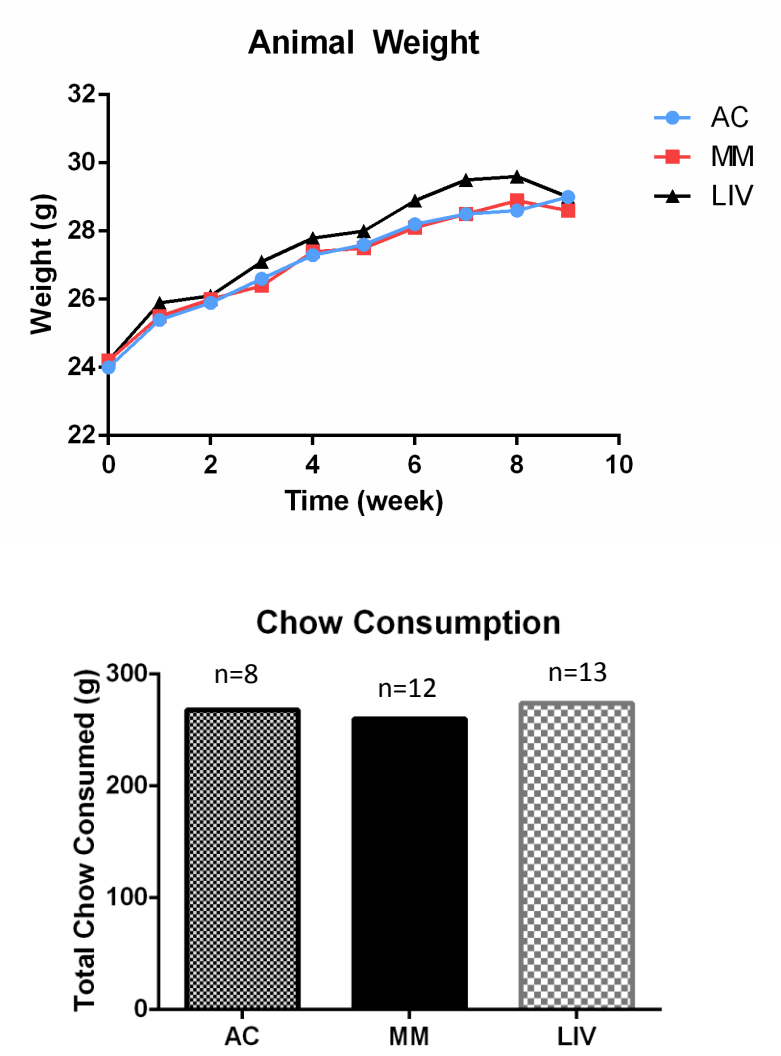

Figure 7. Animal weights taken over the course of the myeloma study for 9w. Weights were measured at 7w of age starting from week 0 (day of injection) until week 9 (day of sacrifice). Though a -1% decrease was measured in MM as compared to AC and a +1% increase in LIV was measured as compared to MM, these deviations were not statistically significant (p=0.73). Average chow consumption did not deviate over the course of the study.

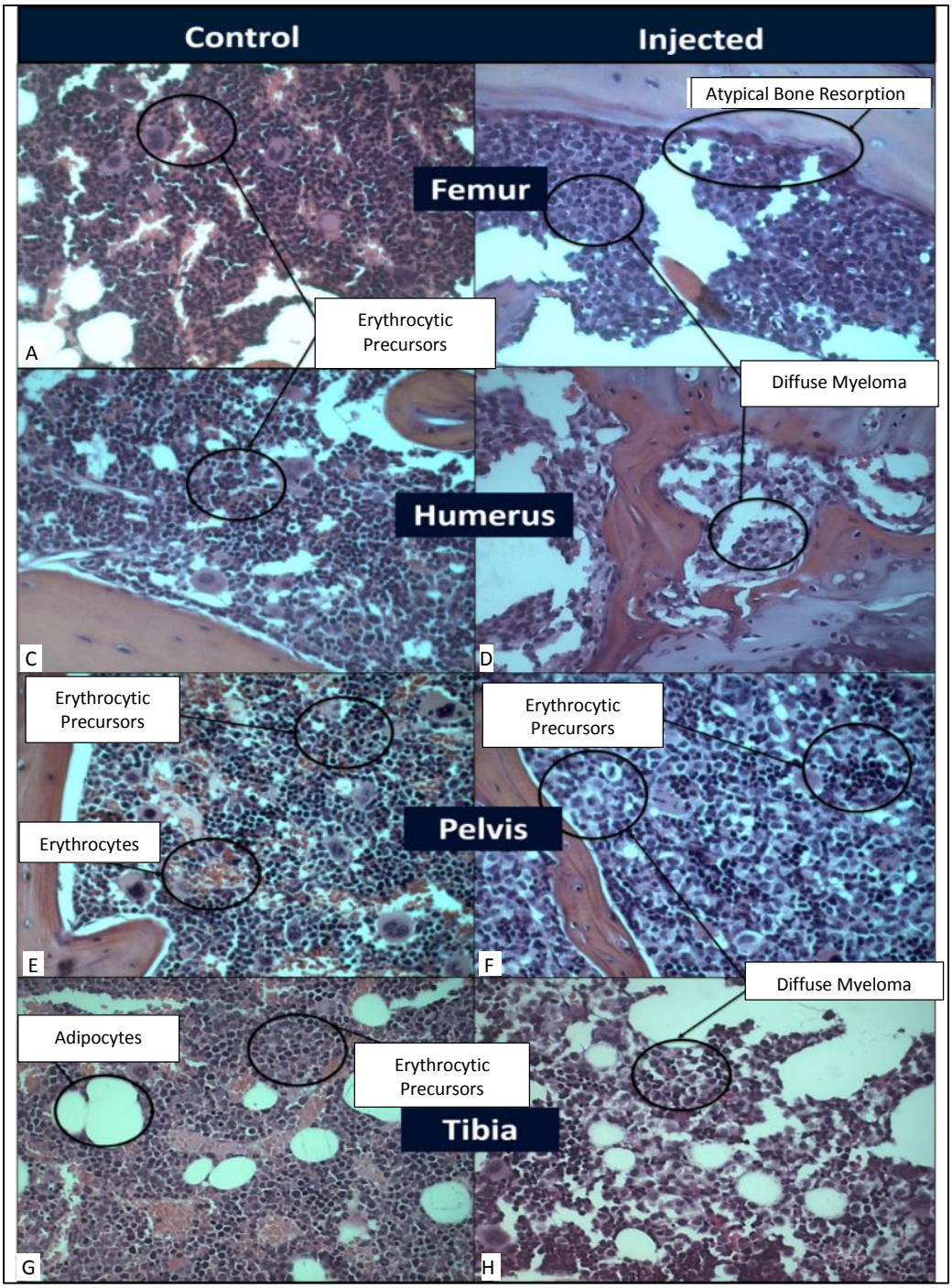

Figure 8. (Above) Histological sections (H&E, 40x) of bones along the axial skeleton of AC (A, C, E, and G) and injected samples. Following the 8w injection, $2x10^6$ **U266β1** cells, have infiltrated the marrow space in the represented bones: D) proximal humerus, F) iliac crest, and along the length of the B) femur and H) tibia. The hallmark "clockface" pattern was visible only in injected animals. At each anatomical site, clusters of myeloma cells were visible at resorption sites (pits) along the endosteal surface. Anemia and neutropenia were observed in MM and LIV samples where erythrocytes, adipocytes, and granulocytes were forced out of the bone marrow, thus, altering the niche phenotype.

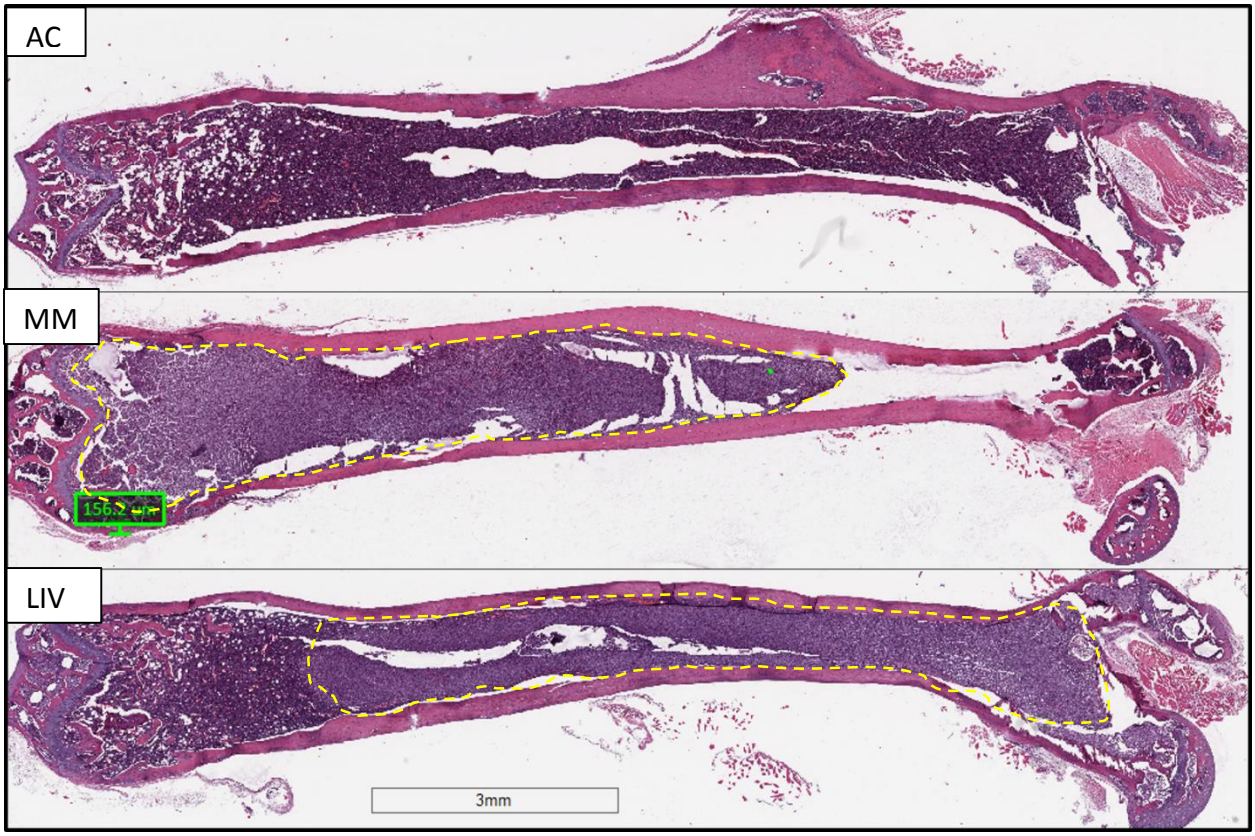

Figure 9. Longitudinal 5µm histological sections (0.7x) of H&E-stained femurs across the medullary cavity. AC marrow contains healthy hematopoietic cells throughout the cavity. The cortical bone is continuous throughout the length of the femur. In MM the confluent tumor burden is quite evident (yellow-dashed line) in the marrow space, with a continuous sheet of plasma cells encroaching on the growth plate and found within endosteal resorption pits that perforate the cortical shell. Trabecular bone is also significantly reduced in MM. LIV bone also reveals a tumor burden (yellow-dashed line), but to a lesser extent than that of MM, extending from the diaphysis to the proximal end of the femur. Cortical resorption is also visible, but these pits to do not puncture the periosteal surface of the bone. Mitigation of trabecular bone at the distal metaphysis is also visible in LIV as compared to MM.

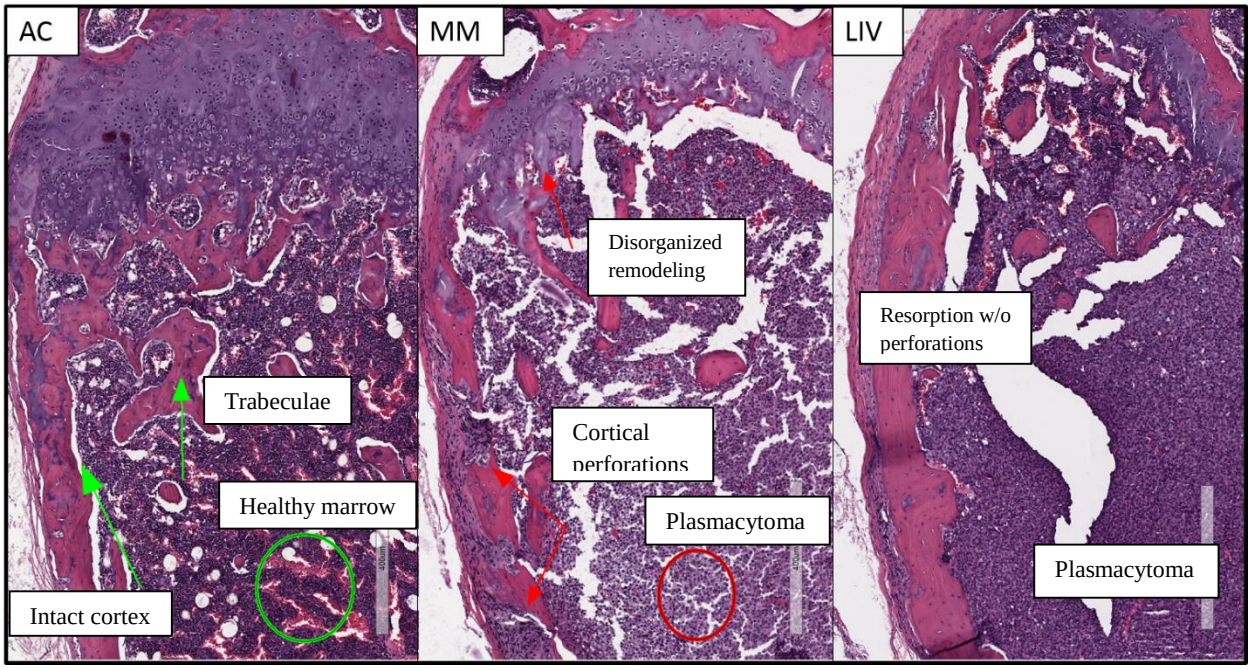

Figure 10. Histological sections of nuclear-stained (H&E) femurs (6.3x) at the distal metaphysis. AC bone shows no evidence of damage to the cortical shell or trabeculae. Healthy marrow in AC is evidenced by an abundance erythrocyte, adipocyte, granulocyte, and reticulocyte presence. Conversely, the endosteal surface in MM reveals extensive cortical perforations (osteolytic lesions) proximal to the growth plate which are filled with myeloma cells as well as disorganized, woven bone along the endosteal surface and at the growth plate. Confluent sheets of myeloma cells are visible across the marrow space in MM without the presence of healthy marrow constituents, leading to a diagnosis of anemia, neutropenia, and leukopenia. While the tumor burden is present in the metaphysis, moderate evidence of healthy marrow is also visible in the marrow of LIV. Though sites of resorption along the endosteal surface are visible in LIV, they have not reached the periosteal surface. Together, this demonstrates myelomas osteolytic capacity, and LIV's ability to mitigate the effects on both the bone and the marrow.

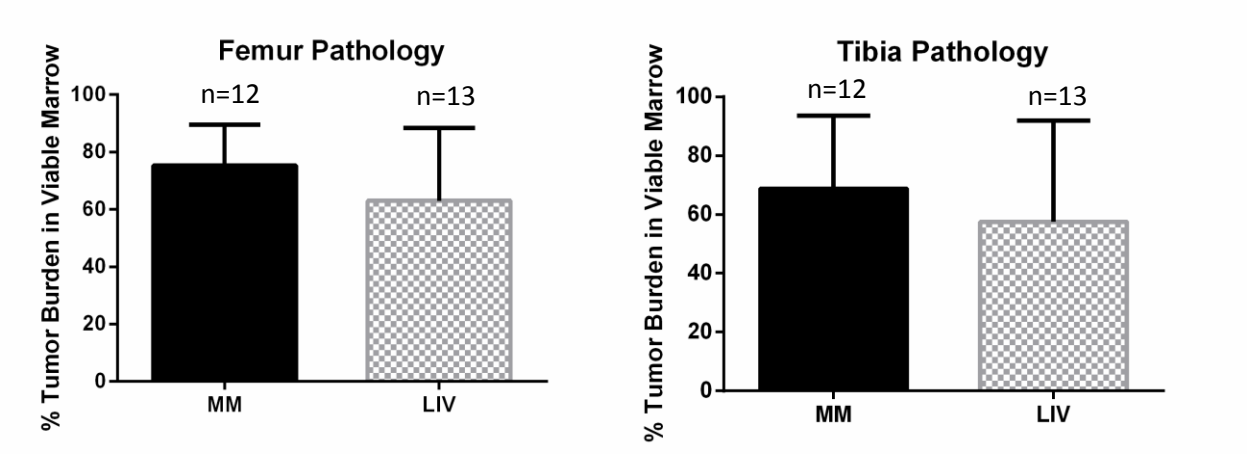

Figure 11. Gross histological quantification of total percentage of viable plasmacytoma infiltration throughout the marrow cavity. Semi-quantitative histopathological estimates of the tumor burden in the viable marrow across the femoral marrow space indicate a 75% infiltration of the disease in MM, with a 61% (p=0.07) invasion in LIV (Fig. 10). The same analysis was performed with the tibial marrow space resulting in 69% occupation of MM marrow, contrasted by 57% (p=0.18) in the marrow of LIV. These values were not statistically significant, but demonstrate a trend towards reduced tumor burden within the bone marrow.

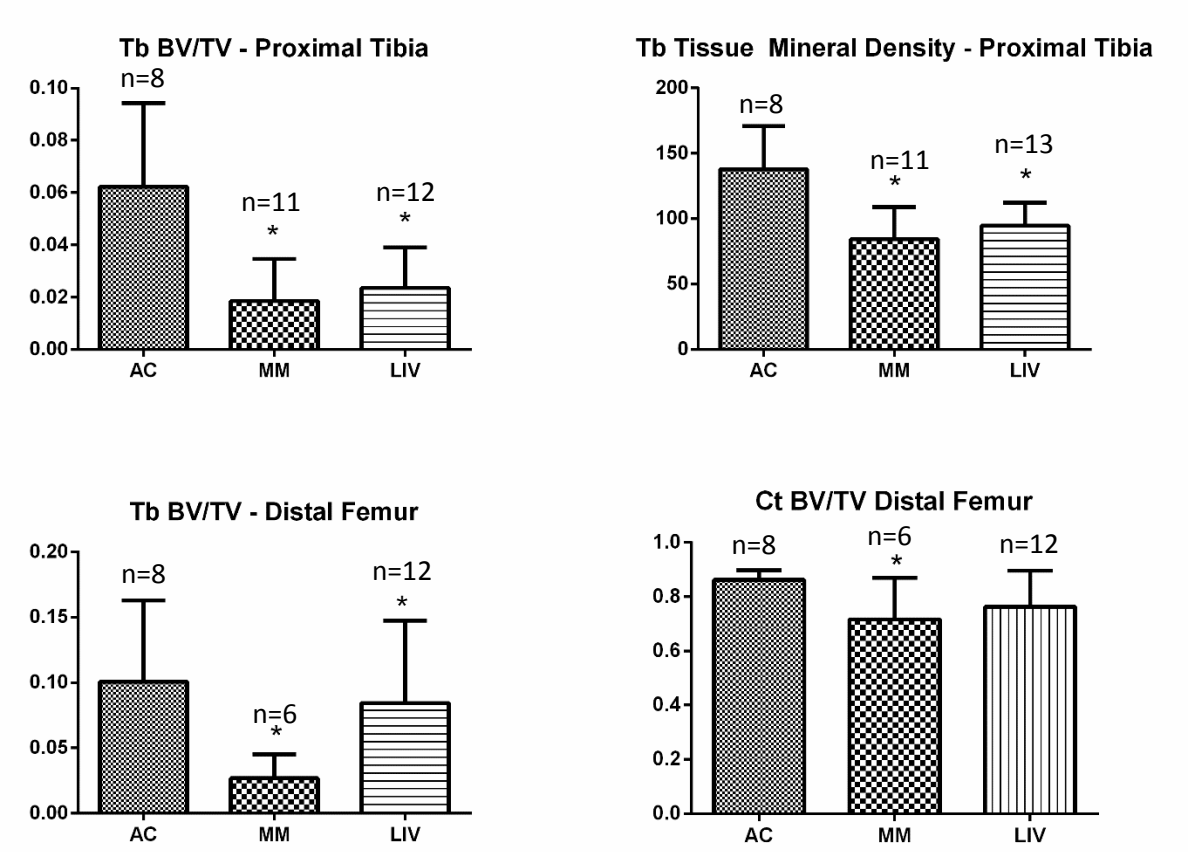

Figure 12. Micro-CT analysis of segmented bone parameters in the femur and tibia were used to measure differences in bone quantity and quality. Distal femora demonstrated a -73% ($p<0.04$) lower trabecular bone volume fraction (BV/TV) in MM as compared to AC. In contrast, the mechanically stimulated LIV group had a +36% greater BV/TV ($p<0.05$) as compared to MM. Cortical BV/TV of the femoral diaphysis was -16% ($p<0.03$) lower in MM as compared to AC, while LIV was +6% greater than MM (nsd). Trabecular BV/TV in the proximal tibiae was -70% lower in MM versus AC, but +27% greater in LIV vs AC (nsd). Tissue mineral density in the tibiae (Tb. Mean 1) was -39% ($p<0.001$) lower in MM as compared to AC, while a +13% (nsd) increase was measured in LIV as compared to MM.

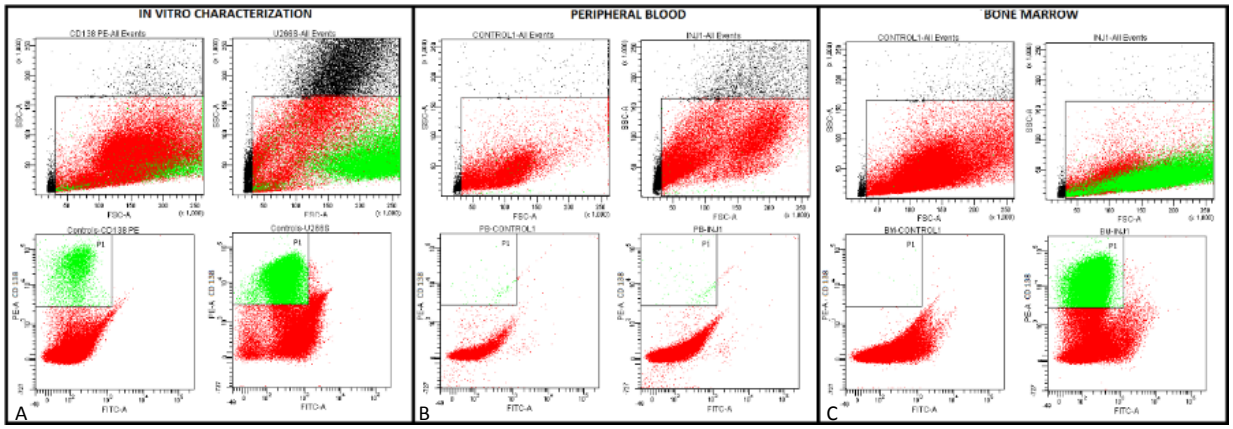

Figure 13. Engraftment efficacy of U266β1 partially determined by FACS analysis. A) *In vitro* characterization of the surface marker CD138 for the U266β1 cell line. B) At sacrifice PB was harvested and tested for presence of $CD138^{+}$ cells, which were undetected in all animals. C) Homing of the injected cells exclusively to the bone marrow cavity was confirmed in 25 of the U266β1-injected animals, reflecting the phenotype observed in *in vitro* cultures.

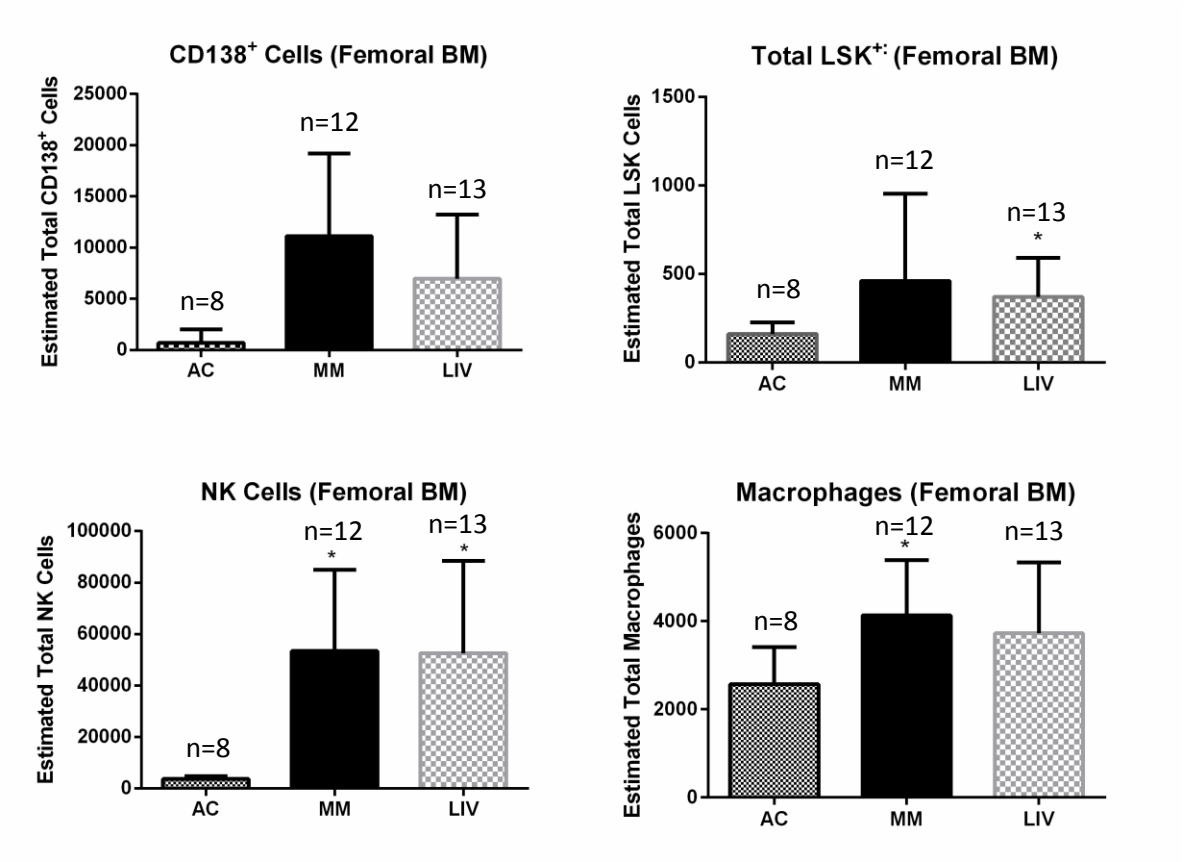

Figure 14. FACS analysis of femoral bone marrow hematopoietic component. At sacrifice and as compared to AC, FACS of BM from the left femur of LIV revealed a -37% (p=0.08) decrease in $CD138^+$ cells as compared to MM. NK cells in MM were 1330% (p=0.0029) greater than in AC, while there were -20% (p=0.94) fewer in LIV as compared to MM. Total mature macrophages were +61% (p=0.0247) greater in MM as compared to AC, while there were -10% (p=0.15) fewer in LIV as compared to MM. LT-HSC (LSK) were +187.5% (p=0.08) greater in MM as compared to AC, while there were -20% (nsd) fewer in LIV versus MM. (* $p<0.05$ relative to AC)

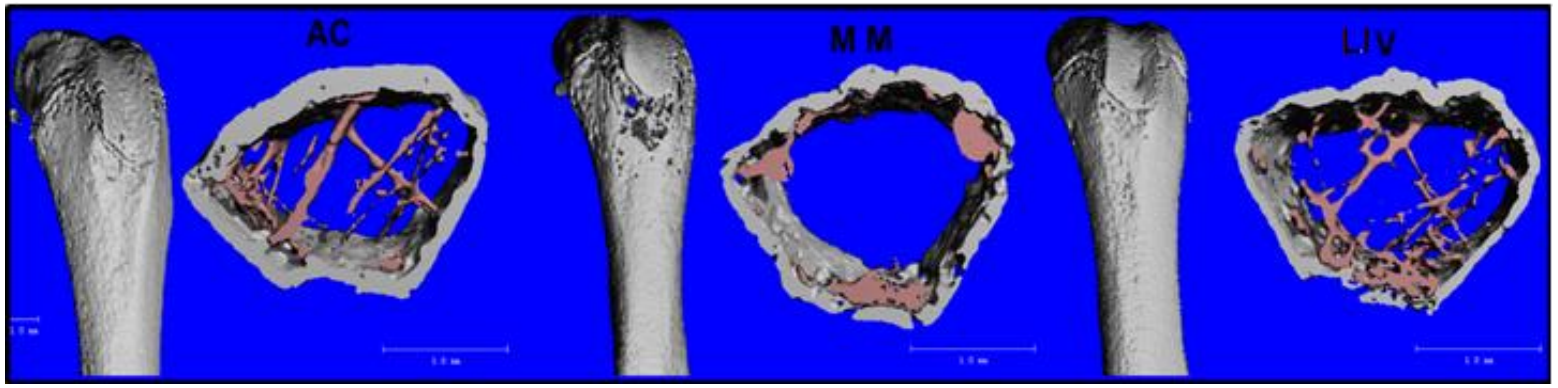

Figure 15. Representative µCT (resolution = 10µm) whole bone and transverse reconstructions of distal femora of 15w-old NSG mice. AC bones demonstrate healthy periosteal surface architecture and intact trabecular bone proximal to the epiphyseal growth plate. Cortical perforations and extensive trabecular destruction were observed in MM, demonstrating the consequences of the engraftment. These losses were somewhat mitigated in LIV, preserving moderate thickness in the cortical shell and retaining trabecular bone volume.

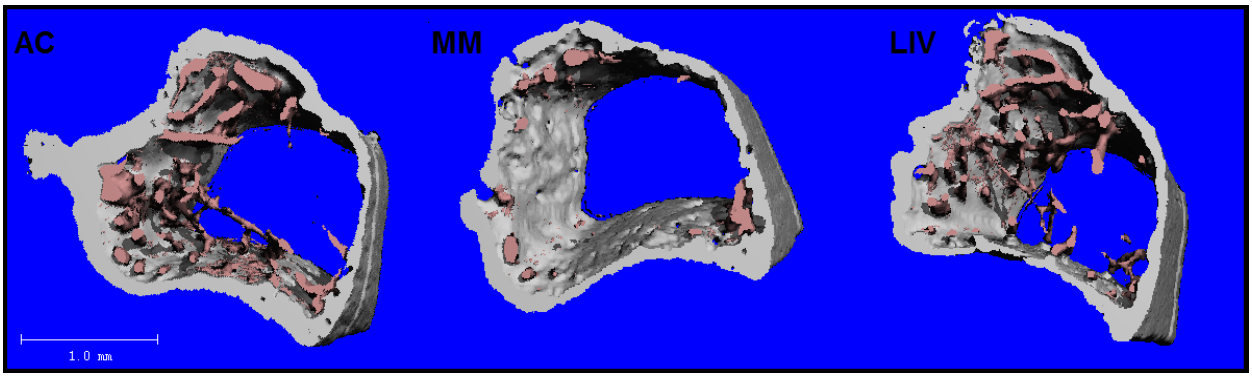

Figure 16. Representative μCT (resolution = 10μm) transverse cross-sectional reconstructions of proximal tibiae in 15w-old NSG mice. AC bones demonstrate healthy trabecular formations distal to the epiphyseal growth plate and a continuous cortical shell. Cortical thinning and extensive trabecular destruction were observed in MM, demonstrating the pathology associated with U266β1's engraftment into the medullary canal. These skeletal losses were somewhat reduced in LIV, preserving moderate thickness in the cortical shell and retaining trabecular integrity.

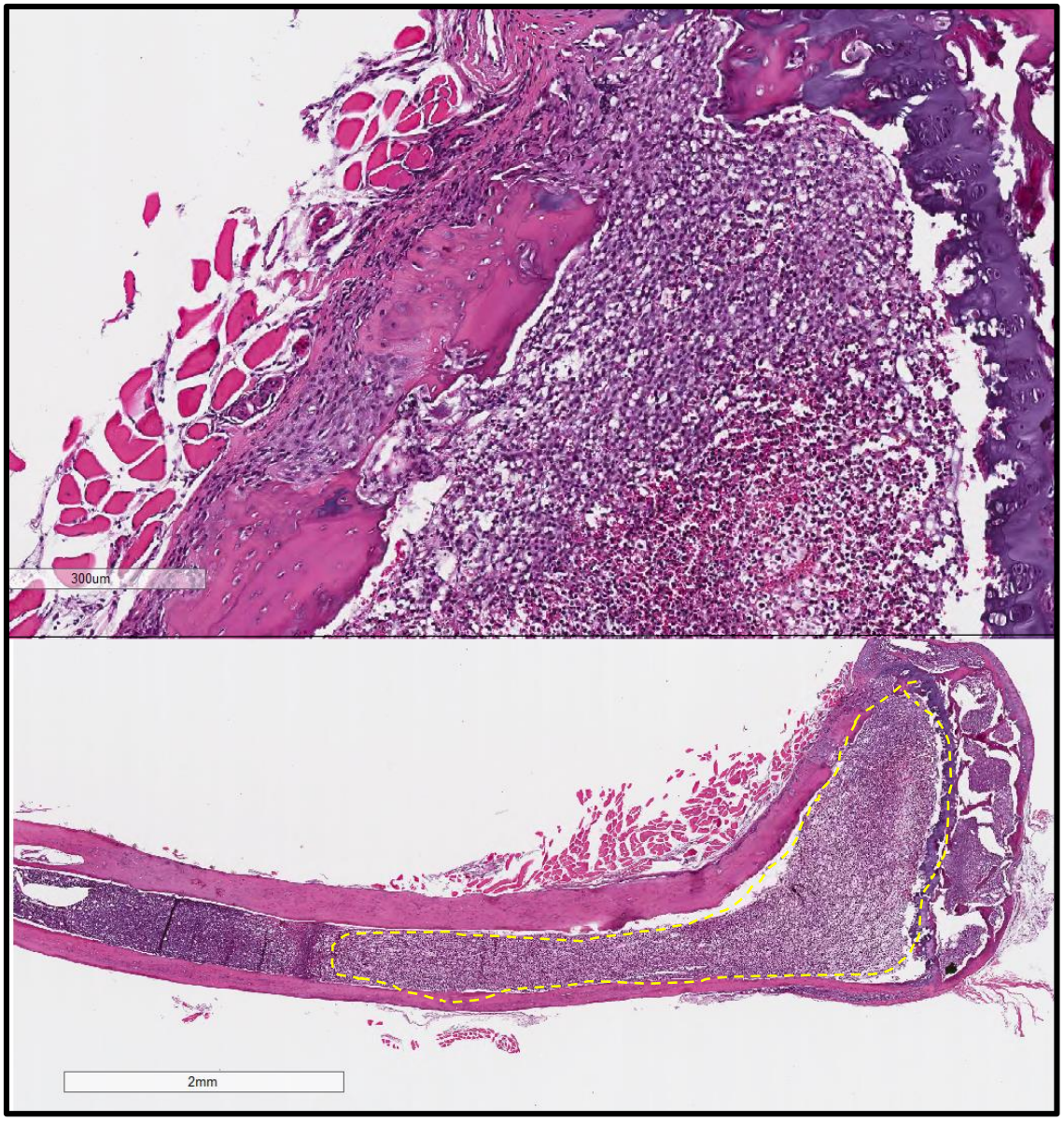

Figure 17. (7.7x, H&E) Focal necrosis (yellow-dashed line) of the tumor within the bone marrow compartment of MM tibiae (n=6). Instance of zonal necrosis of the tumor was isolated to the diseased-only (MM) group indicating the advanced stage of disease progression.

Target Population	Peripheral Blood			Bone Marrow		
	AC	LIV	Difference	AC	LIV	Difference
MSC				4280 ± 2448	2036 ± 981	-52% p = 0.009
HSC				4255 ± 1821	3769 ± 1638	-8% p = 0.25
T-helper Lymphocytes ($CD4^+$)	$2.34x10^5$ ± $2.54x10^5$	$2.79x10^5$ ± $2.22x10^5$	+19% p = 0.28	$2.49x10^5$ ± $1.49x10^5$	$2.08x10^5$ ± $6.84x10^4$	-17% p = 0.13
Cytotoxic T Lymphocytes ($CD8^+$)	$1.13x10^5$ ± $1.53x10^5$	$1.11x10^5$ ± $8.96x10^4$	+2% p = 0.48	$3.99x10^5$ ± $1.03x10^5$	$3.82x10^5$ ± $1.26 x10^5$	-4% p = 0.31
B Lymphocytes ($CD19^+$)	$8.12x10^5$ ± $9.57x10^5$	$9.25x10^5$ ± $8.25x10^5$	+14% p = 0.34	$1.92x10^6$ ± $8.12x10^5$	$1.80x10^6$ ± $8.46x10^5$	-6% p = 0.33

Table 1: Absolute numbers and percent differences (with p-values) of distinct cell populations measured in the peripheral blood of bone marrow, of LIV and AC *SWR* mice, as performed by FACS analysis.

WNT unbound to FZD → Degradation of ß-Catenin

WNT bound to FZD → Translocation of ß-Catenin to nucleus

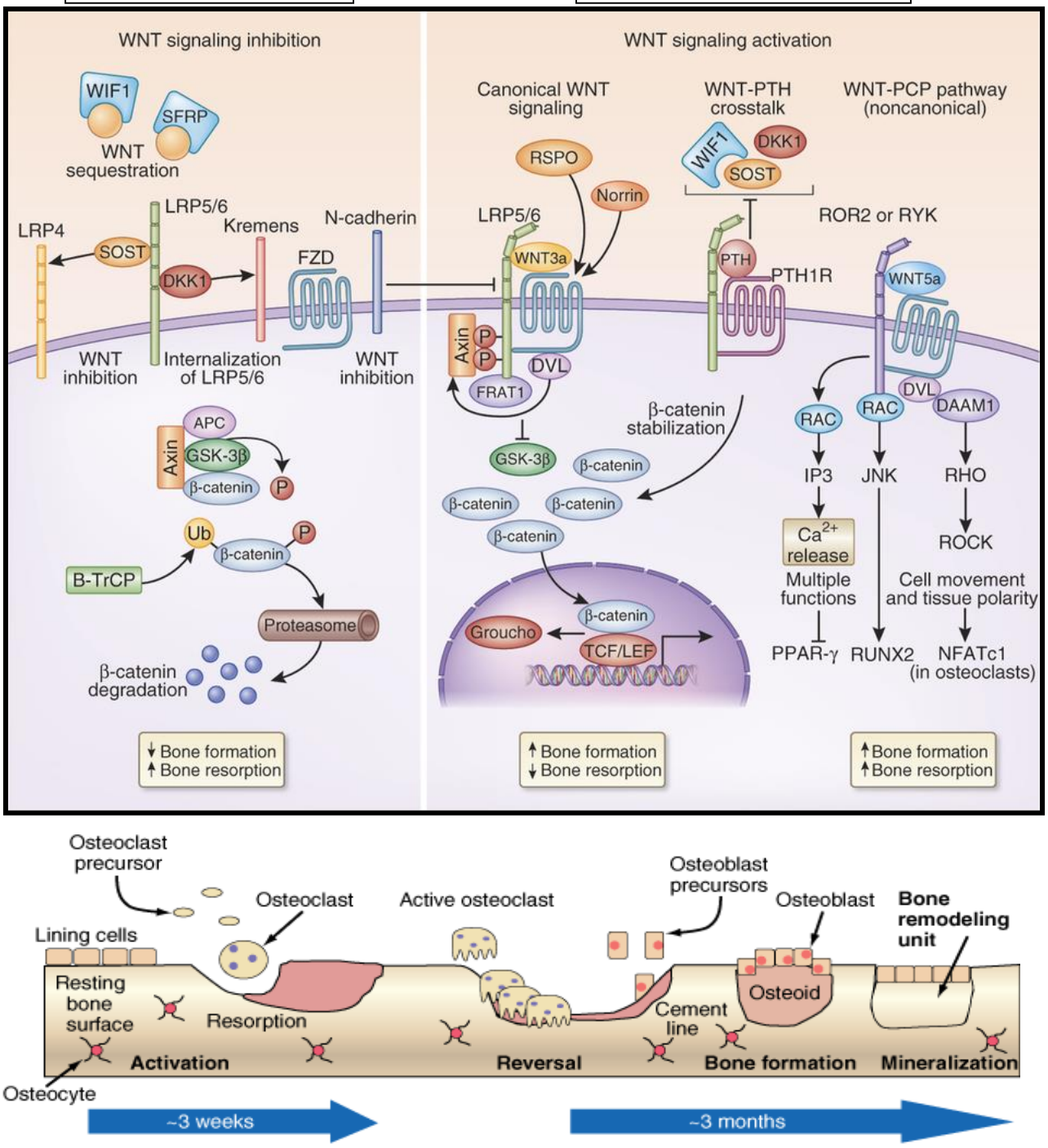

Illustration 1: *Wnt*/β-catenin involvement in bone remodeling. Inhibition of the canonical pathway is conducive to bone resorption, whereas activation is permissive to bone formation. This pathway is shared along the stem cell differentiation pathway. Dysregulation can lead to oncogenic events. Bone remodeling is initiated by resorption of old bone, followed by osteoblast bone formation, and finally osteoid mineralization of the matrix. (Modified from *Nature Medicine* 19, 179–192 (2013) and Fauci AS; *Harrison's Principles of Internal Medicine*; 17th ed.)

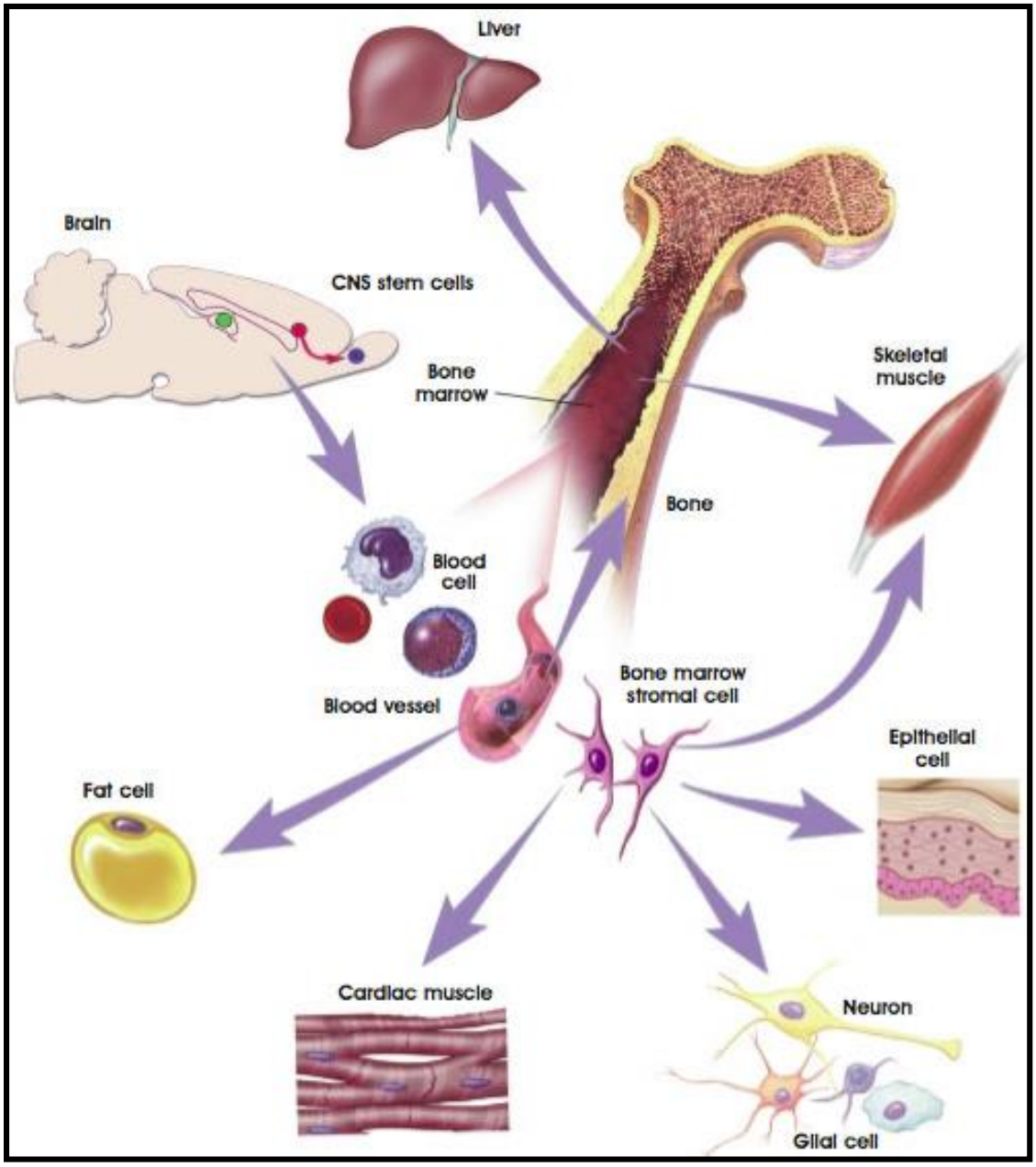

Illustration 2: Bone marrow microenvironment demonstrating mesenchymal (stromal) stem cell differentiation from pluripotency into epithelial, muscle, connective, or nervous tissue depending on molecular and mechanical signaling cues. (Reprinted from *National Institutes of Health*; 2001)

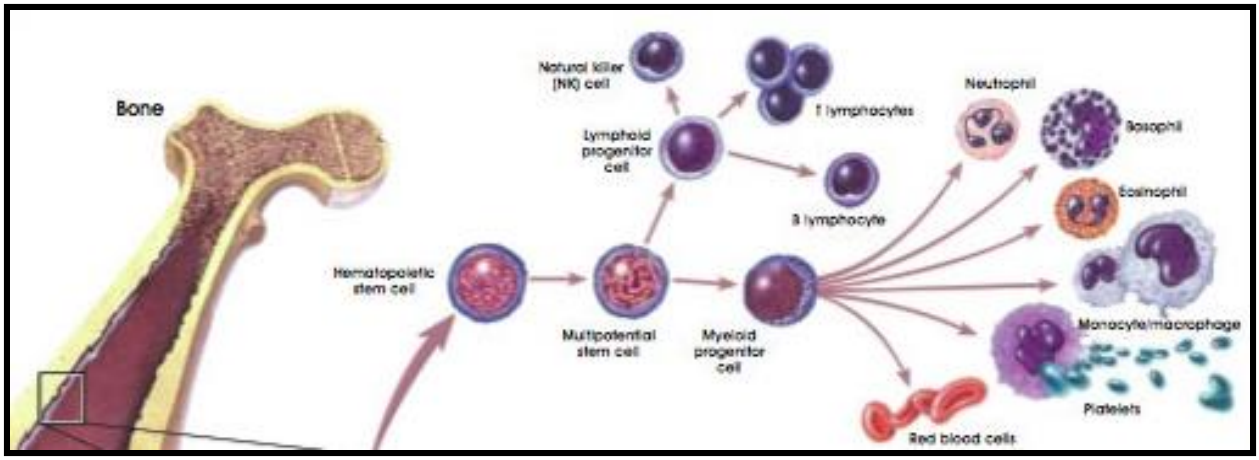

Illustration 3: Bone marrow microenvironment detailing the hematopoietic stem cell differentiation pathway from pluripotency to either lymphoid or myeloid lineage specification. (Reprinted from *National Institutes of Health*; 2001)

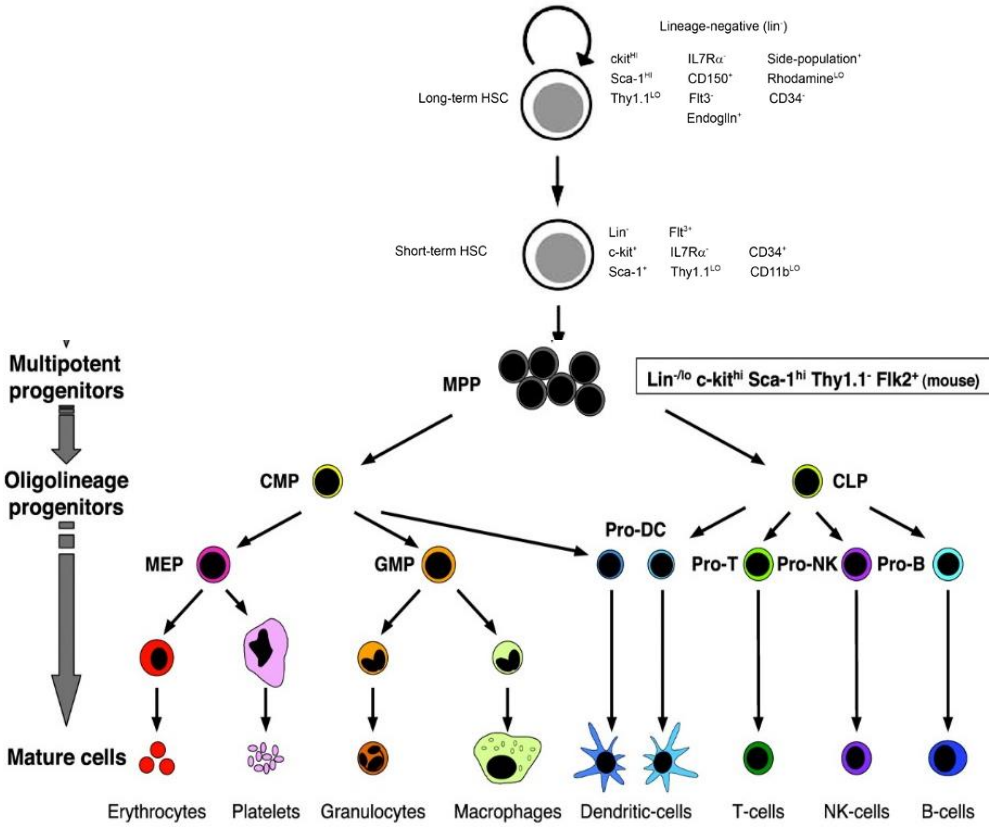

Illustration 4: Hematopoietic stem cell and progenitor differentiation pathways. Long-term HSCs (SP^{KLS}) are capable of self-renewal and differentiating into LSK (short-term HSCs). LSK HSCs are abundant during immune responses as they subsequently undergo lineage specific differentiation. (Modified from *PNAS; 2003,100 (supp1)* and Nameth D, et al; *Cell Research* (2007) **17:**746–758.)

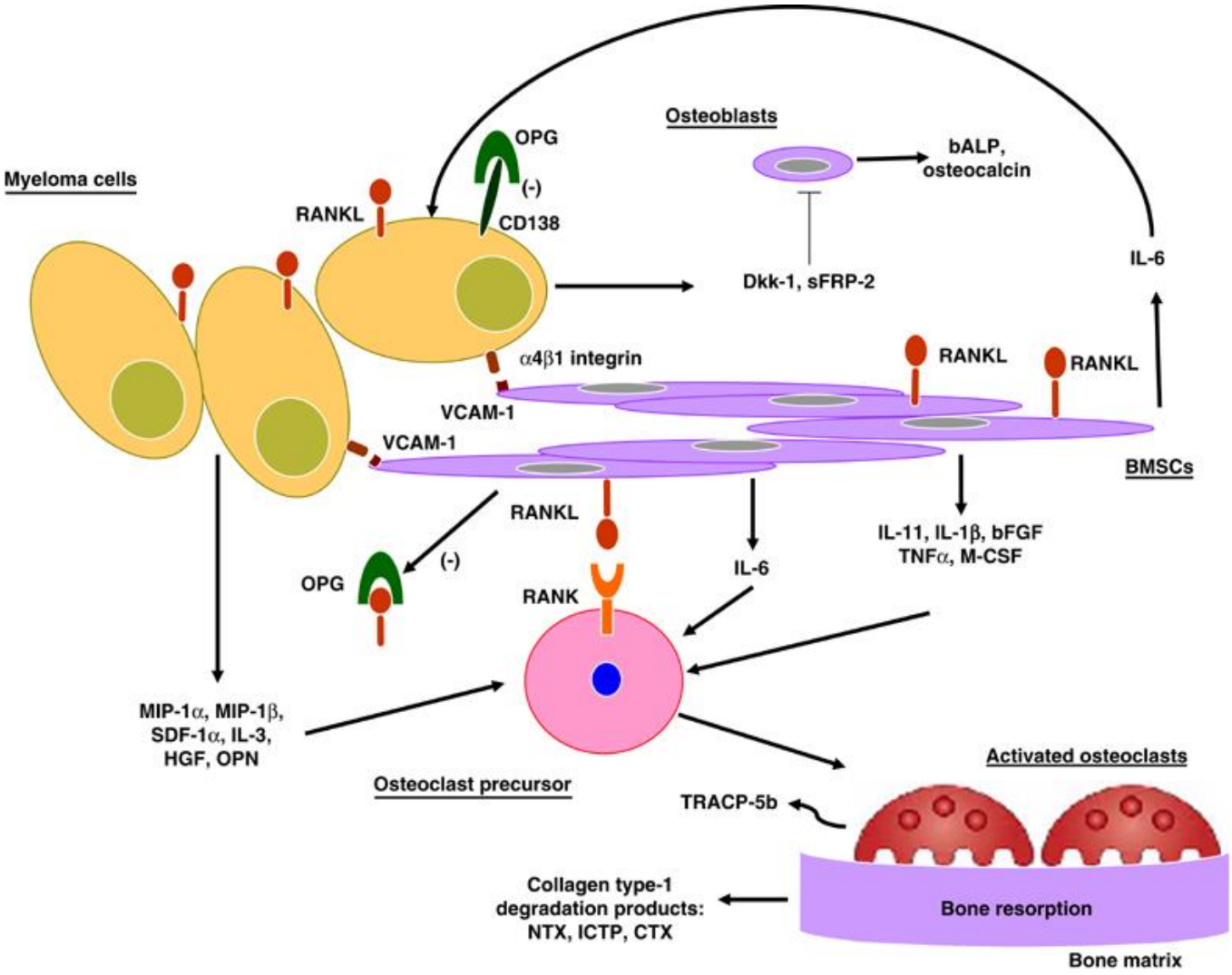

Illustration 5: Mechanism of myeloma bone disease. Myeloma plasma cells and bone marrow-derived MSCs secrete factors that drive hematopoiesis of osteoclastic precursors. RANKL, bound to MSCs and myeloma cells, activate osteoclasts to resorb bone matrix and release TRAP-5b. OPG is produced in lower concentrations and is also eliminated by MM-bound CD138 so the ratio of RANKL:OPG favors osteoclast-mediated resorption. IL6, also secreted by MSCs, feeds back to myeloma cells to further tumorigenesis and at the same time activates osteoclast activity. Myeloma cells secrete DKK-1 to inhibit bone formation by down regulating osteoblast activity. Inflammatory factors are secreted by the myeloma cells and released from resorbed bone, which furthers the persistence of resorption-activity. (Reprinted from *Leukemia* (2007) **21,** 1875–1884)

Bibiology graphy

1. Wolff, J., *The Law of Bone Remodeling*, 1986, Springer: Berlin. p. 126.
2. Wolff, J., *The Law of Transformation of the Bone.* Virchow's Archiv, 1870. **50**(3): p. 389-453.
3. Burstein, A.H., et al., *The ultimate properties of bone tissue: the effects of yielding.* J Biomech, 1972. **5**(1): p. 35-44.
4. Reilly, D.T., A.H. Burstein, and V.H. Frankel, *The elastic modulus for bone.* J Biomech, 1974. **7**(3): p. 271-5.
5. Carter, D.R., et al., *Uniaxial fatigue of human cortical bone. The influence of tissue physical characteristics.* J Biomech, 1981. **14**(7): p. 461-70.
6. Warden, S.J., et al., *Bone adaptation to a mechanical loading program significantly increases skeletal fatigue resistance.* J Bone Miner Res, 2005. **20**(5): p. 809-16.
7. Qin, Y.X., C.T. Rubin, and K.J. McLeod, *Nonlinear dependence of loading intensity and cycle number in the maintenance of bone mass and morphology.* J Orthop Res, 1998. **16**(4): p. 482-9.
8. Rubin, J., C. Rubin, and C.R. Jacobs, *Molecular pathways mediating mechanical signaling in bone.* Gene, 2006. **367**: p. 1-16.
9. Crockett, J.C., et al., *Bone remodelling at a glance.* J Cell Sci, 2011. **124**(Pt 7): p. 991-8.
10. Boyce, B.F. and L. Xing, *The RANKL/RANK/OPG pathway.* Curr Osteoporos Rep, 2007. **5**(3): p. 98-104.
11. Boyce, B.F. and L. Xing, *Biology of RANK, RANKL, and osteoprotegerin.* Arthritis Res Ther, 2007. **9 Suppl 1**: p. S1.
12. Castillo, A.B., et al., *Estrogen receptor-beta regulates mechanical signaling in primary osteoblasts.* Am J Physiol Endocrinol Metab, 2014. **306**(8): p. E937-44.
13. Young, S.R., et al., *Focal adhesion kinase is important for fluid shear stress-induced mechanotransduction in osteoblasts.* J Bone Miner Res, 2009. **24**(3): p. 411-24.
14. Jones, E.A., et al., *Mesenchymal stem cells and skeletal regeneration*. vi, 66 pages.
15. Prockop, D.J., *Marrow stromal cells as stem cells for nonhematopoietic tissues.* Science, 1997. **276**(5309): p. 71-4.
16. Pittenger, M.F., et al., *Multilineage potential of adult human mesenchymal stem cells.* Science, 1999. **284**(5411): p. 143-147.
17. Caplan, A.I., *Mesenchymal stem cells.* J Orthop Res, 1991. **9**(5): p. 641-50.
18. Jones, E. and X. Yang, *Mesenchymal stem cells and bone regeneration: current status.* Injury, 2011. **42**(6): p. 562-8.
19. Ohishi, M. and E. Schipani, *Bone marrow mesenchymal stem cells.* J Cell Biochem, 2010. **109**(2): p. 277-82.
20. Pittenger, M.F., et al., *Multilineage potential of adult human mesenchymal stem cells.* Science, 1999. **284**(5411): p. 143-7.
21. Bielby, R., E. Jones, and D. McGonagle, *The role of mesenchymal stem cells in maintenance and repair of bone.* Injury, 2007. **38 Suppl 1**: p. S26-32.
22. Blanchet, M.R. and K.M. McNagny, *Stem cells, inflammation and allergy.* Allergy Asthma Clin Immunol, 2009. **5**(1): p. 13.
23. Challen, G.A., et al., *Mouse hematopoietic stem cell identification and analysis.* Cytometry A, 2009. **75**(1): p. 14-24.

24. Fischer, K.D. and D.K. Agrawal, *Hematopoietic stem and progenitor cells in inflammation and allergy.* Front Immunol, 2013. **4**: p. 428.
25. Weinberg, R.A., *The biology of cancer*. 2007, New York: Garland Science.
26. Bapat, S., *Cancer stem cells*. 2009, Hoboken, N.J.: John Wiley & Sons. xiv, 245 p., 12 p. of plates.
27. Mortensen, B.T., et al., *Changing bone marrow micro-environment during development of acute myeloid leukaemia in rats.* Br J Haematol, 1998. **102**(2): p. 458-64.
28. Gerson, S.L., *Mesenchymal stem cells: no longer second class marrow citizens.* Nat Med, 1999. **5**(3): p. 262-4.
29. Kim, H., J.H. Lee, and H. Suh, *Interaction of mesenchymal stem cells and osteoblasts for in vitro osteogenesis.* Yonsei Med J, 2003. **44**(2): p. 187-97.
30. Martins, A., et al., *The influence of patterned nanofiber meshes on human mesenchymal stem cell osteogenesis.* Macromol Biosci, 2011. **11**(7): p. 978-87.
31. Park, J.S., et al., *The promotion of chondrogenesis, osteogenesis, and adipogenesis of human mesenchymal stem cells by multiple growth factors incorporated into nanosphere-coated microspheres.* Biomaterials, 2011. **32**(1): p. 28-38.
32. Gershovich, J.G., et al., *Enhanced osteogenesis in cocultures with human mesenchymal stem cells and endothelial cells on polymeric microfiber scaffolds.* Tissue Eng Part A, 2013. **19**(23-24): p. 2565-76.
33. Kaivosoja, E., et al., *Osteogenesis of human mesenchymal stem cells on micro-patterned surfaces.* J Biomater Appl, 2013. **27**(7): p. 862-71.
34. Nikukar, H., et al., *Osteogenesis of mesenchymal stem cells by nanoscale mechanotransduction.* ACS Nano, 2013. **7**(3): p. 2758-67.
35. He, Y., et al., *Ectopic osteogenesis and scaffold biodegradation of tissue engineering bone composed of chitosan and osteo-induced bone marrow mesenchymal stem cells in vivo.* Chin Med J (Engl), 2014. **127**(2): p. 322-8.
36. Dabiri, G., D. Heiner, and V. Falanga, *The emerging use of bone marrow-derived mesenchymal stem cells in the treatment of human chronic wounds.* Expert Opin Emerg Drugs, 2013.
37. Kearney, E.M., et al., *Tensile strain as a regulator of mesenchymal stem cell osteogenesis.* Ann Biomed Eng, 2010. **38**(5): p. 1767-79.
38. Manier, S., et al., *Bone marrow microenvironment in multiple myeloma progression.* J Biomed Biotechnol, 2012. **2012**: p. 157496.
39. Nair, J.R., C.H. Rozanski, and K.P. Lee, *Under one roof: The bone marrow survival niche for multiple myeloma and normal plasma cells.* Oncoimmunology, 2012. **1**(3): p. 388-389.
40. Noll, J.E., et al., *Tug of war in the haematopoietic stem cell niche: do myeloma plasma cells compete for the HSC niche?* Blood Cancer J, 2012. **2**: p. e91.
41. Mazziotti, G., E. Canalis, and A. Giustina, *Drug-induced osteoporosis: mechanisms and clinical implications.* Am J Med. **123**(10): p. 877-84.
42. Rubin, C.D., *Emerging concepts in osteoporosis and bone strength.* Curr Med Res Opin, 2005. **21**(7): p. 1049-56.
43. Galea, G.L., et al., *Estrogen receptor alpha mediates proliferation of osteoblastic cells stimulated by estrogen and mechanical strain, but their acute down-regulation of the Wnt antagonist Sost is mediated by estrogen receptor beta.* J Biol Chem, 2013. **288**(13): p. 9035-48.

44. Armstrong, V.J., et al., *Wnt/beta-catenin signaling is a component of osteoblastic bone cell early responses to load-bearing and requires estrogen receptor alpha.* J Biol Chem, 2007. **282**(28): p. 20715-27.
45. Kondoh, S., et al., *Estrogen receptor alpha in osteocytes regulates trabecular bone formation in female mice.* Bone, 2014. **60**: p. 68-77.
46. Melville, K.M., et al., *Female mice lacking estrogen receptor-alpha in osteoblasts have compromised bone mass and strength.* J Bone Miner Res, 2014. **29**(2): p. 370-9.
47. Rubinacci, A., et al., *Ovariectomy sensitizes rat cortical bone to whole-body vibration.* Calcif Tissue Int, 2008. **82**(4): p. 316-26.
48. Jiang, J.M., S.M. Sacco, and W.E. Ward, *Ovariectomy-induced hyperphagia does not modulate bone mineral density or bone strength in rats.* J Nutr, 2008. **138**(11): p. 2106-10.
49. Pfeilschifter, J. and I.J. Diel, *Osteoporosis due to cancer treatment: pathogenesis and management.* J Clin Oncol, 2000. **18**(7): p. 1570-93.
50. Tisdale, M.J., *Wasting in cancer.* J Nutr, 1999. **129**(1S Suppl): p. 243S-246S.
51. Ramaswamy, B. and C.L. Shapiro, *Osteopenia and osteoporosis in women with breast cancer.* Semin Oncol, 2003. **30**(6): p. 763-75.
52. Raghavan, D., *Textbook of uncommon cancer / editors, Derek Raghavan ... [et al.]*. 3rd ed. 2006, Chichester, West Sussex, England ; Hoboken, NJ: Wiley. xvii, 857 p.
53. Sehouli, J., et al., *Granulosa cell tumor of the ovary: 10 years follow-up data of 65 patients.* Anticancer Res, 2004. **24**(2C): p. 1223-9.
54. Wolf, J.K., et al., *Radiation treatment of advanced or recurrent granulosa cell tumor of the ovary.* Gynecol Oncol, 1999. **73**(1): p. 35-41.
55. Vassilopoulou-Sellin, R., et al., *Osteopenia in young adult survivors of childhood cancer.* Med Pediatr Oncol, 1999. **32**(4): p. 272-8.
56. Krishnamoorthy, P., et al., *Osteopenia in children who have undergone posterior fossa or craniospinal irradiation for brain tumors.* Arch Pediatr Adolesc Med, 2004. **158**(5): p. 491-6.
57. Body, J.J., *Increased fracture rate in women with breast cancer: a review of the hidden risk.* BMC Cancer, 2011. **11**: p. 384.
58. Baxter, N.N., et al., *Risk of pelvic fractures in older women following pelvic irradiation.* JAMA, 2005. **294**(20): p. 2587-93.
59. Barr, R.D., et al., *Osteopenia in children surviving brain tumours.* Eur J Cancer, 1998. **34**(6): p. 873-7.
60. McKean, H., et al., *Are cancer survivors/patients knowledgeable about osteoporosis? Results from a survey of 285 chemotherapy-treated cancer patients and their companions.* J Nutr Educ Behav, 2008. **40**(3): p. 144-8.
61. Ratzkowski, E., M. Frankel, and A. Hochman, *Bone metastases, osteoporosis and radiation necrosis in breast cancer.* Clin Radiol, 1967. **18**(2): p. 146-53.
62. Roodman, G.D., *Pathogenesis of myeloma bone disease.* J Cell Biochem, 2010. **109**(2): p. 283-91.
63. Galson, D.L., R. Silbermann, and G.D. Roodman, *Mechanisms of multiple myeloma bone disease.* Bonekey Rep, 2012. **1**: p. 135.
64. Green, D.E., et al., *Altered Composition of Bone as Triggered by Irradiation Facilitates the Rapid Erosion of the Matrix by Both Cellular and Physicochemical Processes.* Plos One, 2013. **8**(5).

65. Green, D.E., et al., *Devastation of adult stem cell pools by irradiation precedes collapse of trabecular bone quality and quantity.* J Bone Miner Res, 2012. **27**(4): p. 749-59.
66. Cao, X., et al., *Irradiation induces bone injury by damaging bone marrow microenvironment for stem cells.* Proc Natl Acad Sci U S A, 2011. **108**(4): p. 1609-14.
67. Chabner, B. and D.L. Longo, *Cancer chemotherapy and biotherapy : principles and practice*. 4th ed. 2006, Philadelphia: Lippincott Williams & Wilkins. xv, 879 p.
68. Lu, J.J., L.W. Brady, and A.A. Abitbol, *Radiation oncology : an evidence-based approach*. Medical radiology - radiation oncology. 2008, Berlin: Springer. xx, 675 p.
69. Kastler, B. and H. Boulahdour, *Interventional radiology in pain treatment*. 2007, Berlin ; New York: Springer. xx, 202 p.
70. Colombo, N., et al., *Non-epithelial ovarian cancer: ESMO Clinical Practice Guidelines for diagnosis, treatment and follow-up.* Ann Oncol, 2012. **23 Suppl 7**: p. vii20-6.
71. Moreau, P., et al., *Multiple myeloma: ESMO Clinical Practice Guidelines for diagnosis, treatment and follow-up.* Ann Oncol, 2013. **24 Suppl 6**: p. vi133-7.
72. Graham-Pole, J., et al., *High-dose melphalan therapy for the treatment of children with refractory neuroblastoma and Ewing's sarcoma.* Am J Pediatr Hematol Oncol, 1984. **6**(1): p. 17-26.
73. Lazarus, H.M., et al., *Intensive melphalan chemotherapy and cryopreserved autologous bone marrow transplantation for the treatment of refractory cancer.* J Clin Oncol, 1983. **1**(6): p. 359-67.
74. Reimer, R.R., et al., *Acute leukemia after alkylating-agent therapy of ovarian cancer.* N Engl J Med, 1977. **297**(4): p. 177-81.
75. Einhorn, N., *Acute leukemia after chemotherapy (melphalan).* Cancer, 1978. **41**(2): p. 444-7.
76. Rosner, F. and H. Grunwald, *Multiple myeloma terminating in acute leukemia. Report of 12 cases and review of the literature.* Am J Med, 1974. **57**(6): p. 927-39.
77. Garrett, M.J., *Letter: Teratogenic effects of combination chemotherapy.* Ann Intern Med, 1974. **80**(5): p. 667.
78. Ficarra, G. and F. Beninati, *Bisphosphonate-related osteonecrosis of the jaws: an update on clinical, pathological and management aspects.* Head Neck Pathol, 2007. **1**(2): p. 132-40.
79. Wehrhan, F., et al., *Bisphosphonate-associated osteonecrosis of the jaw is linked to suppressed TGFbeta1-signaling and increased Galectin-3 expression: a histological study on biopsies.* J Transl Med, 2011. **9**: p. 102.
80. Orwoll, E.S., et al., *The effect of teriparatide [human parathyroid hormone (1-34)] therapy on bone density in men with osteoporosis.* J Bone Miner Res, 2003. **18**(1): p. 9-17.
81. McTiernan, A., et al., *The Physical Activity for Total Health (PATH) Study: rationale and design.* Med Sci Sports Exerc, 1999. **31**(9): p. 1307-12.
82. Kushi, L.H., et al., *American Cancer Society Guidelines on Nutrition and Physical Activity for cancer prevention: reducing the risk of cancer with healthy food choices and physical activity.* CA Cancer J Clin, 2006. **56**(5): p. 254-81; quiz 313-4.
83. Campbell, K.L. and A. McTiernan, *Exercise and biomarkers for cancer prevention studies.* J Nutr, 2007. **137**(1 Suppl): p. 161S-169S.
84. Warden, S.J., et al., *Exercise when young provides lifelong benefits to bone structure and strength.* J Bone Miner Res, 2007. **22**(2): p. 251-9.

85. (US), S.G., in *Bone Health and Osteoporosis: A Report of the Surgeon General*. 2004: Rockville (MD).
86. Del Fabbro, E., *Nutrition and the cancer patient*. 2010, Oxford ; New York: Oxford University Press. xiv, 519 p.
87. Rogers, L.Q., et al., *Effects of a physical activity behavior change intervention on inflammation and related health outcomes in breast cancer survivors: pilot randomized trial.* Integr Cancer Ther, 2013. **12**(4): p. 323-35.
88. Lynch, B.M., H.K. Neilson, and C.M. Friedenreich, *Physical activity and breast cancer prevention.* Recent Results Cancer Res, 2011. **186**: p. 13-42.
89. Rogers, C.J., et al., *Physical activity and cancer prevention : pathways and targets for intervention.* Sports Med, 2008. **38**(4): p. 271-96.
90. Friedenreich, C.M. and M.R. Orenstein, *Physical activity and cancer prevention: etiologic evidence and biological mechanisms.* J Nutr, 2002. **132**(11 Suppl): p. 3456S-3464S.
91. Brown, J.K., et al., *Nutrition and physical activity during and after cancer treatment: an American Cancer Society guide for informed choices.* CA Cancer J Clin, 2003. **53**(5): p. 268-91.
92. Rubin, C., et al., *Anabolism. Low mechanical signals strengthen long bones.* Nature, 2001. **412**(6847): p. 603-4.
93. Rubin, C., et al., *Mechanical strain, induced noninvasively in the high-frequency domain, is anabolic to cancellous bone, but not cortical bone.* Bone, 2002. **30**(3): p. 445-52.
94. Ozcivici, E., et al., *Mechanical signals as anabolic agents in bone.* Nat Rev Rheumatol. **6**(1): p. 50-9.
95. Sen, B., et al., *Mechanical strain inhibits adipogenesis in mesenchymal stem cells by stimulating a durable beta-catenin signal.* Endocrinology, 2008. **149**(12): p. 6065-75.
96. Pearse, R.N., *Wnt antagonism in multiple myeloma: a potential cause of uncoupled bone remodeling.* Clin Cancer Res, 2006. **12**(20 Pt 2): p. 6274s-6278s.
97. Jiang, Y.G., et al., *Role of Wnt/beta-catenin signaling pathway in epithelial-mesenchymal transition of human prostate cancer induced by hypoxia-inducible factor-1alpha.* Int J Urol, 2007. **14**(11): p. 1034-9.
98. Rubin, C.T. and L.E. Lanyon, *Limb mechanics as a function of speed and gait: a study of functional strains in the radius and tibia of horse and dog.* J Exp Biol, 1982. **101**: p. 187-211.
99. Holguin, N., et al., *Short applications of very low-magnitude vibrations attenuate expansion of the intervertebral disc during extended bed rest.* Spine J, 2009. **9**(6): p. 470-7.
100. Rubin, C., et al., *Prevention of postmenopausal bone loss by a low-magnitude, high-frequency mechanical stimuli: a clinical trial assessing compliance, efficacy, and safety.* J Bone Miner Res, 2004. **19**(3): p. 343-51.
101. Ward, K., et al., *Low magnitude mechanical loading is osteogenic in children with disabling conditions.* J Bone Miner Res, 2004. **19**(3): p. 360-9.
102. Rittweger, J., et al., *Prevention of bone loss during 56 days of strict bed rest by side-alternating resistive vibration exercise.* Bone, 2010. **46**(1): p. 137-47.
103. Wang, H., et al., *Resistive vibration exercise retards bone loss in weight-bearing skeletons during 60 days bed rest.* Osteoporos Int, 2012. **23**(8): p. 2169-78.

104. Ozcivici, E., et al., *Low-level vibrations retain bone marrow's osteogenic potential and augment recovery of trabecular bone during reambulation.* PLoS One, 2010. **5**(6): p. e11178.
105. Xie, L., C. Rubin, and S. Judex, *Enhancement of the adolescent murine musculoskeletal system using low-level mechanical vibrations.* J Appl Physiol (1985), 2008. **104**(4): p. 1056-62.
106. Ozcivici, E., et al., *Mechanical signals as anabolic agents in bone.* Nat Rev Rheumatol, 2010. **6**(1): p. 50-9.
107. Rubin, C.T., et al., *Adipogenesis is inhibited by brief, daily exposure to high-frequency, extremely low-magnitude mechanical signals.* Proc Natl Acad Sci U S A, 2007. **104**(45): p. 17879-84.
108. Luu, Y.K., et al., *Development of diet-induced fatty liver disease in the aging mouse is suppressed by brief daily exposure to low-magnitude mechanical signals.* Int J Obes (Lond). **34**(2): p. 401-5.
109. Sen, B., et al., *Mechanically induced focal adhesion assembly amplifies anti-adipogenic pathways in mesenchymal stem cells.* Stem Cells, 2011. **29**(11): p. 1829-36.
110. Thompson, W.R., et al., *Mechanically activated Fyn utilizes mTORC2 to regulate RhoA and adipogenesis in mesenchymal stem cells.* Stem Cells, 2013. **31**(11): p. 2528-37.
111. Luu, Y.K., et al., *Mechanical Stimulation of Mesenchymal Stem Cell Proliferation and Differentiation Promotes Osteogenesis While Preventing Dietary-Induced Obesity.* Journal of Bone and Mineral Research, 2009. **24**(1): p. 50-61.
112. Sen, B., et al., *Mechanical loading regulates NFATc1 and beta-catenin signaling through a GSK3beta control node.* J Biol Chem, 2009. **284**(50): p. 34607-17.
113. Robinson, J.A., et al., *Wnt/beta-catenin signaling is a normal physiological response to mechanical loading in bone.* J Biol Chem, 2006. **281**(42): p. 31720-8.
114. Sen, B., et al., *mTORC2 regulates mechanically induced cytoskeletal reorganization and lineage selection in marrow-derived mesenchymal stem cells.* J Bone Miner Res, 2014. **29**(1): p. 78-89.
115. Uzer, G., et al., *Vibration induced osteogenic commitment of mesenchymal stem cells is enhanced by cytoskeletal remodeling but not fluid shear.* J Biomech, 2013. **46**(13): p. 2296-302.
116. Dezorella, N., et al., *Mesenchymal stromal cells revert multiple myeloma cells to less differentiated phenotype by the combined activities of adhesive interactions and interleukin-6.* Exp Cell Res, 2009. **315**(11): p. 1904-13.
117. Fowler, J.A., et al., *Bone marrow stromal cells create a permissive microenvironment for myeloma development: a new stromal role for Wnt inhibitor Dkk1.* Cancer Res, 2012. **72**(9): p. 2183-9.
118. Atsuta, I., et al., *Mesenchymal stem cells inhibit multiple myeloma cells via the Fas/Fas ligand pathway.* Stem Cell Res Ther, 2013. **4**(5): p. 111.
119. Zhu, Y., et al., *Human mesenchymal stem cells inhibit cancer cell proliferation by secreting DKK-1.* Leukemia, 2009. **23**(5): p. 925-33.
120. Al-Tonbary, Y.A., et al., *Bone mineral density in newly diagnosed children with neuroblastoma.* Pediatr Blood Cancer, 2011. **56**(2): p. 202-5.
121. Winters-Stone, K.M., et al., *Bone Health and Falls: Fracture Risk in Breast Cancer Survivors With Chemotherapy-Induced Amenorrhea.* Oncol Nurs Forum, 2009. **36**(3): p. 315-325.

122. Edwards, B.J., et al., *Cancer therapy associated bone loss: implications for hip fractures in mid-life women with breast cancer.* Clin Cancer Res, 2011. **17**(3): p. 560-8.
123. Guise, T.A., *Bone loss and fracture risk associated with cancer therapy.* Oncologist, 2006. **11**(10): p. 1121-31.
124. Meyerhardt, J.A., et al., *Physical activity and survival after colorectal cancer diagnosis.* J Clin Oncol, 2006. **24**(22): p. 3527-34.
125. Ogunleye, A.A. and M.D. Holmes, *Physical activity and breast cancer survival.* Breast Cancer Res, 2009. **11**(5): p. 106.
126. Cancer, N.I.o., *Cancer Trends Progress Report - 2007*, 2009.
127. Ligibel, J.A. and H.D. Strickler, *Obesity and its impact on breast cancer: tumor incidence, recurrence, survival, and possible interventions.* Am Soc Clin Oncol Educ Book, 2013: p. 52-9.
128. Wang, R., et al., *Glioblastoma stem-like cells give rise to tumour endothelium.* Nature, 2010. **468**(7325): p. 829-33.
129. Kemp, K., et al., *Chemotherapy-induced mesenchymal stem cell damage in patients with hematological malignancy.* Ann Hematol, 2010. **89**(7): p. 701-13.
130. Gardner, R.V., et al., *Assessing permanent damage to primitive hematopoietic stem cells after chemotherapy using the competitive repopulation assay.* Cancer Chemother Pharmacol, 1993. **32**(6): p. 450-4.
131. Rubin, C., G. Xu, and S. Judex, *The anabolic activity of bone tissue, suppressed by disuse, is normalized by brief exposure to extremely low-magnitude mechanical stimuli.* FASEB J, 2001. **15**(12): p. 2225-9.
132. Judex, S., S. Gupta, and C. Rubin, *Regulation of mechanical signals in bone.* Orthod Craniofac Res, 2009. **12**(2): p. 94-104.
133. Rubin, C., S. Judex, and Y.X. Qin, *Low-level mechanical signals and their potential as a non-pharmacological intervention for osteoporosis.* Age Ageing, 2006. **35 Suppl 2**: p. ii32-ii36.
134. Thompson, W.R., C.T. Rubin, and J. Rubin, *Mechanical regulation of signaling pathways in bone.* Gene, 2012. **503**(2): p. 179-93.
135. Schuster, D.P., *Changes in physiology with increasing fat mass.* Semin Pediatr Surg, 2009. **18**(3): p. 126-35.
136. Cao, J.J., *Effects of obesity on bone metabolism.* J Orthop Surg Res, 2011. **6**: p. 30.
137. Moerman, E.J., et al., *Aging activates adipogenic and suppresses osteogenic programs in mesenchymal marrow stroma/stem cells: the role of PPAR-gamma2 transcription factor and TGF-beta/BMP signaling pathways.* Aging Cell, 2004. **3**(6): p. 379-89.
138. Sen, B., et al., *Mechanical signal influence on mesenchymal stem cell fate is enhanced by incorporation of refractory periods into the loading regimen.* J Biomech, 2010.
139. Li, L., et al., *Human mesenchymal stem cells play a dual role on tumor cell growth in vitro and in vivo.* J Cell Physiol, 2011. **226**(7): p. 1860-7.
140. Roorda, B.D., et al., *Bone marrow-derived cells and tumor growth: contribution of bone marrow-derived cells to tumor micro-environments with special focus on mesenchymal stem cells.* Crit Rev Oncol Hematol, 2009. **69**(3): p. 187-98.
141. Studeny, M., et al., *Mesenchymal stem cells: potential precursors for tumor stroma and targeted-delivery vehicles for anticancer agents.* J Natl Cancer Inst, 2004. **96**(21): p. 1593-603.

142. Spaeth, E.L., et al., *Mesenchymal stem cell transition to tumor-associated fibroblasts contributes to fibrovascular network expansion and tumor progression.* PLoS One, 2009. **4**(4): p. e4992.
143. Sakai, A., *[Space flight/bedrest immobilization and bone. Osteocyte as a sensor of mechanical stress and Wnt signal]*. Clin Calcium, 2012. **22**(12): p. 1829-35.
144. Case, N., et al., *Beta-catenin levels influence rapid mechanical responses in osteoblasts.* J Biol Chem, 2008. **283**(43): p. 29196-205.
145. Gregory, C.A., et al., *The promise of canonical Wnt signaling modulators in enhancing bone repair.* Drug News Perspect, 2006. **19**(8): p. 445-52.
146. Johnson, M.L. and M.A. Kamel, *The Wnt signaling pathway and bone metabolism.* Curr Opin Rheumatol, 2007. **19**(4): p. 376-82.
147. Morin, P.J., *beta-catenin signaling and cancer.* Bioessays, 1999. **21**(12): p. 1021-30.
148. Arend, R.C., et al., *The Wnt/beta-catenin pathway in ovarian cancer: a review.* Gynecol Oncol, 2013. **131**(3): p. 772-9.
149. Zhang, W.M., et al., *Effect of WNT-1 on beta-catenin expression and its relation to Ki-67 and tumor differentiation in oral squamous cell carcinoma.* Oncol Rep, 2005. **13**(6): p. 1095-9.
150. Chen, J., et al., *Wnt/beta-catenin signaling plays an essential role in activation of odontogenic mesenchyme during early tooth development.* Dev Biol, 2009. **334**(1): p. 174-85.
151. Qiao, L., et al., *Dkk-1 secreted by mesenchymal stem cells inhibits growth of breast cancer cells via depression of Wnt signalling.* Cancer Lett, 2008. **269**(1): p. 67-77.
152. Chao, K.C., H.T. Yang, and M.W. Chen, *Human umbilical cord mesenchymal stem cells suppress breast cancer tumourigenesis through direct cell-cell contact and internalization.* J Cell Mol Med, 2012. **16**(8): p. 1803-15.
153. Karnoub, A.E., et al., *Mesenchymal stem cells within tumour stroma promote breast cancer metastasis.* Nature, 2007. **449**(7162): p. 557-U4.
154. Xu, S., et al., *Bone marrow-derived mesenchymal stromal cells are attracted by multiple myeloma cell-produced chemokine CCL25 and favor myeloma cell growth in vitro and in vivo.* Stem Cells, 2012. **30**(2): p. 266-79.
155. McLean, K., et al., *Human ovarian carcinoma-associated mesenchymal stem cells regulate cancer stem cells and tumorigenesis via altered BMP production.* J Clin Invest, 2011.
156. Beamer, W.G., et al., *Mouse model for malignant juvenile ovarian granulosa cell tumors.* Toxicol Pathol, 1998. **26**(5): p. 704-10.
157. Gocze, P.M., et al., *Hormone synthesis and responsiveness of spontaneous granulosa cell tumors in (SWR x SWXJ-9) F1 mice.* Gynecol Oncol, 1997. **65**(1): p. 143-8.
158. Beamer, W.G., P.C. Hoppe, and W.K. Whitten, *Spontaneous malignant granulosa cell tumors in ovaries of young SWR mice.* Cancer Res, 1985. **45**(11 Pt 2): p. 5575-81.
159. Soleimani, M. and S. Nadri, *A protocol for isolation and culture of mesenchymal stem cells from mouse bone marrow.* Nat Protoc, 2009. **4**(1): p. 102-6.
160. Zhou, Y.F., et al., *Spontaneous transformation of cultured mouse bone marrow-derived stromal cells.* Cancer Res, 2006. **66**(22): p. 10849-54.
161. Weksberg, D.C., et al., *CD150- side population cells represent a functionally distinct population of long-term hematopoietic stem cells.* Blood, 2008. **111**(4): p. 2444-51.
162. Judex, S., et al., *Genetically based influences on the site-specific regulation of trabecular and cortical bone morphology.* J Bone Miner Res, 2004. **19**(4): p. 600-6.

163. Lublinsky, S., E. Ozcivici, and S. Judex, *An automated algorithm to detect the trabecular-cortical bone interface in micro-computed tomographic images.* Calcif Tissue Int, 2007. **81**(4): p. 285-93.
164. Pawloski, P.A., et al., *Fracture risk in older, long-term survivors of early-stage breast cancer.* J Am Geriatr Soc, 2013. **61**(6): p. 888-95.
165. Kaste, S.C., et al., *QCT versus DXA in 320 survivors of childhood cancer: association of BMD with fracture history.* Pediatr Blood Cancer, 2006. **47**(7): p. 936-43.
166. Chen, Z., et al., *Fracture risk among breast cancer survivors: results from the Women's Health Initiative Observational Study.* Arch Intern Med, 2005. **165**(5): p. 552-8.
167. Holmes, S.J., et al., *Reduced bone mineral density in men following chemotherapy for Hodgkin's disease.* Br J Cancer, 1994. **70**(2): p. 371-5.
168. Kwong, F.N. and M.B. Harris, *Recent developments in the biology of fracture repair.* J Am Acad Orthop Surg, 2008. **16**(11): p. 619-25.
169. Pountos, I., et al., *Pharmacological agents and impairment of fracture healing: what is the evidence?* Injury, 2008. **39**(4): p. 384-94.
170. Theriault, R.L., *The role of bisphosphonates in breast cancer.* J Natl Compr Canc Netw, 2003. **1**(2): p. 232-41.
171. Coleman, R.E., *Clinical features of metastatic bone disease and risk of skeletal morbidity.* Clin Cancer Res, 2006. **12**(20 Pt 2): p. 6243s-6249s.
172. Ruggiero, S.L. and B. Mehrotra, *Bisphosphonate-related osteonecrosis of the jaw: diagnosis, prevention, and management.* Annu Rev Med, 2009. **60**: p. 85-96.
173. Aguirre, J.I., et al., *Oncologic doses of zoledronic acid induce osteonecrosis of the jaw-like lesions in rice rats (Oryzomys palustris) with periodontitis.* J Bone Miner Res, 2012. **27**(10): p. 2130-43.
174. Black, D.M., et al., *Bisphosphonates and Fractures of the Subtrochanteric or Diaphyseal Femur.* New England Journal of Medicine, 2010. **362**(19): p. 1761-1771.
175. Friedenreich, C.M., et al., *Alberta Physical Activity and Breast Cancer Prevention Trial: Sex Hormone Changes in a Year-Long Exercise Intervention Among Postmenopausal Women.* Journal of Clinical Oncology, 2010. **28**(9): p. 1458-1466.
176. Rubin, C.T. and L.E. Lanyon, *Dynamic strain similarity in vertebrates; an alternative to allometric limb bone scaling.* J Theor Biol, 1984. **107**(2): p. 321-7.
177. Case, N. and J. Rubin, *Beta-catenin--a supporting role in the skeleton.* J Cell Biochem, 2010. **110**(3): p. 545-53.
178. Pontes, J., Jr., et al., *E-cadherin and beta-catenin loss of expression related to bone metastasis in prostate cancer.* Appl Immunohistochem Mol Morphol, 2010. **18**(2): p. 179-84.
179. Gilsanz, V., et al., *Low-level, high-frequency mechanical signals enhance musculoskeletal development of young women with low BMD.* J Bone Miner Res, 2006. **21**(9): p. 1464-74.
180. Ward, K., et al., *Low magnitude mechanical loading is osteogenic in children with disabling conditions.* Journal of Bone and Mineral Research, 2004. **19**(3): p. 360-369.
181. Weiderpass, E., *Lifestyle and cancer risk.* J Prev Med Public Health, 2010. **43**(6): p. 459-71.
182. World Health Organization., *Global health risks : mortality and burden of disease attributable to selected major risks*. 2009, Geneva, Switzerland: World Health Organization. vi, 62 p.
183. Society, A.C., 2009.

184. Giuliani, N., V. Rizzoli, and G.D. Roodman, *Multiple myeloma bone disease: Pathophysiology of osteoblast inhibition.* Blood, 2006. **108**(13): p. 3992-6.
185. Bowell, B.J., *Current Controversies in Bone Marrow Transplantation*. 2000, Totowa, NJ: Humana Press. 322.
186. Bishop, M.R., *Hematopoietic stem cell transplantation. Introduction.* Cancer Treat Res, 2009. **144**: p. ix-x.
187. Pagnotti, G.M., et al., *Low magnitude mechanical signals mitigate osteopenia without compromising longevity in an aged murine model of spontaneous granulosa cell ovarian cancer.* Bone, 2012. **51**(3): p. 570-7.
188. Miyakawa, Y., et al., *Establishment of a new model of human multiple myeloma using NOD/SCID/gammac(null) (NOG) mice.* Biochem Biophys Res Commun, 2004. **313**(2): p. 258-62.
189. Mirandola, L., et al., *Tracking human multiple myeloma xenografts in NOD-Rag-1/IL-2 receptor gamma chain-null mice with the novel biomarker AKAP-4.* BMC Cancer, 2011. **11**: p. 394.
190. Machida, K., et al., *Higher susceptibility of NOG mice to xenotransplanted tumors.* J Toxicol Sci, 2009. **34**(1): p. 123-7.
191. Radl, J., et al., *Animal model of human disease. Multiple myeloma.* Am J Pathol, 1988. **132**(3): p. 593-7.
192. Shultz, L.D., et al., *Human lymphoid and myeloid cell development in NOD/LtSz-scid IL2R gamma null mice engrafted with mobilized human hemopoietic stem cells.* J Immunol, 2005. **174**(10): p. 6477-89.
193. Hjorth-Hansen, H., et al., *Marked osteoblastopenia and reduced bone formation in a model of multiple myeloma bone disease in severe combined immunodeficiency mice.* J Bone Miner Res, 1999. **14**(2): p. 256-63.
194. Reme, T., et al., *Growth and immortalization of human myeloma cells in immunodeficient severe combined immunodeficiency mice: a preclinical model.* Br J Haematol, 2001. **114**(2): p. 406-13.
195. Huang, Y.W., et al., *Disseminated growth of a human multiple myeloma cell line in mice with severe combined immunodeficiency disease.* Cancer Res, 1993. **53**(6): p. 1392-6.
196. Sala, A. and R.D. Barr, *Osteopenia and cancer in children and adolescents: the fragility of success.* Cancer, 2007. **109**(7): p. 1420-31.
197. Lemaire, M., et al., *The microenvironment and molecular biology of the multiple myeloma tumor.* Adv Cancer Res, 2011. **110**: p. 19-42.
198. Wiggins, M.S. and E.M. Simonavice, *Cancer prevention, aerobic capacity, and physical functioning in survivors related to physical activity: a recent review.* Cancer Manag Res, 2010. **2**: p. 157-64.
199. Fairey, A.S., et al., *Effect of exercise training on C-reactive protein in postmenopausal breast cancer survivors: a randomized controlled trial.* Brain Behav Immun, 2005. **19**(5): p. 381-8.
200. Friedenreich, C.M., *Physical activity and breast cancer: review of the epidemiologic evidence and biologic mechanisms.* Recent Results Cancer Res, 2011. **188**: p. 125-39.
201. Michigami, T., et al., *Cell-cell contact between marrow stromal cells and myeloma cells via VCAM-1 and alpha(4)beta(1)-integrin enhances production of osteoclast-stimulating activity.* Blood, 2000. **96**(5): p. 1953-60.

202. Charafe-Jauffret, E., et al., *Aldehyde dehydrogenase 1-positive cancer stem cells mediate metastasis and poor clinical outcome in inflammatory breast cancer.* Clin Cancer Res, 2010. **16**(1): p. 45-55.
203. Dick, J.E., *Acute myeloid leukemia stem cells.* Ann N Y Acad Sci, 2005. **1044**: p. 1-5.
204. Matsui, W., et al., *Characterization of clonogenic multiple myeloma cells.* Blood, 2004. **103**(6): p. 2332-6.
205. Britton, K.M., et al., *Cancer stem cells and side population cells in breast cancer and metastasis.* Cancers (Basel), 2011. **3**(2): p. 2106-30.
206. Fowler, J.A., C.M. Edwards, and P.I. Croucher, *Tumor-host cell interactions in the bone disease of myeloma.* Bone, 2011. **48**(1): p. 121-8.